

AD-A034 457

HUGHES HELICOPTERS CULVER CITY CALIF

F/G 1/3

DESIGN, FABRICATION, AND TESTING OF ADVANCED COMPOSITE AH-1G TA--ETC(U)

NOV 76 J F NEEDHAM

DAAJ02-73-C-0079

UNCLASSIFIED

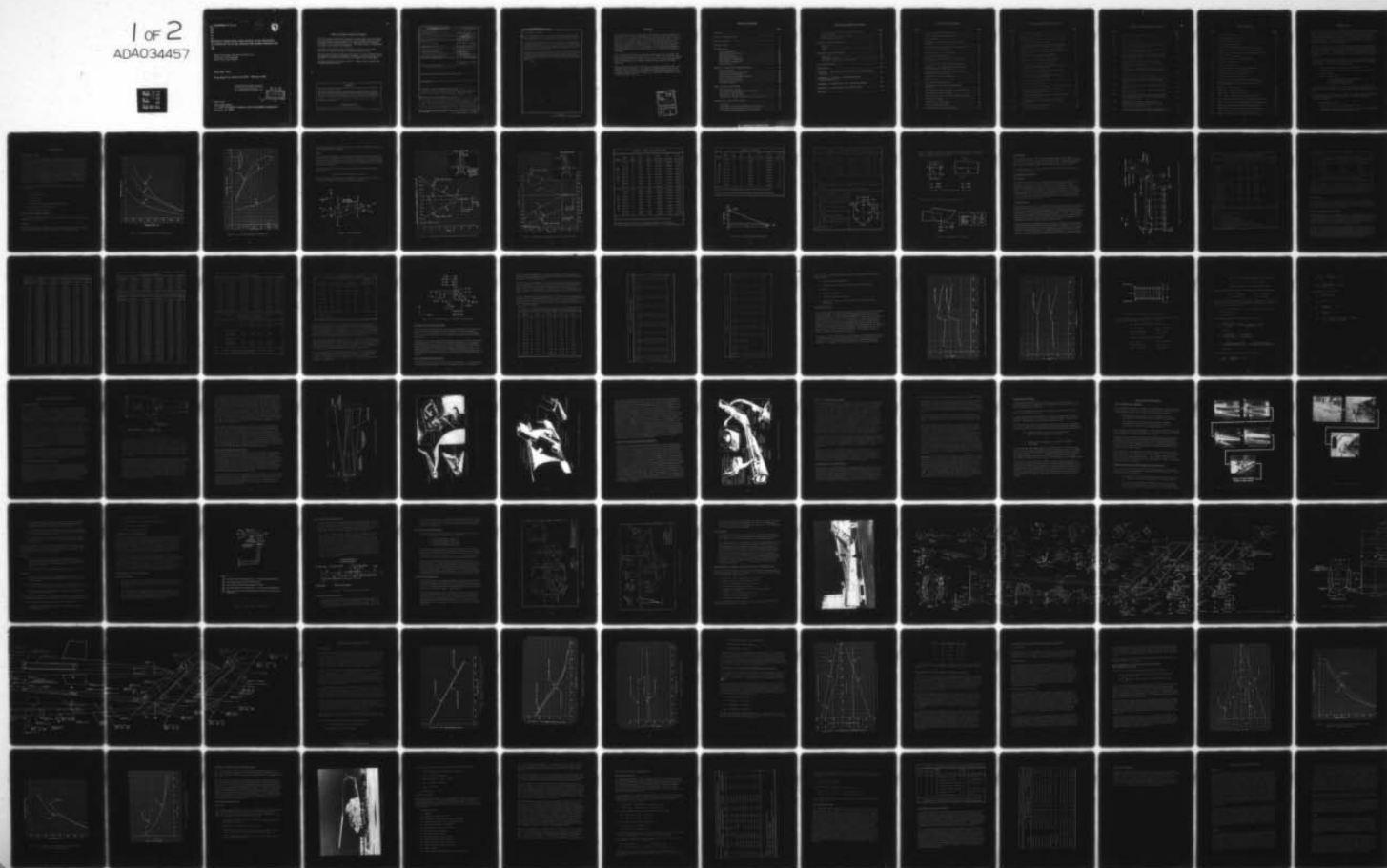
HH-76-50

USAAMRDL-TR-76-24

NL

1 OF 2

ADA034457



AD 1034457

USAAMRDL-TR-76-24

12



FC

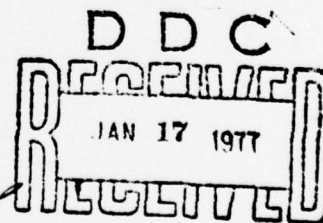
DESIGN, FABRICATION, AND TESTING OF AN ADVANCED
COMPOSITE AH-1G TAIL SECTION (TAIL BOOM/VERTICAL FIN)

Hughes Helicopters, Division of Summa Corp.
Centinela and Teale Streets
Culver City, Calif. 90230

November 1976

Final Report for Period July 1973 - February 1976

Approved for public release;
distribution unlimited.



Prepared for

EUSTIS DIRECTORATE
U. S. ARMY AIR MOBILITY RESEARCH AND DEVELOPMENT LABORATORY
Fort Eustis, Va. 23604

EUSTIS DIRECTORATE POSITION STATEMENT

This report documents the research, development, and testing efforts involved in designing, fabricating, structural testing, and flight testing of a primary fuselage structure for a helicopter using advanced composite materials. The selected component was the tailboom and vertical fin for the AH-1G Cobra helicopter. The tailboom design is a semimonocoque construction using a sandwich wall construction.

The research and development program established that helicopter primary fuselage structures can be efficiently fabricated from advanced composite materials.

The report has been reviewed by the Eustis Directorate, U. S. Army Air Mobility Research and Development Laboratory (AVSCOM) and is considered to be technically sound. It is published for the exchange of information and the stimulation of future development.

The technical monitor for this program was Mr. T. L. Mazza, Structures Technical Area, Technology Applications Division.

DISCLAIMERS

The findings in this report are not to be construed as an official Department of the Army position unless so designated by other authorized documents.

When Government drawings, specifications, or other data are used for any purpose other than in connection with a definitely related Government procurement operation, the United States Government thereby incurs no responsibility nor any obligation whatsoever; and the fact that the Government may have formulated, furnished, or in any way supplied the said drawings, specifications, or other data is not to be regarded by implication or otherwise as in any manner licensing the holder or any other person or corporation, or conveying any rights or permission, to manufacture, use, or sell any patented invention that may in any way be related thereto.

Trade names cited in this report do not constitute an official endorsement or approval of the use of such commercial hardware or software.

DISPOSITION INSTRUCTIONS

Destroy this report when no longer needed. Do not return it to the originator.

Unclassified

SECURITY CLASSIFICATION OF THIS PAGE (When Data Entered)

REPORT DOCUMENTATION PAGE		READ INSTRUCTIONS BEFORE COMPLETING FORM	
1. REPORT NUMBER USAAMRDL-TR-76-24 ✓	2. GOVT ACCESSION NO.	3. RECIPIENT'S CATALOG NUMBER	
4. TITLE (and Subtitle) DESIGN, FABRICATION, AND TESTING OF AN ADVANCED COMPOSITE AH-1G TAIL SECTION (TAIL BOOM/VERTICAL FIN) ✓		5. TYPE OF REPORT & PERIOD COVERED Final July 1973 to February 1976	
7. AUTHOR(s) James F. Needham		6. PERFORMING ORG. REPORT NUMBER HH-76-50	
9. PERFORMING ORGANIZATION NAME AND ADDRESS Hughes Helicopters, Division of Summa Corp. Centinela & Teale Streets Culver City, Ca. 90230		8. CONTRACT OR GRANT NUMBER(s) DAAJ02-73-C-0079 NEW	
11. CONTROLLING OFFICE NAME AND ADDRESS Eustis Directorate, U. S. Army Air Mobility Research & Development Laboratory Fort Eustis, Virginia 23604		10. PROGRAM ELEMENT, PROJECT, TASK AREA & WORK UNIT NUMBERS 63211A 1F263211DB41 00 001 EK	
14. MONITORING AGENCY NAME & ADDRESS (if different from Controlling Office)		12. REPORT DATE November 1976	
		13. NUMBER OF PAGES 157 (2) 163 p.	
		15. SECURITY CLASS. (of this report)	
		15a. DECLASSIFICATION/DOWNGRADING SCHEDULE	
16. DISTRIBUTION STATEMENT (of this Report) Approved for public release; distribution unlimited.			
17. DISTRIBUTION STATEMENT (of the abstract entered in Block 20, if different from Report)			
18. SUPPLEMENTARY NOTES			
19. KEY WORDS (Continue on reverse side if necessary and identify by block number) Composite, Graphite, Sandwich, Filament Winding, Primary, Structural, Component, Tail Boom, Helicopter, Strength, Weight, Life-Cycle Cost, Static, Fatigue, Flight, Test, Criteria, Design, Fabrication, AH-1G			
20. ABSTRACT (Continue on reverse side if necessary and identify by block number) The purpose of this program was to design and fabricate a primary structural component for a helicopter using advanced composite materials. The com- ponent selected was the tail boom and vertical fin of the AH-1G Cobra heli- copter. The composite tail boom was required to meet the existing metal tail boom structural design and stiffness criteria, and to be interchangeable with the metal tail boom. Design objectives were to reduce the life cycle			

DD FORM 1 JAN 73 1473 EDITION OF 1 NOV 65 IS OBSOLETE

Unclassified
SECURITY CLASSIFICATION OF THIS PAGE (When Data Entered)

409 164
lpg

Unclassified

SECURITY CLASSIFICATION OF THIS PAGE(When Data Entered)

20. Abstract - continued

costs, to minimize the parts count, and to lower the overall weight of the existing structure. The composite tail boom successfully met the design criteria and objectives and completed all the structural and flight tests.

The composite tail boom structure is a semimonocoque configuration using a sandwich wall construction. The inner and outer skins are fabricated of Thornel 300 graphite filaments with an epoxy resin, and the sandwich core is Nomex honeycomb. The wet-filament-winding technique was used in the fabrication of the major components.

This research and development program established that primary helicopter components could be efficiently fabricated from composite materials. The resulting structure would have a higher fatigue strength and a lower life-cycle cost than the metal structure, and it would have an improved ballistic tolerance.

Unclassified

SECURITY CLASSIFICATION OF THIS PAGE(When Data Entered)

PREFACE

This final report describes the design, fabrication, structural testing, and flight testing of a composite aft fuselage tail section for the AH-1G Cobra helicopter. The program was conducted under Contract DAAJ02-73-C-0079 between the Eustis Directorate, U. S. Army Air Mobility Research and Development Laboratory (USAAMRDL), Fort Eustis, Virginia, and Hughes Helicopters (HH), Culver City, California. The program was under the technical cognizance of Mr. Thomas Mazza of the Technology Applications Division, AMRDL and technical supervision of Mr. Herb Lund of Hughes Helicopters.

As a subcontractor to HH, the design and fabrication of the composite tail boom was accomplished at Fiber Science, Inc. (FSI). The structural testing was accomplished at HH facilities in Culver City, California, and the flight test demonstrations were conducted at HH Palomar Airport, Carlsbad, California.

The principal contributors to the design, fabrication and testing of the composite tail boom were Herb Lund, Advanced Design Manager, and James Needham, Design Specialist, of Hughes Helicopters; Dale Abildskov, Vice President Engineering, Larry Ashton, Vice President, and Sam Yao, Chief Engineer, of Fiber Science.

ACCESSION for	
DTIC	White Section <input checked="" type="checkbox"/>
DOC	Belt Section <input type="checkbox"/>
UNANNOUNCED	<input type="checkbox"/>
JUSTIFICATION	
BY	
DISTRIBUTION/AVAILABILITY CODES	
Dist.	AVAIL. SEC. & SPECIAL
A	

TABLE OF CONTENTS

	<u>Page</u>
PREFACE	3
LIST OF ILLUSTRATIONS.....	7
LIST OF TABLES	10
INTRODUCTION	11
DETAIL DESIGN	12
Design Discussion	12
Structural Design Criteria	12
Materials Selection	22
Initial Design Configuration	25
Second Design Configuration	30
Final Design Configuration	30
Stress Analysis	34
ORIGINAL FABRICATION METHODOLOGY	40
Filament Winding	40
Initial Boom Fabrication Concept	40
Initial Fabrication Problems	42
Initial Fin Spar Fabrication Concept	46
Initial Fabrication Review	48
Attachment Test Tail Boom	48
Fabrication Review	50
FINAL BOOM FABRICATION	51
New Fabrication Concept	51
Fabrication of the Structural Test Tail Boom	51
Fabrication of the Fin Spar	55
Fabrication of the Tail Boom	55
Fabrication of Flight Test Tail Boom and Vertical Fin	61
STRUCTURAL AND FLIGHT TESTS	67
Discussion	67
Test Results of Tool-Proof (Specimen A) Tail Boom	71
Test Results of the Attachment Test Tail Boom	73
Test Results of the Structural Test Tail Boom	74

TABLE OF CONTENTS - Continued

	<u>Page</u>
Proof Loading of the Flight Test Tail Boom and Vertical Fin Spar	75
Lateral Control System Proof Load	80
Flight Demonstration	80
REVIEW OF DESIGN OBJECTIVES	90
General	90
Weight	90
Costs	91
ADVANCED TAIL BOOM DESIGN	94
Discussion	94
Component Redesign	94
Tail Boom Construction Cost Estimate	97
RECOMMENDATIONS	103
REFERENCES	104
APPENDIX A - SECTION PROPERTIES COMPUTER PROGRAM "SECPRO"	106
APPENDIX B - FOUR BOLT AND VERTICAL FIN ATTACHMENT TEST	111
APPENDIX C - STRUCTURAL TEST AND EVALUATION	124
APPENDIX D - STRUCTURAL EVALUATION TEST	144
SYMBOLS	156

LIST OF ILLUSTRATIONS

<u>Figure</u>		<u>Page</u>
1	Section Properties for Existing Boom	13
2	Section Properties for Existing Fin	14
3	Sign Convention	15
4	Vertical Fin Chordwise Bending and Torsional Moments	16
5	Vertical Fin Spanwise Shear and Bending Moment	17
6	Fin-Chord Load Distribution	19
7	Synchronized Elevator Limit Loads	21
8	Tail Bumper Limit Loads	21
9	Geometry and Station Location, Tail Boom and Vertical Fin	23
10	Computer Program "SECPRO" Nomenclature	30
11	Comparison of Ultimate Compressive Stress to Allowable Stress - Outer Skin	35
12	Comparison of Ultimate Compressive Stress to Allowable Stress - Inner Skin	36
13	Notations for Sandwich Composite	37
14	Geodesic Path	41
15	Forward Attachment Fitting	43
16	Composite Tail Boom Forward Attachment Assembly	44
17	Composite Tail Boom Fin Spar to Boom Assembly	45
18	Composite Tail Boom Assembly	47
19	Manufacturing Process for the Composite Tail Boom	52
20	Forming in the Mold	53
21	Final Fin Spar Configuration	56
22	Typical Reinforcement Doily	57
23	Tail Rotor Gearbox Mounting Bracket	59

LIST OF ILLUSTRATIONS - Continued

<u>Figure</u>		<u>Page</u>
24	Fin Aft Structure Assembly	60
25	Flight Test Tail Section	62
26	Structural Assembly of the Tail Boom Cobra AH-1G. . . .	63
27	Tail Boom Assembly and Installation	65
28	Comparison of Tail Boom Lateral Bending Moments (M_z) for Condition V, +15 degrees Yaw, Recovery	68
29	Comparison of Tail Boom Vertical Bending Moments (M_y) for Condition V, +15 degrees Yaw, Recovery	69
30	Comparison of Tail Boom Torque (M_x) for Condition V, +15 degrees Yaw, Recovery	70
31	Structural Test Tail Boom Fatigue Loading	72
32	Proof Loading for Flight Test Tail Boom	76
33	Comparison of Vertical Bending Stiffness of AH-1G Structure to Composite Structure	77
34	Comparison of Lateral Bending Stiffness AH-1G Structure to Composite Structure	78
35	Comparison of Torsional Stiffness of AH-1G Structure to Composite Structure	79
36	Composite Tail Section in Flight	81
37	Advanced Tail Boom Design	95
38	Manufacturing Unit Cost Estimates - Composite Tail Boom.	102
A-1	Computer Program "SECPRO" Nomenclature	106
A-2	Section Elements BS 122, 33	107
B-1	Test Load and Deflection Locations and Test Results, Tail Boom Specimen "A"	117
B-2	Load Stations and Instrumentation, Tail Boom Specimen "B"	118
B-3	Test Setup Tail Boom Specimen A	119
B-4	Failure Tail Boom Specimen A	120

LIST OF ILLUSTRATIONS - Continued

<u>Figure</u>		<u>Page</u>
B-5	Test Setup, Tail Boom Specimen B	121
B-6	Spar Failure, Right Side	122
B-7	Boom Failure, Right Side	123
C-1	View of Test Setup of AH-1G Basic Test Tail Boom (Configuration II) Structural Tests	137
C-2	View of Test Setup of AH-1G Basic Test Tail Boom (Configuration II) Structural Tests	138
C-3	Schematic Representation of Load Point Locations and Load Direction for the AH-1G Basic Test Tail Boom Structural Tests	139
C-4	Schematic Representation of Deflection and Accelerometer Locations for AH-1G Basic Test Tail Boom Structural Tests	140
C-5	Schematic Representation of Strain Gage Locations for the AH-1G Basic Test Tail Boom Structural Tests	141
C-6	View of Both 0.50-Inch Diameter Holes	142
C-7	Schematic Representation of Location of 0.50-Inch Diameter Holes and Location of Path Steel Ball Traveled	143
D-1	View of Test Setup of AH-1G Flight Test Tail Boom Static Proof Test	151
D-2	View of Test Setup of AH-1G Flight Test Tail Boom Static Proof Test	152
D-3	Schematic Representation of Load Point Locations and Load Direction for the AH-1G Flight Test Tail Boom Structural Test	153
D-4	Schematic Representation of Deflection and Accelerometer Locations for the AH-1G Flight Test Tail Boom Structural Test	154
D-5	Schematic Representation of Strain Gage Locations for the AH-1G Flight Test Tail Boom Structural Test . . .	155

LIST OF TABLES

<u>Table</u>		<u>Page</u>
1	Limit Loads for Boom	18
2	Attachment Bolt Loads - BS 41.32	20
3	Graphite Material Summary	24
4	Resin Property Summary	25
5	Thornel 300 Graphite/Standard Epoxy Properties	26
6	Thornel 300 Graphite/Bi-Modal Epoxy Properties	27
7	Comparison of Composite Moduli Calculated and Tested	28
8	Sandwich Core Properties	29
9	Calculated Tail Boom Section Properties	31
10	Tail Boom Inside Skin	32
11	Tail Boom Outside Skin	33
12	Measured Flight Strain and Load Factor Data	85
13	Summary of Observed Skin Temperatures	87
14	Comparison of Gearbox Accelerations	88
15	Tail Section Weight Comparison	92
16	Production Unit Cost Estimate - Advanced Design	98
17	Advanced Design - Unit Production Cost Estimate Calculation Table	99
18	Initial Fabrication Cost	100
A-1	Input Data - Tail Boom BS 122.33	108
A-2	Output Data - Tail Boom BS 122.33	109
B-1	Test Loading Conditions, Tail Boom Specimen "B"	115
B-2	Test Results at 100 Percent Limit Load, Tail Boom "B"	116
C-1	Test Program Summary, AH-1G Basic Test Tail Boom	132
C-2	Maximum Applied Loads, Deflections and Strains	133
C-3	Applied Test Loads, AH-1G Basic Test Tail Boom	135
C-4	Fatigue Test Summary, AH-1G Basic Test Tail Boom	136
D-1	Maximum Applied Loads, Deflections and Strains	150

INTRODUCTION

A composite tail section for the AH-1G Cobra helicopter was designed, fabricated and tested by Hughes Helicopters (HH) and Fiber Science, Incorporated (FSI). The tail boom structure is a semimonocoque configuration using a sandwich wall construction. The inner and outer skins are fabricated of Thornel 300 graphite filaments with an epoxy resin, and the sandwich core is Nomex honeycomb. The wet-filament-winding technique was used in the fabrication of all the major components.

The AH-1G composite tail section was required to meet the existing metal tail boom structural design and stiffness criteria. It was to be interchangeable with the existing metal tail boom, including the installation of all the operational hardware. Design objectives were to reduce the life-cycle costs, to minimize the parts count, and to lower the overall weight of the existing structure.

A thorough structural testing of the final composite tail boom configuration was required to structurally substantiate the tail boom prior to the flight demonstration. The structural tests included:

1. Static testing to the maximum design limit loads.
2. Static testing to the ultimate for the critical loading condition.
3. Fatigue testing.
4. Selective static testing.
 - a. Simulated forward attach bolt failure
 - b. Simulated ballistic damage
 - c. One-pound ball impact.

The composite tail section successfully completed all the structural tests with the results of the fatigue tests indicating essentially an infinite service life.

The final phase of the program was a flight demonstration with the composite tail boom installed on an AH-1G helicopter. The flight test envelope included the following:

- Airspeeds to 190 knots
- Maximum helicopter cg load factors of 3.4 g.
- Maneuvers including turns, pull-ups, push-overs, power transitions, and control reversals at airspeeds to 171 knots.

DETAIL DESIGN

DESIGN DISCUSSION

The AH-1G composite tail boom was designed to the existing metal tail boom design and stiffness criteria, using the wet-filament-winding process for fabricating all the major components. The composite tail boom was to be interchangeable with the existing metal tail boom, including the installation of all operational hardware (i.e., drive shaft, covers, sync elevator, gear-boxes, controls, electronic equipment, etc), with adequate accessibility. The tail boom and vertical fin spar were designed as a sandwich-wall construction with the faces filament-wound. The locations of all access doors and panels on the existing tail boom were incorporated in the composite tail boom. The doors were designed to be nonstructural. The tail boom construction was such that the number of internal parts (frames, bulkheads, stiffeners, etc.) were minimized. The outside contour lines were required to be within ± 0.1 inch of the metal boom.

The design approach was governed by the following criteria -- in order of importance:

1. Life-cycle cost
2. Minimum part count
3. Weight saving
4. Flyaway cost
5. Simplicity in tooling and fabrication procedure
6. Reliability and maintainability
7. Safety and survivability

STRUCTURAL DESIGN CRITERIA

The tail boom and vertical fin structures were designed to meet the following structural design criteria:

Stiffness

The bending and torsional stiffness are taken from Reference 2 for the AH-1G metal tail boom and vertical fin, and are shown in Figures 1 and 2.

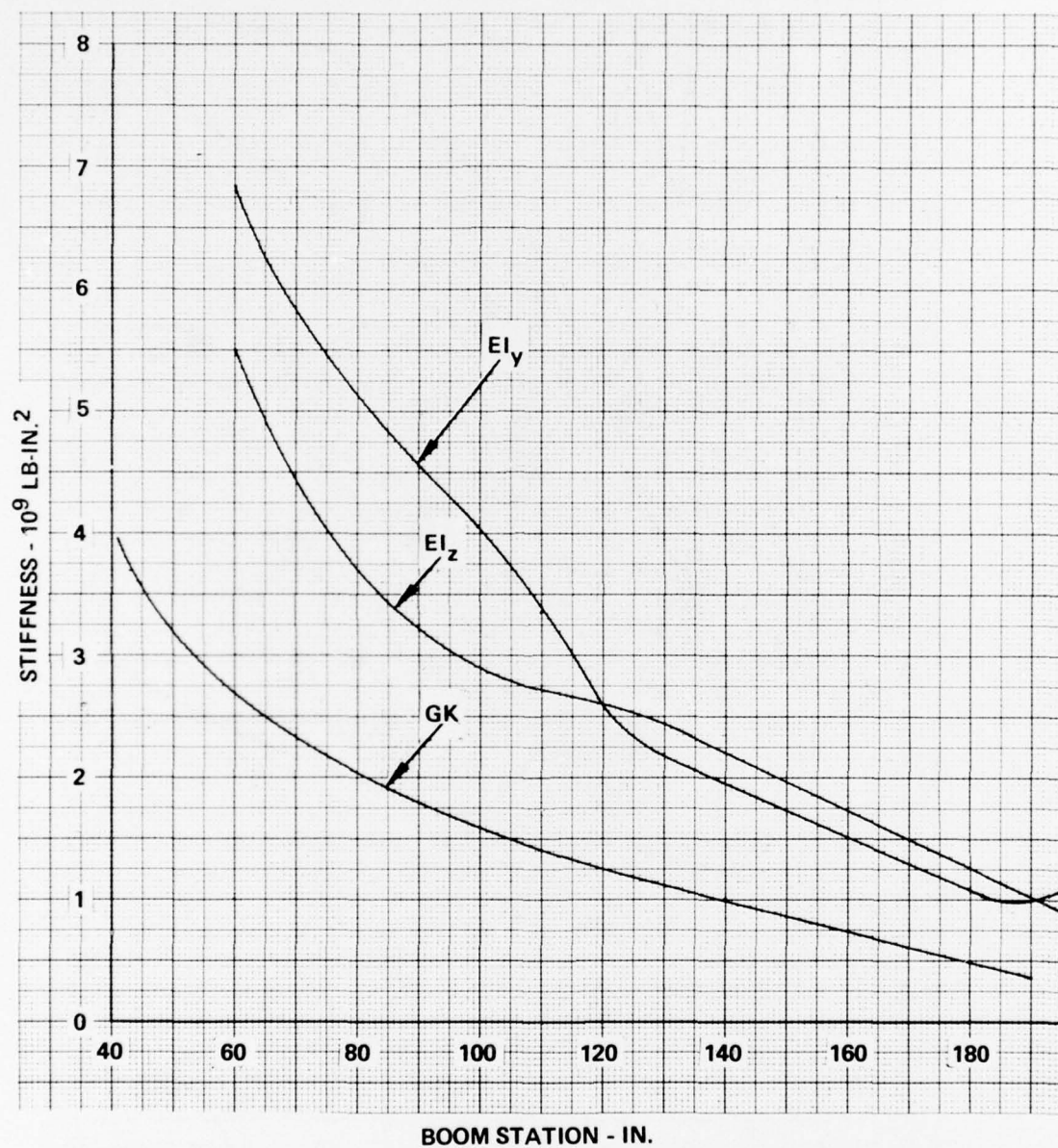


Figure 1. Section Properties for Existing Boom.

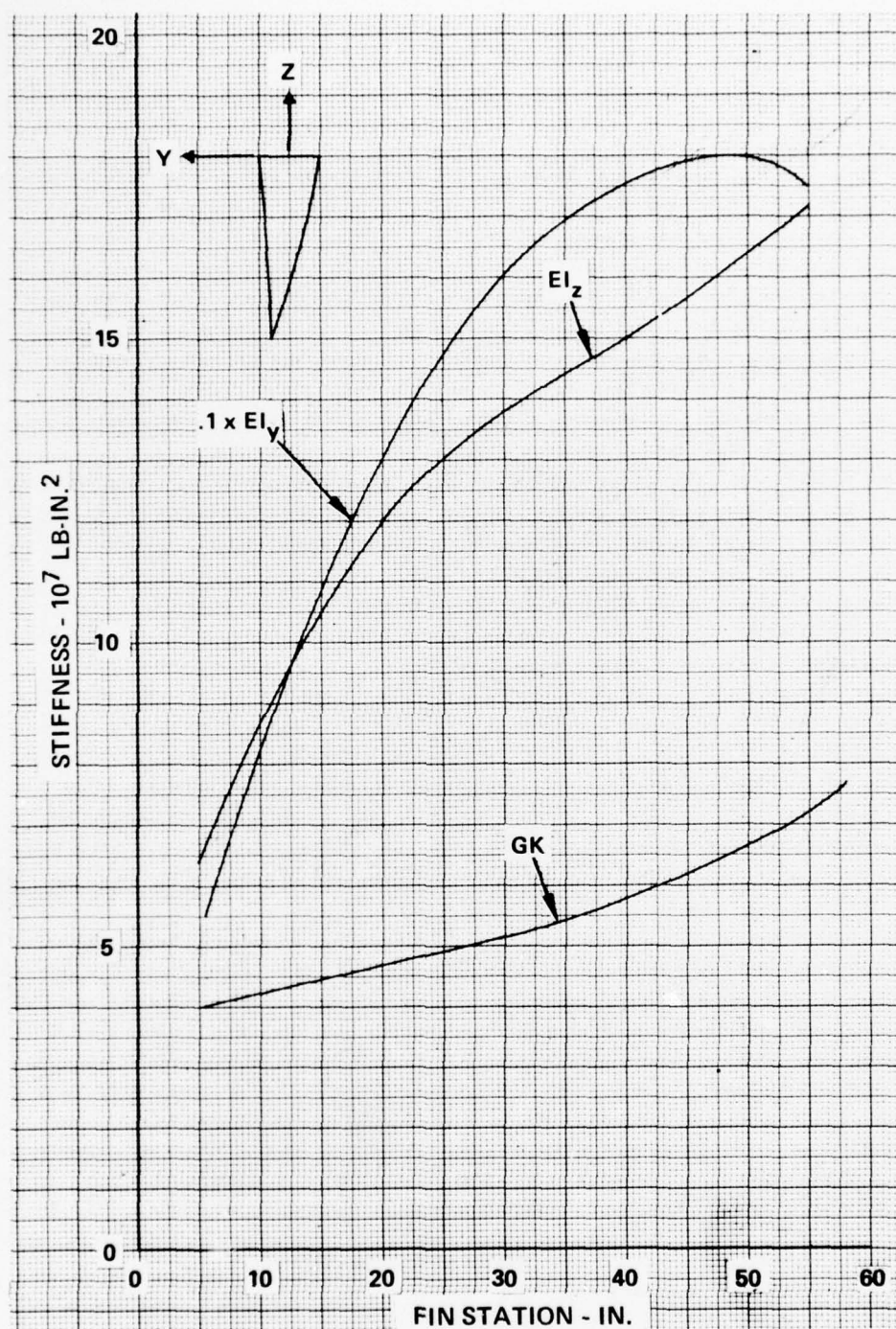


Figure 2. Section Properties for Existing Fin.

A design object of the composite tail boom was that it be within ± 10 percent of the metal tail boom stiffness.

Loads

The composite tail boom was required to have the strength equivalent to or greater than the standard AH-1G tail boom. Figures 3, 4, and 5 and Tables 1 and 2 (taken from Reference 1) show the sign convention and the maximum design limit loads. Unless otherwise noted, the ultimate loads are 1.5 times that of the limit loads.

The fin limit air load distribution was derived from information found in Reference 1.

$$\text{Average Pressure Loading} = 0.758 \text{ psi}$$

The fin-chord load distribution, assuming the center of pressure at 0.30 chord and a triangular distribution, is shown in Figure 6.

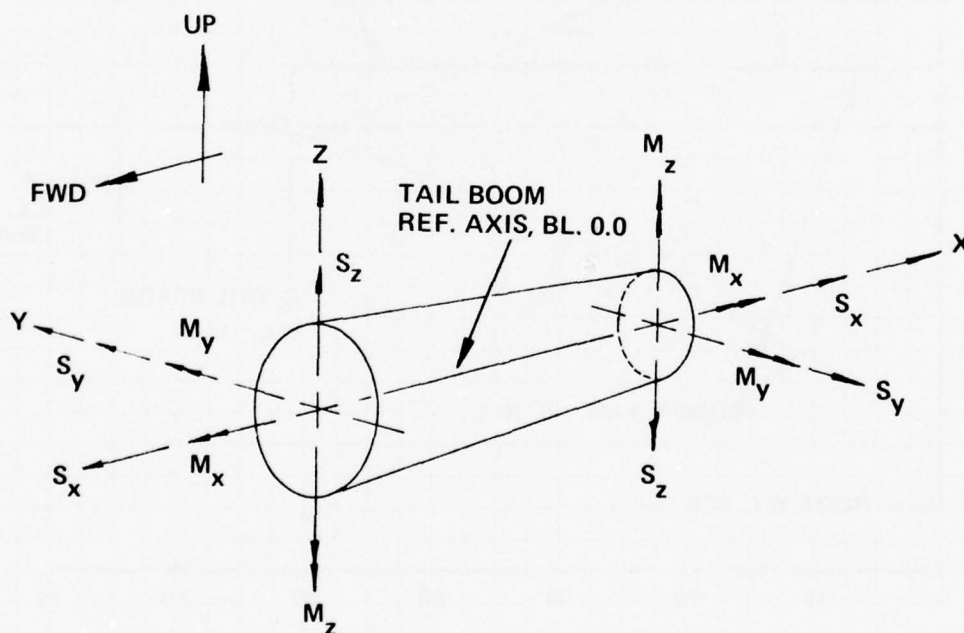


Figure 3. Sign Convention.

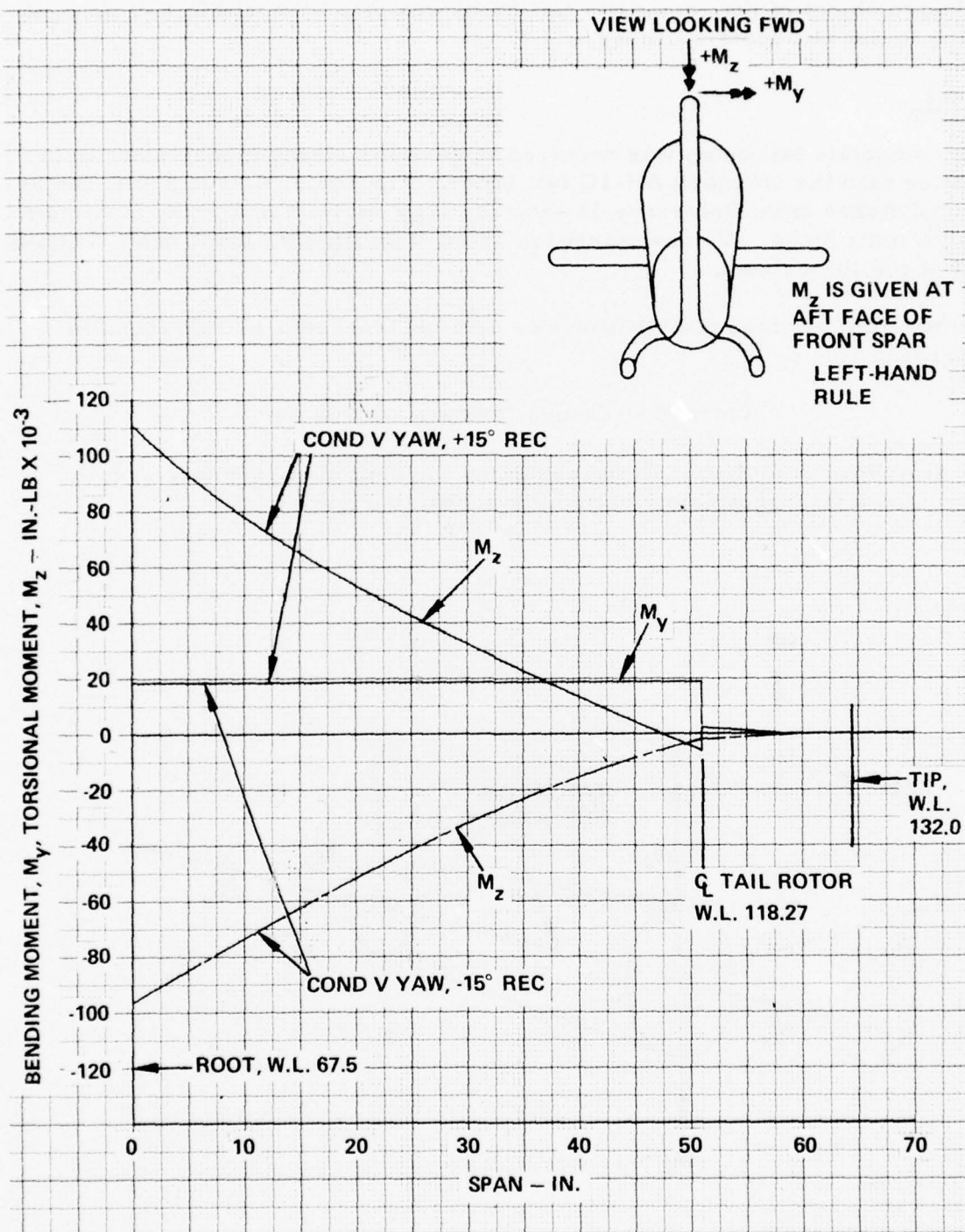


Figure 4. Vertical Fin Chordwise Bending and Torsional Moments.

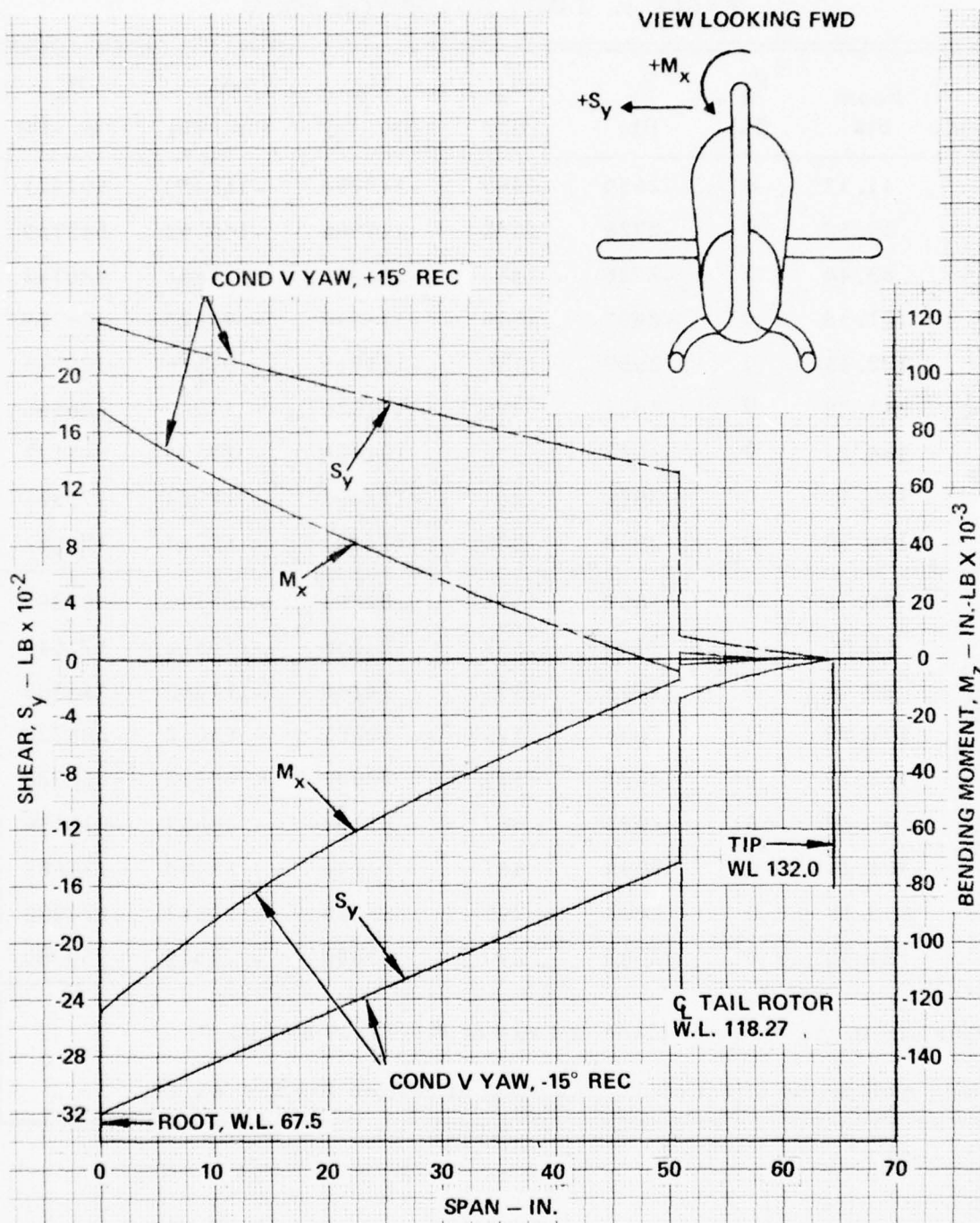


Figure 5. Vertical Fin Spanwise Shear and Bending Moment.

TABLE 1. LIMIT LOADS FOR BOOM

Cond.	Boom Sta	S _x (lb)	S _y (lb)	S _z (lb)	M _x (in. -lb)	M _y (in. -lb)	M _z (in. -lb)
V, YAW +15° REC	41.32	0	-2659	1450	-112734	-166459	591941
	59.50	0	-2726	1352	-113966	-140152	543727
	80.44	0	-2726	1352	-113966	-111888	486743
	101.38	0	-2957	1136	-111916	- 83623	429759
	122.33	0	-2957	1136	-111916	- 61516	386743
	143.28	0	-3027	476	-111326	- 37797	306485
	164.23	0	-3027	476	-111326	- 27825	243173
	185.18	0	-2922	284	-113491	- 17953	179861
	194.30	0	-2922	284	-113491	- 15283	152461
V, YAW -15° REC	41.32	0	1668	1432	82993	-165305	-401897
	59.50	0	1744	1332	84246	-139322	-371648
	80.44	0	1744	1332	84246	-111467	-335188
	101.38	0	2001	1113	82001	- 83612	-288728
	122.33	0	2001	1113	82001	- 60112	-256528
	143.28	0	2093	487	81294	- 38633	-215436
	164.23	0	2093	487	81294	- 28440	-171688
	185.18	0	2002	290	83580	- 18247	-127900
	194.30	0	2002	290	83580	- 15517	-109050
Loads are in the fuselage plane and are at WL 63.09 and BL 0.							
Loads include the effect of 100 lb ballast at Station 470 and WL 60.							

TABLE 1. Continued							
Cond.	Boom Sta	S_x (lb)	S_y (lb)	S_z (lb)	M_x (in. -lb)	M_y (in. -lb)	M_z (in. -lb)
XIV Tail Down Landing	41.32	0	0	-1851	0	367038	0
	59.50	0	0	-1851	0	333388	0
	80.44	0	0	-1851	0	294628	0
	101.38	0	0	-1851	0	255868	0
	122.33	0	0	-1851	0	217089	0
	143.28	0	0	-1851	0	178311	0
	164.23	0	0	-1851	0	139532	0
	185.18	0	0	-1851	0	100754	0
	194.30	0	0	-1851	0	83873	0
Loads are in the fuselage plane and are at WL 76.81 and BL 0.							
Loads include the effect of 100 lb ballast at Station 470 and WL 60.							

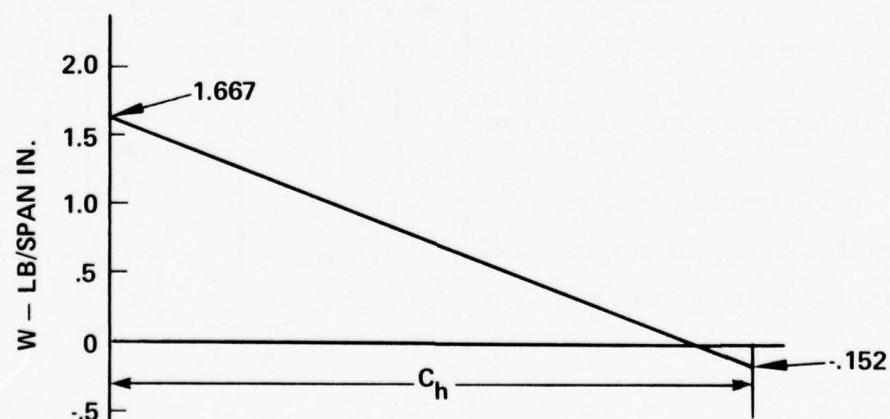


Figure 6. Fin-Chord Load Distribution.

TABLE 2. ATTACHMENT BOLT LOADS - BS 41.32

Condition	No. 2 (UR)			No. 5 (LR)			No. 7 (LL)			No. 10 (UL)		
	P_x	P_y	P_z	P_x	P_y	P_z	P_x	P_y	P_z	P_x	P_y	P_z
1	-7860	-1878	1504	-17511	548	1504	10743	548	-780	14541	-1878	-780
2	10458	1298	-468	6724	-454	-468	-13417	-454	1182	-3823	1278	1182
3	5194	-550	1236	-11918	238	1236	-6395	238	494	11942	-550	494
4	-6757	0	-461	6804	0	-461	8083	0	-461	-8014	0	-461
5	-8425	0	-583	8484	0	-583	11079	0	-583	-9993	0	-583
6	3828	-547	1039	-9898	235	1038	-4199	235	303	10278	-547	303
7	4123	-465	1098	-10056	142	1098	-4661	142	528	10393	-464	528
8	-308	-988	1304	-11214	522	1309	948	522	-113	10425	-988	-113

NOTES:

P_x is the axial load from the unsymmetrical bending and is a positive tension.

All loads are limit except condition 5, which is ultimate.

No.	Condition
1	VA, Yaw +15°, fwd, CG, 9500 lb
2	VA, Yaw -15°, fwd, CG, 9500 lb
3	XI, 6600 lb, Landing/drag lim fwd CG
4	XIV, Reserve Energy, Tail down landing
5	XIV, Tail down landing - Reserve Energy
6	VI, Jump TO fwd CG 6600 lb
7	II, 6600 lb - Sym pull out, fwd CG
8	IV, 6600 lb, Rolling PO, RT, fwd CG
From Reference 1.	

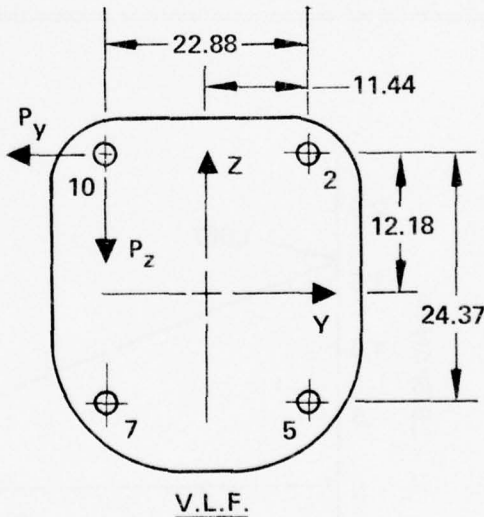


Diagram illustrating the geometry and loading of a rectangular attachment plate (V.L.F.) with four bolts (2, 5, 7, 10). The plate is centered on a coordinate system with Z pointing up, Y pointing right, and Pz pointing down. The dimensions are as follows:

- Horizontal distance between bolt centers: 22.88
- Horizontal distance from center to bolt 2: 11.44
- Vertical distance from center to bolt 5: 12.18
- Vertical distance from center to bolt 10: 24.37

Labels: V.L.F.

The synchronized elevator limit loads taken from Reference 1 are shown in Figure 7. Bell's factor for the ultimate load is 2.25, (Reference 1); this includes a static fatigue factor of 1.5.

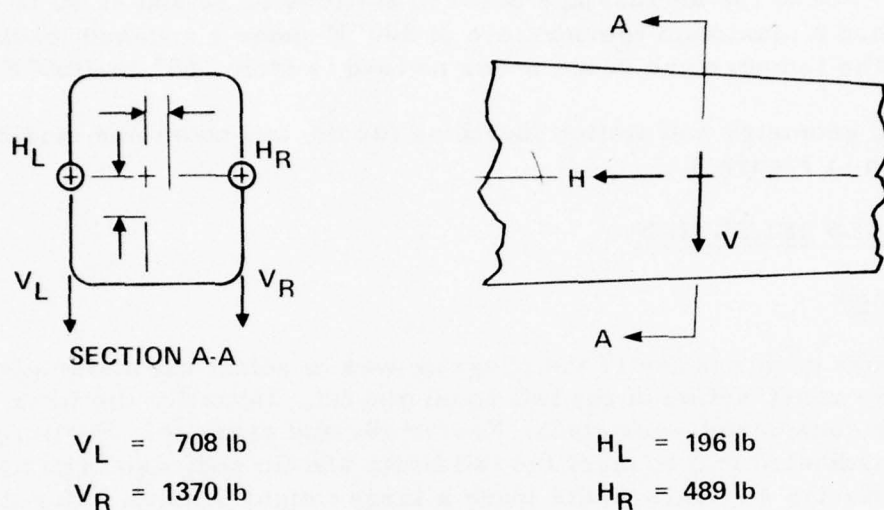


Figure 7. Synchronized Elevator Limit Loads.

The tail bumper limit loads are shown in Figure 8.

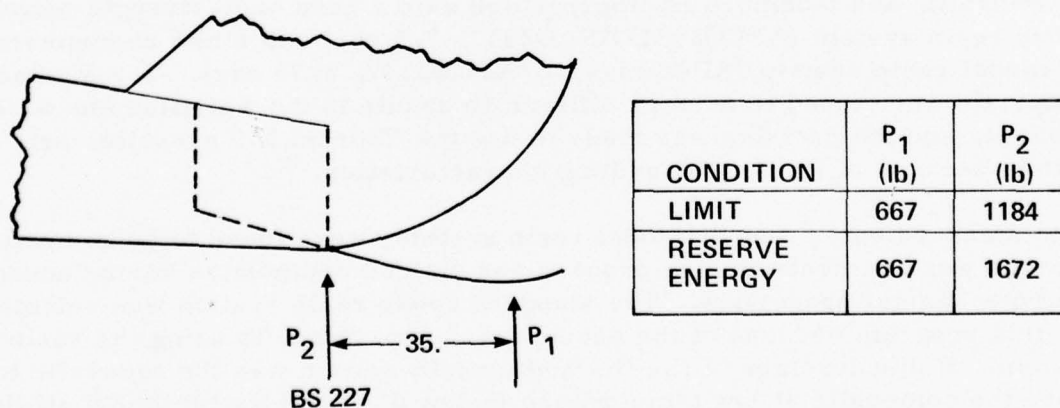


Figure 8. Tail Bumper Limit Loads.

Temperature

The temperature range under maximum load is from -65° to $+120^{\circ}$ F. The upper surface of the aft fuselage between stations 41.32 and 81.00 is designed to withstand a maximum temperature of 300° F under a reduced loading condition. The temperature range under no load is from -65° to $+165^{\circ}$ F.

The basic geometry and station locations for the tail boom and vertical fin are shown in Figure 9.

MATERIALS SELECTION

Introduction

The purpose of this phase of the program was to select the materials to be used in the construction of the tail boom and fin. Initially, the fiber materials considered were glass, Kevlar 49, and graphite. Preliminary analysis indicated that to meet the tail boom and fin stiffness criteria with glass or Kevlar 49 fibers would incur a large weight penalty. The stiffness criteria dictated that the tail boom be of sandwich-wall construction, fabricated using wet-filament-wound, graphite/epoxy skins, and a low-density core. An additional criterion was that as much of the structure be made of composite materials as practical.

Graphite/Epoxy

The characteristics and costs of the candidate materials are shown in Table 3. Filament-wound tubular test specimens were fabricated using Thornel 300, Modmore II, and Modmore III impregnated with a good high-strength (standard) epoxy resin system (APCO2434/APCO2347, 7.5 phr) and a new experimental Bi-modal resin system (APCO23-97-2/APCO2347, 5.75 phr). The Modmore materials were found to be very difficult to handle in the wet-filament-winding process, and the decision was made to use the Thornel 300 graphite, primarily because of its better handling characteristics.

Both standard epoxy and Bi-Modal resin systems were found to be compatible with the wet-filament-winding process and yielded composites having acceptable mechanical properties. The standard epoxy resin system was selected for this program because of the accumulated experience in using the resin system. A disadvantage of the Bi-Modal resin system was the necessity to store the composite at low temperature (below 0° F) and its limited shelf life.

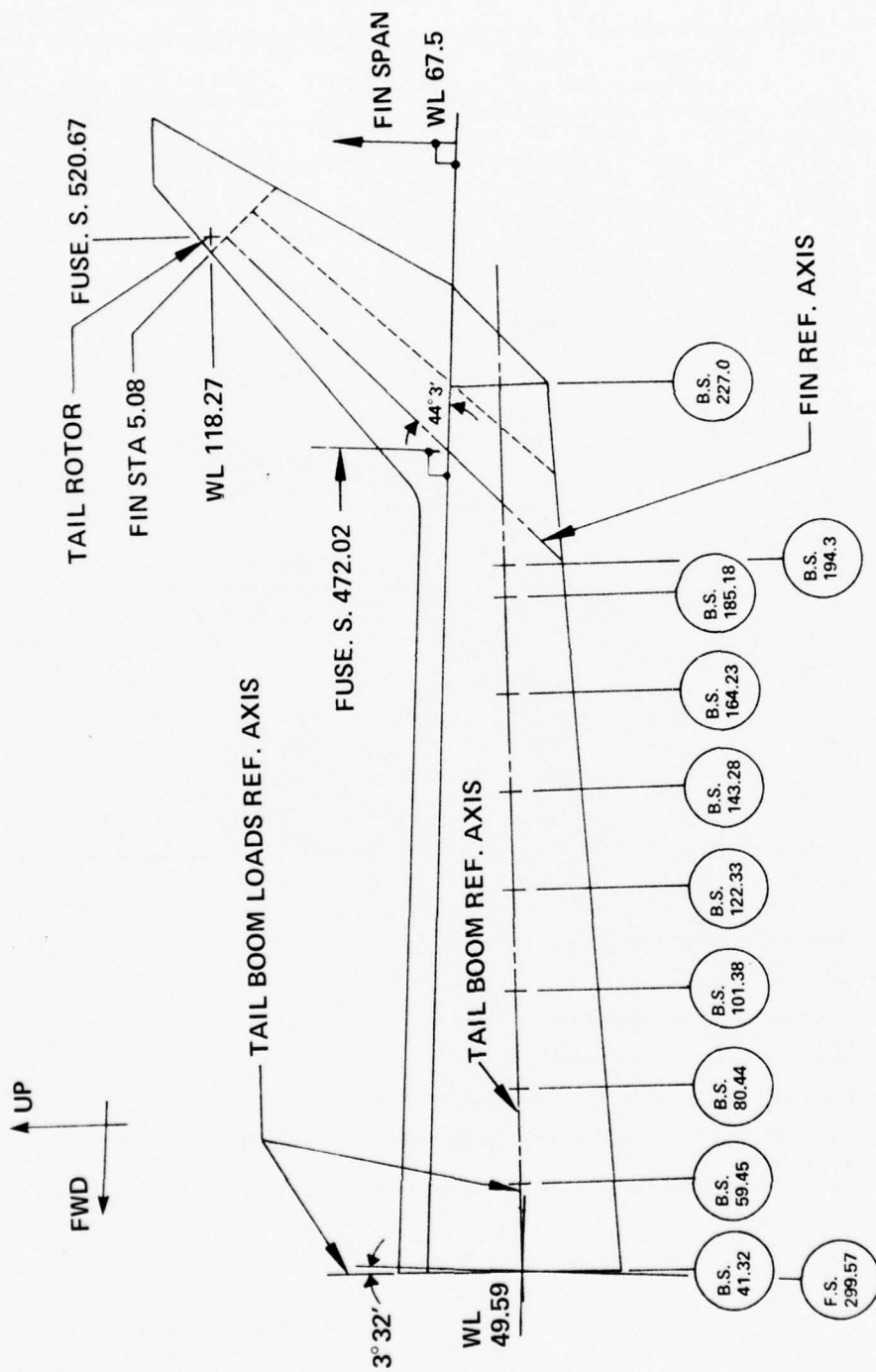


Figure 9. Geometry and Station Locations, Tail Boom and Vertical Fin.

TABLE 3. GRAPHITE MATERIAL SUMMARY

	Cost (\$/lb)	Density (lb/in. ³)	E (10 ⁶ psi)	F _{tu} (psi)	e (%)	Comment
Union Carbide Corp.						
Thornel 300	50	0.0636	34.0	360,000	1.1	1
Thornel 400	275	0.0640	34.0	450,000	1.3	2
Thornel 50S	205	0.0600	57.0	285,000	0.53	2
Thornel 75S	275	0.0650	78.0	345,000	0.53	2
Hercules						
A	55	0.0650	30.0	400,000		3
H.T.	75	0.0625	36.0	380,000		3
H.M.	90	0.0680	55.5	320,000		3
Great Lakes Carbon Corp.						
Fortafil CG-3	40	0.0650	25.0	250,000		
Fortafil CG-5	48	0.0650	45.0	350,000		
Fortafil 3-T	55	0.0650	30.0	300,000		
Fortafil 4-T		0.0650	38.0	350,000	0.92	
Fortafil 5-T	75	0.0650	48.0	400,000	0.83	
Fortafil 6-T	90	0.0686	58.0	420,000	0.72	
Fortafil 4-R	55	0.0650	38.0	450,000	1.2	4
Morganite Modmor Inc.						
Modmore I	95	0.0672	58.0	360,000		5
Modmore II	80	0.0618	42.0	360,000		5
Modmore III	55	0.0639	34.0	350,000		5
Celanese Corp.						
Celcon GY-70	75	0.0708	77.0	250,000		6
Comments:						
1. Good handling characteristics						
2. Prohibitive Cost						
3. Poor handling characteristics						
4. Available only in small quantities						
5. Difficult to use in wet winding process at FSI						
6. Not suitable for filament winding using present FSI Equipment (3 foot wide tape only)						

The mechanical properties of the standard and Bi-Modal epoxy resins are shown in Table 4.

TABLE 4. RESIN PROPERTY SUMMARY		
Property	Standard*	Bi-Modal**
E, 10^6 psi	0.470	0.383
F _{tu} , 10^6 psi	9600	8800
e, in./in.	0.0250	0.0278
ρ , lb/in. ³	0.0412	0.0412
*APCO 2434/APCO 2347 7.5 phr (FSCS - 118 ET)		
**APCO 23-97-2/APCO 2347 5.75 phr (Bi-Modal)		

Tables 5 and 6 show the calculated composite properties obtained by a computer program (Reference 7) for $\pm\alpha$ wound laminates of Thornel 300/epoxy. Table 7 presents a comparison of the calculated and the tested values of composite moduli using Thornel 300 graphite with Standard epoxy and with Bi-modal epoxy. The test specimens were wet-filament-wound tublar specimens. The fiber volume was 50 percent.

Sandwich Core

The materials selected as candidates for the sandwich core were polymethacrylimid (PMI) rigid foam, polyvinylchloride (PVC) rigid foam and HRH 10/OX-3/16-3.0 Nomex honeycomb. The properties of the candidate sandwich core materials are shown in Table 8.

INITIAL DESIGN CONFIGURATION

The materials used in the construction of the initial tail boom design were Thornel 300 graphite fibers, APCO 2434/2347, 7.5 phr (standard) epoxy resin, and PMI rigid foam core. Glass (S-1014) rovings and E-Glass fabric were used to reinforce the frames and bulkheads, the vertical fin aft airfoil, and the fittings because of their higher strength and lower cost.

The tail boom was designed as a sandwich-wall construction with the faces filament-wound and the core material configured by a thermal deforming process. The basic fiber winding patterns for the tail boom were $\pm\alpha$ (25 to 35 degrees) combined with 0 degree longitudinal fibers called longos. Local areas requiring strength and/or stiffness in the circumferential direction were reinforced with noncontinuous 90-degree circular windings.

TABLE 5. THORNEL 300 GRAPHITE/STANDARD EPOXY PROPERTIES

Alpha (deg)	EX (psi)	EY (psi)	GXY (psi)	UXY	UXY
0.00	1.723E+07	8.775E+05	5.095E+05	0.2850	0.0145
1.00	1.722E+07	8.776E+05	5.143E+05	0.2903	0.0148
2.00	1.718E+07	8.779E+05	5.286E+05	0.3063	0.0156
3.00	1.712E+07	8.784E+05	5.523E+05	0.3327	0.0171
4.00	1.703E+07	8.791E+05	5.853E+05	0.3692	0.0191
5.00	1.691E+07	8.800E+05	6.275E+05	0.4156	0.0216
6.00	1.676E+07	8.811E+05	6.786E+05	0.4713	0.0248
7.00	1.658E+07	8.825E+05	7.385E+05	0.5357	0.0285
8.00	1.636E+07	8.841E+05	8.068E+05	0.6078	0.0329
9.00	1.610E+07	8.860E+05	8.831E+05	0.6868	0.0378
10.00	1.581E+07	8.882E+05	9.671E+05	0.7713	0.0433
11.00	1.547E+07	8.906E+05	1.058E+06	0.8601	0.0495
12.00	1.509E+07	8.935E+05	1.157E+06	0.9515	0.0563
13.00	1.468E+07	8.967E+05	1.261E+06	1.0440	0.0638
14.00	1.422E+07	9.003E+05	1.372E+06	1.1357	0.0719
15.00	1.372E+07	9.043E+05	1.486E+06	1.2248	0.0807
16.00	1.319E+07	9.089E+05	1.608E+06	1.3095	0.0902
17.00	1.283E+07	9.140E+05	1.733E+06	1.3882	0.1004
18.00	1.205E+07	9.196E+05	1.861E+06	1.4594	0.1114
19.00	1.144E+07	9.260E+05	1.992E+06	1.5217	0.1231
20.00	1.883E+07	9.331E+05	2.126E+06	1.5741	0.1356
21.00	1.821E+07	9.409E+05	2.261E+06	1.6160	0.1489
22.00	9.591E+06	9.497E+05	2.397E+06	1.6471	0.1631
23.00	8.981E+06	9.594E+05	2.534E+06	1.6673	0.1781
24.00	8.385E+06	9.703E+05	2.670E+06	1.6768	0.1940
25.00	7.809E+06	9.823E+05	2.805E+06	1.6762	0.2109
26.00	7.255E+06	9.957E+05	2.939E+06	1.6662	0.2287
27.00	6.728E+06	1.011E+06	3.870E+06	1.6477	0.2475
28.00	6.230E+06	1.027E+06	3.198E+06	1.6217	0.2673
29.00	5.763E+06	1.045E+06	3.323E+06	1.5890	0.2882
30.00	5.327E+06	1.066E+06	3.443E+06	1.5509	0.3102
31.00	4.922E+06	1.988E+06	3.559E+06	1.5882	0.3334
32.00	4.547E+06	1.113E+06	3.670E+06	1.4618	0.3578
33.00	4.203E+06	1.141E+06	3.774E+06	1.4126	0.3834
34.00	3.887E+06	1.172E+06	3.872E+06	1.3615	0.4103
35.00	3.598E+06	1.206E+06	3.964E+06	1.3290	0.4386
36.00	3.335E+06	1.244E+06	4.048E+06	1.2557	0.4682
37.00	3.096E+06	1.286E+06	4.124E+06	1.2022	0.4993
38.00	2.878E+06	1.332E+06	4.192E+06	1.1489	0.5318
39.00	2.881E+06	1.384E+06	4.252E+06	1.0951	0.5658
40.00	2.502E+06	1.441E+06	4.303E+06	1.0442	0.6014

TABLE 5. Continued					
Alpha(deg)	EX (psi)	EY (psi)	GXY (psi)	UXY	UXY
41.00	2.341E+06	1.585E+06	4.346E+06	0.9933	0.6385
42.00	2.195E+06	1.576E+06	4.379E+06	0.9436	0.6773
43.00	2.064E+06	1.654E+06	4.402E+06	0.8954	0.7177
44.00	1.945E+06	1.741E+06	4.417E+06	0.8486	0.7597
45.00	1.838E+06	1.838E+06	4.421E+06	0.8033	0.8033

TABLE 6. THORNEL 300 GRAPHITE/BI-MODAL EPOXY PROPERTIES					
Alpha(deg)	EX (psi)	EY (psi)	GXY (psi)	UXY	UXY
0.00	1.719E+07	7.918E+05	4.263E+05	0.2850	0.0131
1.00	1.718E+07	7.918E+05	4.311E+05	0.2910	0.0134
2.00	1.714E+07	7.928E+05	4.456E+05	0.3090	0.0143
3.00	1.708E+07	7.922E+05	4.697E+05	0.3389	0.0157
4.00	1.698E+07	7.925E+05	5.033E+05	0.3803	0.0177
5.00	1.686E+07	7.930E+05	5.461E+05	0.4329	0.0204
6.00	1.671E+07	7.935E+05	5.980E+05	0.4960	0.0236
7.00	1.652E+07	7.942E+05	6.588E+05	0.5690	0.0274
8.00	1.629E+07	7.950E+05	7.282E+05	0.6509	0.0318
9.00	1.603E+07	7.959E+05	8.057E+05	0.7405	0.0368
10.00	1.572E+07	7.970E+05	8.911E+05	0.8365	0.0424
11.00	1.536E+07	7.984E+05	9.839E+05	0.9373	0.0487
12.00	1.497E+07	7.999E+05	1.084E+06	1.0409	0.0556
13.00	1.453E+07	8.017E+05	1.190E+06	1.1455	0.0632
14.00	1.404E+07	8.037E+05	1.302E+06	1.2490	0.0715
15.00	1.351E+07	8.060E+05	1.420E+06	1.3491	0.0805
16.00	1.295E+07	8.087E+05	1.542E+06	1.4437	0.0901
17.00	1.236E+07	8.118E+05	1.669E+06	1.5309	0.1006
18.00	1.174E+07	8.153E+05	1.799E+06	1.6089	0.1117
19.00	1.110E+07	8.193E+05	1.932E+06	1.6762	0.1237
20.00	1.045E+07	8.238E+05	2.068E+06	1.7317	0.1365
21.00	9.804E+06	8.290E+05	2.205E+06	1.7748	0.1501
22.00	9.159E+06	8.348E+05	2.344E+06	1.8052	0.1645
23.00	8.526E+06	8.414E+05	2.482E+06	1.8230	0.1799
24.00	7.912E+06	8.489E+05	2.621E+06	1.8286	0.1962
25.00	7.321E+06	8.573E+05	2.758E+06	1.8229	0.2134
26.00	6.759E+06	8.668E+05	2.893E+06	1.8067	0.2317
27.00	6.227E+06	8.775E+05	3.027E+06	1.7812	0.2510
28.00	5.729E+06	8.896E+05	3.157E+06	1.7477	0.2714
29.00	5.265E+06	9.032E+05	3.284E+06	1.7072	0.2929
30.00	4.835E+06	9.184E+05	3.406E+06	1.6611	0.3156

TABLE 6. Continued					
Alpha (deg)	EX (psi)	EY (psi)	GXY (psi)	UXY	UXY
31.00	4.439E+06	9.356E+05	3.524E+06	1.6105	0.3395
32.00	4.076E+06	9.548E+05	3.636E+06	1.5564	0.3646
33.00	3.744E+06	9.764E+05	3.742E+06	1.4998	0.3911
34.00	3.443E+06	1.001E+06	3.842E+06	1.4415	0.4190
35.00	3.169E+06	1.028E+06	3.935E+06	1.3823	0.4483
36.00	2.922E+06	1.058E+06	4.020E+06	1.3227	0.4790
37.00	2.699E+06	1.092E+06	4.098E+06	1.2633	0.5113
38.00	2.498E+06	1.161E+06	4.167E+06	1.2045	0.5452
39.00	2.317E+06	1.173E+06	4.228E+06	1.1487	0.5808
40.00	2.154E+06	1.221E+06	4.280E+06	1.0900	0.6180
41.00	2.008E+06	1.275E+06	4.322E+06	1.0349	0.6570
42.00	1.877E+06	1.335E+06	4.356E+06	0.9813	0.6978
43.00	1.760E+06	1.402E+06	4.380E+06	0.9295	0.7404
44.00	1.655E+06	1.477E+06	4.395E+06	0.8794	0.7849
45.00	1.561E+06	1.561E+06	4.399E+06	0.8312	0.8312

TABLE 7. COMPARISON OF COMPOSITE MODULI CALCULATED AND TESTED				
	Cal	Test	Cal	Test
	±25°	±25°	±35°	±35°
Standard Epoxy				
$E_x 10^6 \text{ psi}$	7.809	7.097	3.598	3.877
$G_{xy} 10^6 \text{ psi}$	2.805	2.856	3.964	4.175
Bi-Modal Epoxy				
$E_x 10^6 \text{ psi}$	7.321	6.814	3.169	3.152
$G_{xy} 10^6 \text{ psi}$	2.758	3.180	3.935	4.178
NOTE: Thornel 300 graphite fibers, with a fiber volume of 50 percent, were used.				

TABLE 8. SANDWICH CORE PROPERTIES			
Property	PVC Foam	PMI Foam	Nomex Honeycomb**
ρ , lb/ft ³	4.0 - 5.0	3.12 - 4.37	3.0
E_c , psi	4500 - 6000	9950 - 14,200	18,500
G_c , psi	3500 - 4500	3550 - 5690	3000
F_{tu} , psi	NA - NA	270 - 412	NA
F_{cu} , psi	140 - 210	128 - 213	330
F_{su} , psi	110 - 140	114 - 184	115
HDT, °F	160* - 160*	383 - 374	400
*Estimated			
**HRH 10/0X-3/16-3.0			

All doors were designed to be nonstructural, and the openings were reinforced by replacing the sandwich-wall core material with a combination of graphite fibers and glass fabric (Figure 22). The forward attachment fittings were designed around a manufacturing process of winding the conical shells that are configured in a mold while in the uncured condition. These configured, wound fittings replaced the sandwich-wall core material locally and were bonded to the inner and outer faces over a large area.

The vertical fin consists of a filament-wound, sandwich-wall spar and a laminated glass fabric trailing airfoil. The spar is designed to carry the major portion of the fin loads and was permanently attached to the aft fuselage. The spar bonds directly to the forward and aft bulkheads, which are bonded to both the inner and the outer faces of the tail boom sandwich wall.

A computer program was developed to calculate the tail boom bending and torsional stiffnesses for sandwich wall configurations. The program was developed by Fiber Science, Inc. (FSI) and is entitled "SECPRO." The program nomenclature is shown in Figure 10, and a typical program run is included as Appendix A.

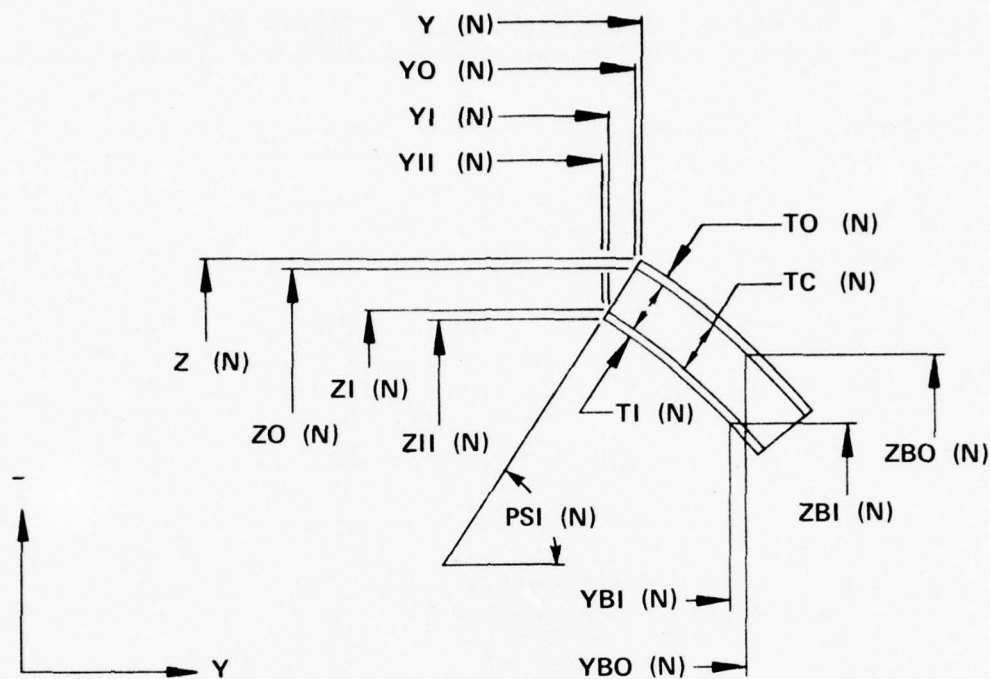


Figure 10. Computer Program "SECPRO" Nomenclature.

SECOND DESIGN CONFIGURATION

The fabrication of the initial tail boom design configuration was unsuccessful, thus a second design configuration was required. The basic fabrication problem was in wet-filament-winding the tail boom skins to a nongeodesic path. The fabrication problems are described in detail under the section on Fabrication.

Redesign of the tail boom skins was completed using combinations of geodesic winding patterns. The new design has nonsymmetrical faces and requires three different winding patterns, whereas the old design had symmetrical inside and outside skins and only one helical winding pattern. Also, the new design eliminates the use of prewound hand-layup, longitudinal fibers and reinforcement in the attachment area. The details of the winding patterns and the method of construction are described in the Attachment Test Tail Boom section.

FINAL DESIGN CONFIGURATION

Fabrication problems still existed with the second design, thus a third design configuration was required. New skin winding patterns were established

for the tail boom and fin spar to meet the stiffness and strength criteria. The final design configuration is described in detail in the Fabrication of the Structural Test Tail Boom section.

The cross-sectional properties of the tail boom were calculated for Boom Stations (BS) 41.32, 59.45, 80.44, 101.38, 105.00, 122.33, 143.28, 164.23, 185.18, 194.43, and 227.00 by the computer and are given in Table 9. Table 10 shows the winding angles, skin thickness, and composite properties for the inner skin, and Table 11 presents similar information for the outer skin.

The fin spar final design configuration was a sandwich-wall construction consisting of Thornel 300 graphite filaments and epoxy resin skins, unidirectional graphite fibers (longos) in the four corners, and a 0.50-inch-thick Nomex honeycomb core. A cross section of the fin spar construction is shown later in the report in Figure 21.

TABLE 9. CALCULATED TAIL BOOM SECTION PROPERTIES

Boom Station	EA 10^6 lb	EIY 10^9 lb-in. ²	EIZ 10^9 lb-in. ²	GK 10^9 lb-in. ²
41.32	70.5	11.92	8.43	3.66
59.45	68.9	10.37	7.19	3.58
59.45	66.8	10.04	6.96	3.49
80.44	61.8	7.78	5.51	3.15
101.38	57.5	6.08	4.31	2.92
105.0	56.9	5.89	4.17	2.89
105.0	51.3	5.24	3.71	1.22
122.33	49.5	4.30	3.05	1.15
143.28	46.1	3.25	2.31	1.07
164.23	42.0	2.33	1.66	0.965
185.18	39.3	1.651	1.185	0.791
194.43	37.7	1.388	0.996	0.724
227.0	29.4	0.602	0.435	0.494

TABLE 10. TAIL BOOM INSIDE SKIN

Boom Station	α_1 (deg)	t_1 (in.)	α_2 (deg)	t_2 (in.)	t_i (in.)	EX^* (10^6 psi)	EY^* (10^6 psi)	GXY^* (10^6 psi)	UXY^*
41.32	17.00	0.0168	90.0	0.0084	0.0252	9.83	6.28	1.26	0.165
59.45	18.20	0.0181	90.0	0.0084	0.0265	9.76	6.01	1.38	0.192
80.44	19.82	0.0198	90.0	0.0084	0.0282	9.67	5.70	1.56	0.231
101.38	21.76	0.0219	90.0	0.0084	0.0303	9.25	5.37	1.79	0.282
105.00	22.14	0.0224	90.0	0.0084	0.0308	9.16	5.31	1.84	0.280
122.33	24.09	0.0246	90.0	0.0084	0.0330	8.73	5.04	2.07	0.348
143.28	27.08	0.0281	90.0	0.0084	0.0365	7.87	4.53	2.44	0.430
164.23	30.00	0.0326	90.0	0.0084	0.0410	6.91	4.25	2.80	0.512
185.18	30.0	0.0375	90.0	0.0084	0.0459	6.95	3.90	2.86	0.562
194.18	30.0	0.0402	90.0	0.0084	0.0486	6.96	3.73	2.89	0.588
227.00	30.0	0.0536	90.0	0.0084	0.0620	6.93	3.12	3.00	0.700

*Calculated by computer program - Reference 7

TABLE 11. TAIL BOOM OUTSIDE SKIN

Boom Station	α_1 (deg)	t_1 (in.)	α_2 (deg)	t_2 (in.)	α_3 (deg)	t_3 (in.)	t_o (in.)	EX* (10^6 psi)	EY* (10^6 psi)	GXY* (10^6 psi)	UXY*
41.32	35.0	0.0168	12.00	0.0168	90.00	0.0168	0.0504	7.96	6.62	1.82	0.233
59.45	37.66	0.0185	12.80	0.0180	90.00	0.0168	0.0533	7.67	6.46	1.97	0.258
59.45	37.66	0.0185	12.80	0.0180	90.00	0.0084	0.0449	8.63	4.46	2.27	0.420
80.44	41.38	0.0211	13.86	0.0195	90.00	0.0084	0.0490	7.93	4.50	2.45	0.445
101.38	46.03	0.0249	15.12	0.0214	90.00	0.0084	0.0547	7.13	4.72	2.63	0.445
105.00	46.97	0.0257	15.37	0.0217	90.00	0.0084	0.0558	6.99	4.75	2.66	0.442
105.00			15.37	0.0217	90.00	0.0084	0.0301	11.02	5.40	1.14	0.179
122.33			16.64	0.0236	90.00	0.0084	0.0320	10.82	5.12	1.31	0.212
143.28			18.50	0.0264	90.00	0.0084	0.0348	10.58	4.78	1.52	0.267
164.23			20.84	0.0301	90.00	0.0084	0.0385	10.11	4.40	1.80	0.345
185.18			23.88	0.0350	90.00	0.0084	0.0434	9.25	4.01	2.18	0.562
194.43			25.54	0.0378	90.00	0.0084	0.0462	8.68	3.83	2.39	0.588
227.00			33.97	0.0532	90.00	0.0084	0.0616	5.40	3.21	3.37	0.700

*Calculated by computer program - Reference 7

The following components remain essentially unchanged from the original design concept:

1. Forward attachment fittings
2. Access holes and stabilizer support area reinforcements
3. Doors
4. Frames and bulkheads
5. Vertical fin aft airfoil section
6. Attachment of fin spar to tail boom with forward and aft cant bulkheads

STRESS ANALYSIS

The tail boom sandwich-wall construction was analyzed for combined bending and shear loading. The allowable compression and shear stresses were essentially equal — the shear stress was approximately 20 percent of the compression stress. The interaction formula for a panel loaded in compression and shear was $R_c + R_s^2 = 1$. Therefore, the sandwich compression stress resulting from the boom bending moments was the critical design parameter. The tail boom outer skin ultimate compression stresses and allowable compression stresses are plotted versus boom stations in Figure 11; the inner skin ultimate compression stresses and allowable stresses are plotted versus the boom stations in Figure 12. The minimum margin of safety is at BS 122 and is 0.29 (see page 29).

A computer program (Reference 7) was developed to determine the allowable compression and shear buckling stresses for various combinations of skins and cores. The computer program was based on the equations given in Reference 4. Figure 13 shows the notations for a sandwich composite.

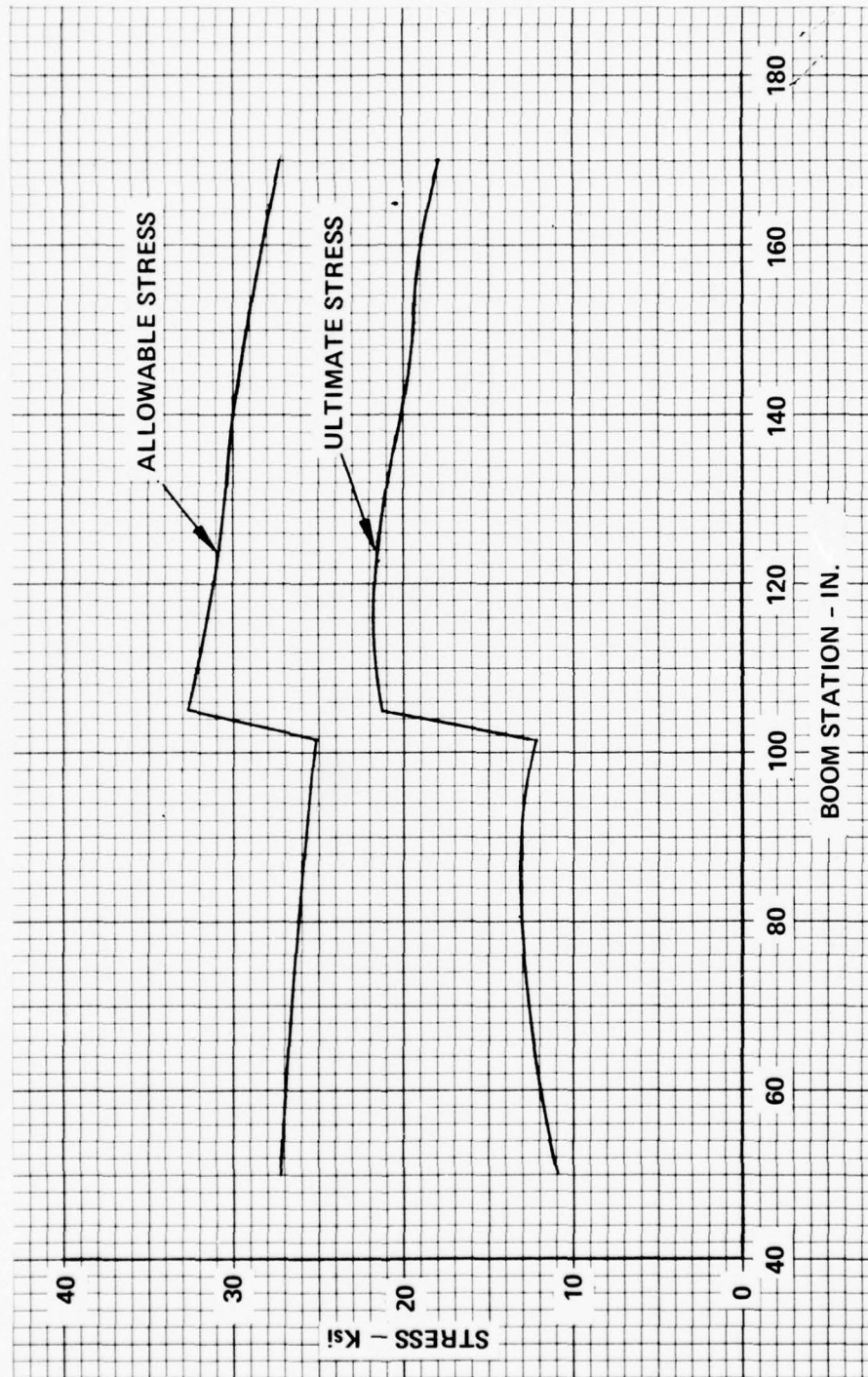


Figure 11. Comparison of Ultimate Compressive Stress to Allowable Stress - Outer Skin.

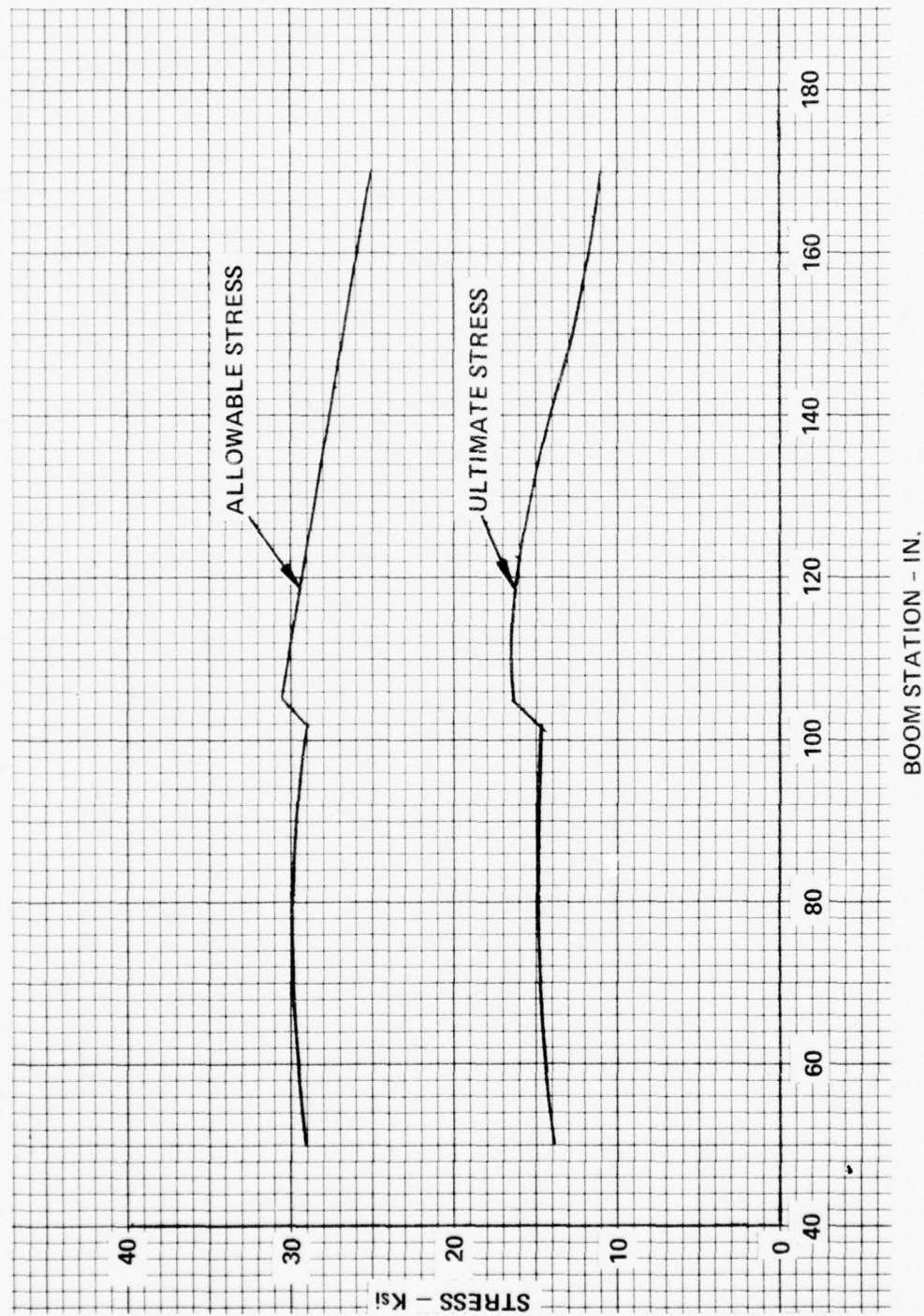


Figure 12. Comparison of Ultimate Compressive Stress to Allowable Stress - Inner Skin.

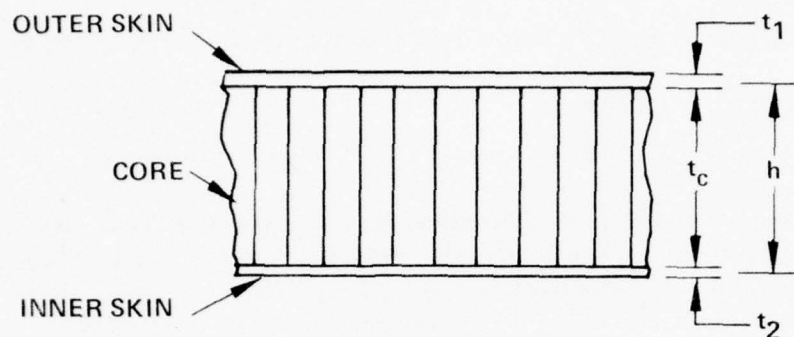


Figure 13. Notations for Sandwich Composite.

The computer input data for Boom Station 122.33 is (refer to Tables 9, 10, 11, A-1 and A-2; for Tables 9 and 10, $t_1 = t_o$ and $t_2 = t_i$)

Outer Skin - Thornel 300 Graphite/Epoxy

$t_1 = 0.0320$	$GXY = 1.31 \text{ E}+06$
$EX_1 = 10.82 \text{ E}+06$	$UXY = 0.212$
$EY_1 = 5.12 \text{ E}+06$	$UYX = 0.100$

Inner Skin - Thornel 300 Graphite/Epoxy

$t_2 = 0.0330$	$GXY = 2.07 \text{ E}+06$
$EX_2 = 8.73 \text{ E}+06$	$UXY = 0.348$
$EY_2 = 5.04 \text{ E}+06$	$UYX = 0.200$

Core - Nomex Honeycomb (HRH 10/OX-3/16 - 3.0)

$$t_c = 0.625$$

$$GC = 3000$$

Estimated panel size is 18 inches by 44 inches.

The resulting allowable compression and shear buckling strengths are:

$$F_{c1} = 31100 \text{ psi}$$

$$F_{s1} = 29500 \text{ psi}$$

$$F_{c2} = 29200 \text{ psi}$$

$$F_{s2} = 27700 \text{ psi}$$

The critical loading condition is Condition V, +15 degrees Yaw, Recovery (Condition A). The limit shear loads and moments at BS 122.33 that produce the critical element stress are:

$$M_x = 111,916 + 2957 (12.97 - .245 + 63.09 - 67.5) = 137,000 \text{ in. -lb}$$

$$M_z = 386,743 \text{ in. -lb}$$

$$S_z = P_z = 1136 \text{ lb}$$

The resulting stresses for the outerskin at $Z = 0$ are:

$$f_{c1} = \frac{(M_z)(Y_o)(EX_1)}{(EIZ)} = \frac{386743 \times 10.415 \times 10.82 \times 10^6}{3.047 \times 10^9}$$
$$= 14303 \text{ psi}$$

$$f_{s1} = \frac{(M_x)(GKO)}{2(AOC)(GK)t_1} + \frac{P_z(EIZO)}{2(Z_1)(EIZ)t_1}$$
$$= \frac{137000(0.486 \times 10^9)}{2(481)(1.153 \times 10^9)0.032} + \frac{1136(1.795 \times 10^9)}{2(25.95)(3.047 \times 10^9)0.032}$$
$$= 2280 \text{ psi}$$

The computation for the ultimate margin of safety is:

$$R_c = \frac{f_{c1}}{F_{c1}} = \frac{14303 \times 1.5}{31100} = 0.690$$

$$R_s = \frac{f_{sl}}{F_{sl}} = \frac{2280 \times 1.5}{29500} = 0.116$$

$$MS = \frac{2}{R_c + \sqrt{R_c^2 + 4R_s^2}} - 1 = \underline{\underline{0.29}}$$

and, similarly, for the inner skin,

$$f_{c2} = 10804 \text{ psi limit}$$

$$f_{s2} = 3080 \text{ psi limit}$$

$$R_c = \frac{10804 \times 1.5}{29200} = 0.555$$

$$R_s = \frac{3080 \times 1.5}{27700} = 0.167$$

$$MS = \frac{2}{0.555 + \sqrt{0.555^2 + 4(0.167)^2}} - 1 = \underline{\underline{0.46}}$$

ORIGINAL FABRICATION METHODOLOGY

FILAMENT WINDING

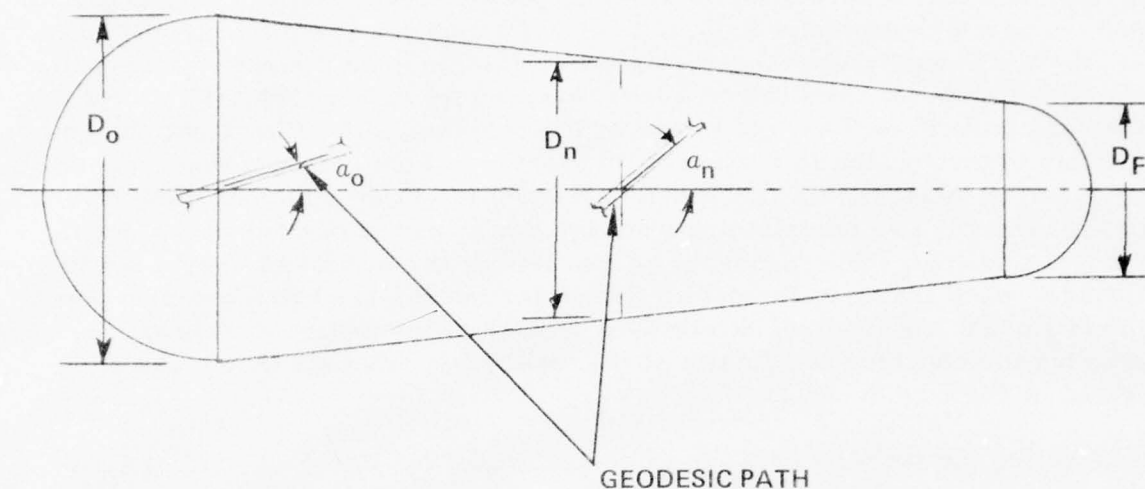
The tail boom and fin spar were designed as a sandwich-wall construction with the faces filament wound. The classical helical winders were used. Helical winders basically wind a helical pattern along a cylindrical mandrel. The machines look like a lathe with a traversing carriage, upon which is mounted a pay-off head that can dispense roving strands in the form of a band of filaments. The rovings are supplied from spools, tensioned evenly, and saturated with a resin from a small bath. They are fed onto the mandrel, which rotates in a positive relationship to the traversing speed of the carriage.

The AH-1G tail boom tapers from the forward attachment to the fin area, requiring the winding mandrel to be conical shaped. To filament wind on a conical shaped mandrel, basically requires the helical path of the filament band to be geodesic. The geodesic path is the shortest helical path from the large end to the small end of the mandrel and, even if friction were zero, the band would not slip under tension loads. The geodesic path requires the helix angle to increase as you progress from the mandrel's large end to the small end (see Figure 14). The change in helix angle affects both the stiffness and the strength properties of the composite, and the properties reduce as the helix angle increases. Winding on a geodesic path would reduce the ability to optimize the tail boom skins.

Scale models representing the mandrel configuration of the tail boom were constructed to determine the amount of deviation from the geodesic path that could be accomplished without incurring slippage of the filaments. It was determined by the tests that a winding pattern with a constant or negative helix angle up to 1 degree per 8 inches of length would not slip.

INITIAL BOOM FABRICATION CONCEPT

Both the inner and outer skins of the initial boom skin fabrication had the same winding patterns, and were made of Thornel 300 graphite filaments, with FSCS-118 ET epoxy resin. The skin winding patterns deviated from the geodesic path and consisted of one helical layer, with the helix (wrap) angle being ± 35 degrees at the forward end (BS 41.32) and reducing to ± 25 degrees at BS 121.32 and remaining constant to the end of the boom. A ply of uni-directional (0 degree) fibers was added to meet overall stiffness and strength requirements; also, in selected areas, hoop (90-degree) fibers were included.



BASIC EQUATION
$$a_n = \sin^{-1} \left[\left(\frac{D_o}{D_n} \right) \sin a_o \right]$$

Figure 14. Geodesic Path.

The core thickness was established at 0.625 inch thick. Initially, PVC (Rigicell 400) was selected for the foam core. Due to a material shortage in the plastic industry, the PVC foam received was poor in quality and exceeded the density requirements by approximately 35 percent. Studies were made of various structural foams, and PMI (Rohacell type 51) was selected to replace the PVC foam. The main advantage was the PMI density of 3.12 pounds per cubic foot versus 4.0 for the PVC foam. The other advantage was the critical elevated temperature of 383° F for the PMI versus 180° F for the PVC.

The fabrication sequence was to wind the outer skin and place in a female mold configured to the outside contour of the AH-1G tail boom. The skin was pressurized by drawing a vacuum between an inner vacuum bag and the mold. The skin was cured at an elevated temperature and remained in the mold. The sandwich foam core and forward attachment fittings were then positioned against the outer skin. The inner skin was wound using the same winding patterns as the outer skin. While still wet (uncured), the inner skin was inserted into the tail boom mold and positioned against the foam core and fittings. The inner skin was pressurized with a vacuum and cured at the same temperature as the outer skin.

The fabrication concept for the four forward attachment fittings consisted of an aluminum alloy metal insert that becomes a short section of the mandrel end, over which is wound S-glass fibers and epoxy. The metal insert has a short "bottle top" shape -- a necked-down section near the end. During the winding operation, the band of fibers is wound down into this neck each time the band traverses from end to end of the mandrel. The fibers buildup and overlap in this region in a manner that forms a thick ring end that completely entraps the metal insert and provides a mechanical attachment of the fibers to the insert. Two complete end fittings are wound at one time on a double conical mandrel. The mandrel is separated at the middle to create the two fittings; each fitting is formed to fit and fare to the sandwich construction of the tail boom and is cured at elevated temperatures under pressure. Sketches showing the construction details of the forward attachment fitting are illustrated in Figures 15 and 16.

Connecting the vertical fin spar to the tail boom consisted of bonding both the forward and the aft surfaces of the spar to the full canted boom bulkheads (see Figure 17). The bulkheads located fore and aft of the fin spar are a precured composite (glass fabric/epoxy) and are molded to fit the inside contour of the boom. The fabrication sequence is to install the forward cant bulkhead from the front end of the boom and bond it to the inner skin of the boom. The forward face of the fin spar is then bonded to the bulkhead with the aid of cleco clamping fasteners. Precured glass fabric/epoxy angles are then used to tie the sides of spar to the inside of the boom. The aft (two piece) canted bulkhead is then installed from the aft end of the boom and bonded to the aft face of the spar and the inner skin of the boom.

INITIAL FABRICATION PROBLEMS

The first structure fabricated was the outer tail boom skin. The skin was over the design weight by approximately 30 percent due to an added ply of 113 fabric applied over its surface and its resin rich condition. Nonuniform coverage was noticeable because of roving slippage, and some skin wrinkling occurred near the forward end that was caused by too large a skin perimeter. A void at the top, near the aft end, occurred due to an uncut hoop ply which limited the helical layer from stretching. The outside surface of the part was very smooth and the overall condition was considered to be adequate for the attachment test tail boom since the primary test was for the forward attach fittings and fin spar/boom attachment.

The material selected for the sandwich core was PMI foam. The fabrication sequence was to heat form the foam to the tail boom shape and bond it to the previously cured outer skin. PMI foam proved to be difficult to form to the tail boom contour, particularly in the corner areas. A compromise approach was taken by using PMI foam in the more flat areas and Nomex honeycomb in the tight corners.

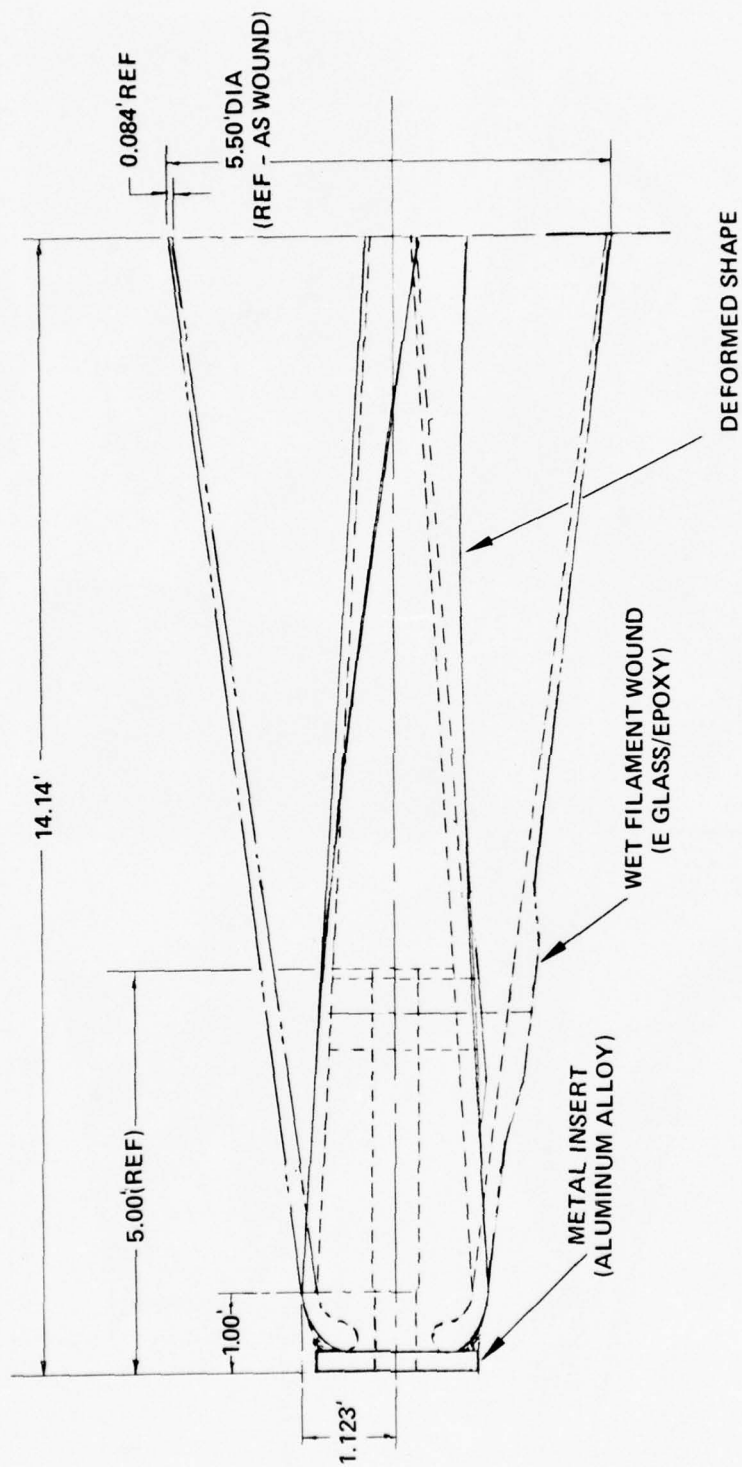


Figure 15. Forward Attachment Fitting.

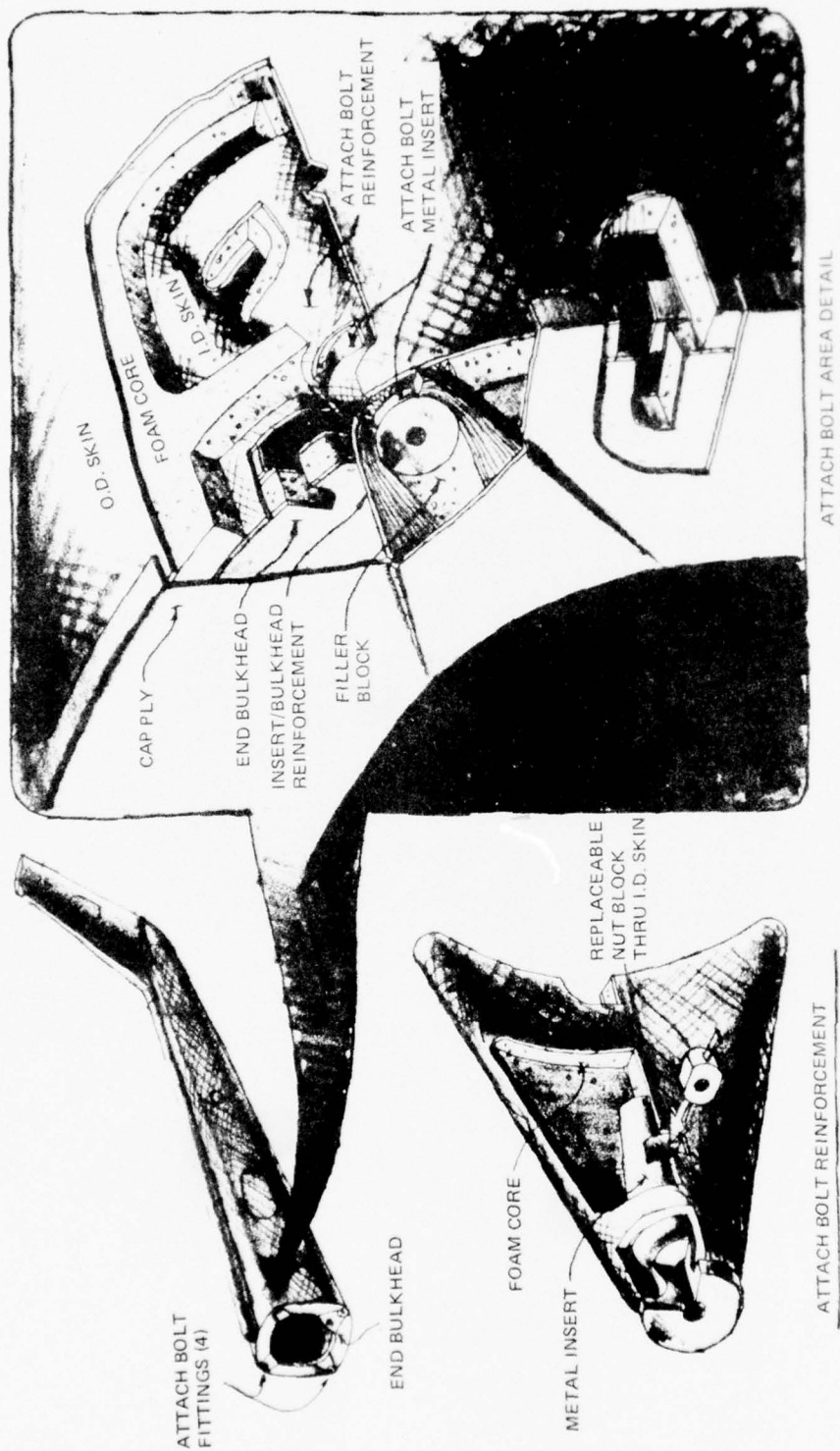


Figure 16. Composite Tail Boom Forward Attachment Assembly.

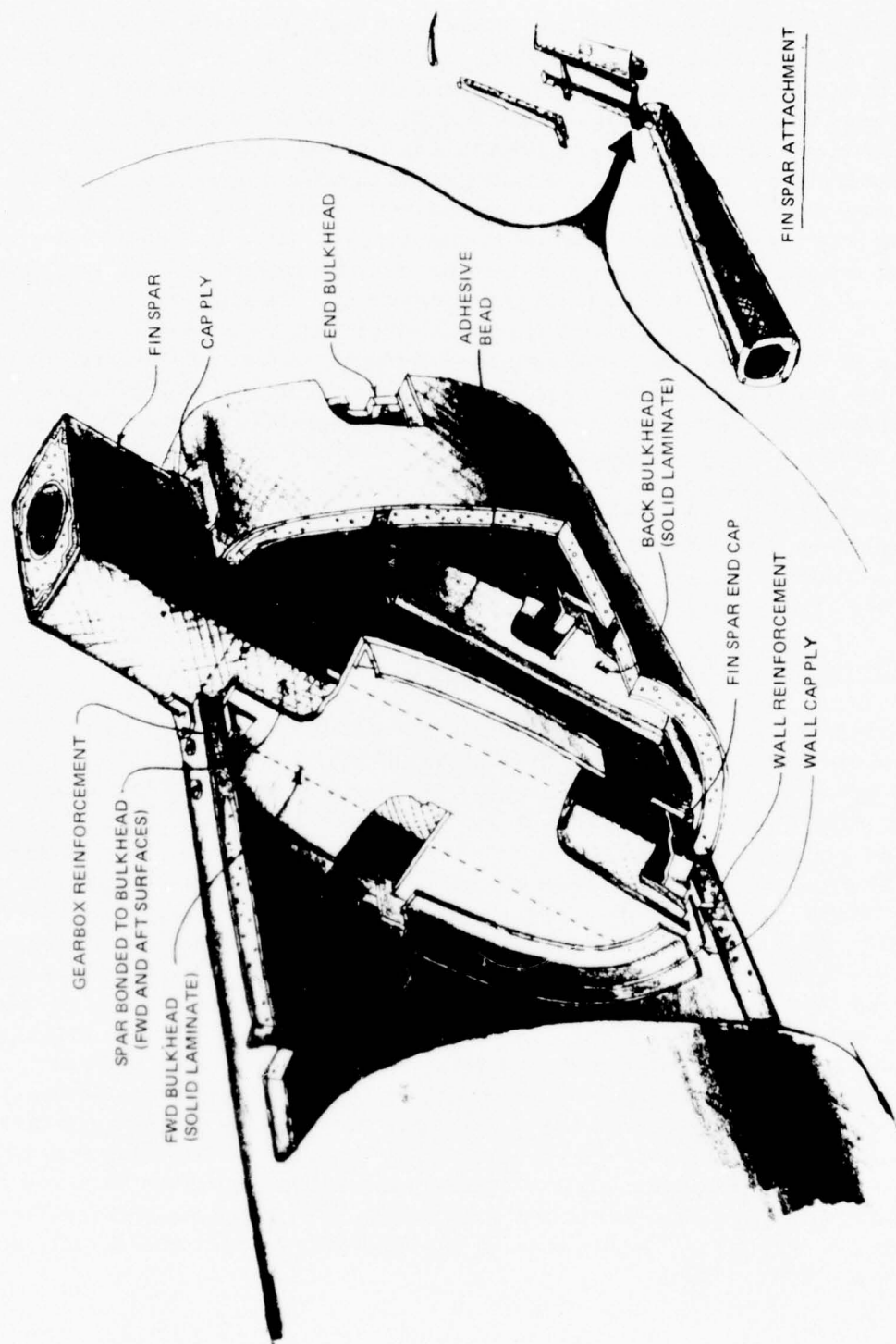


Figure 17. Composite Tail Boom Fin Spar to Boom Assembly.

The tail boom skins were redesigned because of the fabrication problems that existed in fabricating the outer skin. The details of the redesign were described in the Second Design Configuration section. The inner skin was filament wound to the new configuration without fabrication problems. The tail boom fabrication sequence was then to remove the skin intact from the winding mandrel and insert it in the boom mold against the sandwich core. Difficulty was experienced in positioning the skin against the core. A vacuum bag was then installed against the inner skin and attached at the ends to the boom mold. A partial vacuum was produced between the bag and mold which pressed the inner skin against the honeycomb. During the curing operation, the vacuum was lost allowing the inner skin to separate from the sandwich core, creating unbonded areas. However, it was decided to continue with the installation of the forward attachment fittings, the fin spar, and the bulkheads to determine if additional manufacturing problems existed. The fin spar was a dummy spar fabricated from polyurethane foam strengthened with an epoxy gel coat. The fabrication concepts for installing the forward fittings and fin spar were successful, with only minor problems existing due mainly to the irregular surface of the inner skin. The complete tail boom was moved to Hughes Helicopters facility and used to assure its compatibility with the structure test fixture.

INITIAL FIN SPAR FABRICATION CONCEPT

The initial spar configuration selected for fabrication has an approximate trapezoidal cross section. The skin consists of three wraps of ± 30 -degree orientated graphite fibers (Thornel 300), with the thickness varying from 0.054 inch thick at Fin Station 70 to 0.065 inch thick at Fin Station 5.08. Four corner angles composed of unidirectional graphite fibers were added to meet overall strength and stiffness requirements. The corner graphite thickness varies from 0.016 inch thick at Fin Station 5.06 to 0.134 inch thick at Fin Station 70. The skin with added corner fibers was cured in a female mold at elevated temperature and pressure. A rigid foam (polystyrene) and an inner tube of S-glass fibers were added to the inside of the skin to create a sandwich construction; the fibers were ± 45 degrees and 0.010 inch thick. The purpose of the foam and inner tube was to stabilize the spar skin and corner angles for compression and shear loads, thereby obtaining the maximum strength of the graphite fibers. The spar was then to be wrapped circumferentially with one ply of glass fiber. The purpose of the wrap was to prevent peeling of the corner unidirectional graphite fibers and to improve the bonding to the fin skins and tail boom bulkheads. The fin spar construction is illustrated in Figure 18; also shown in the figure are additional details of the tail boom construction.

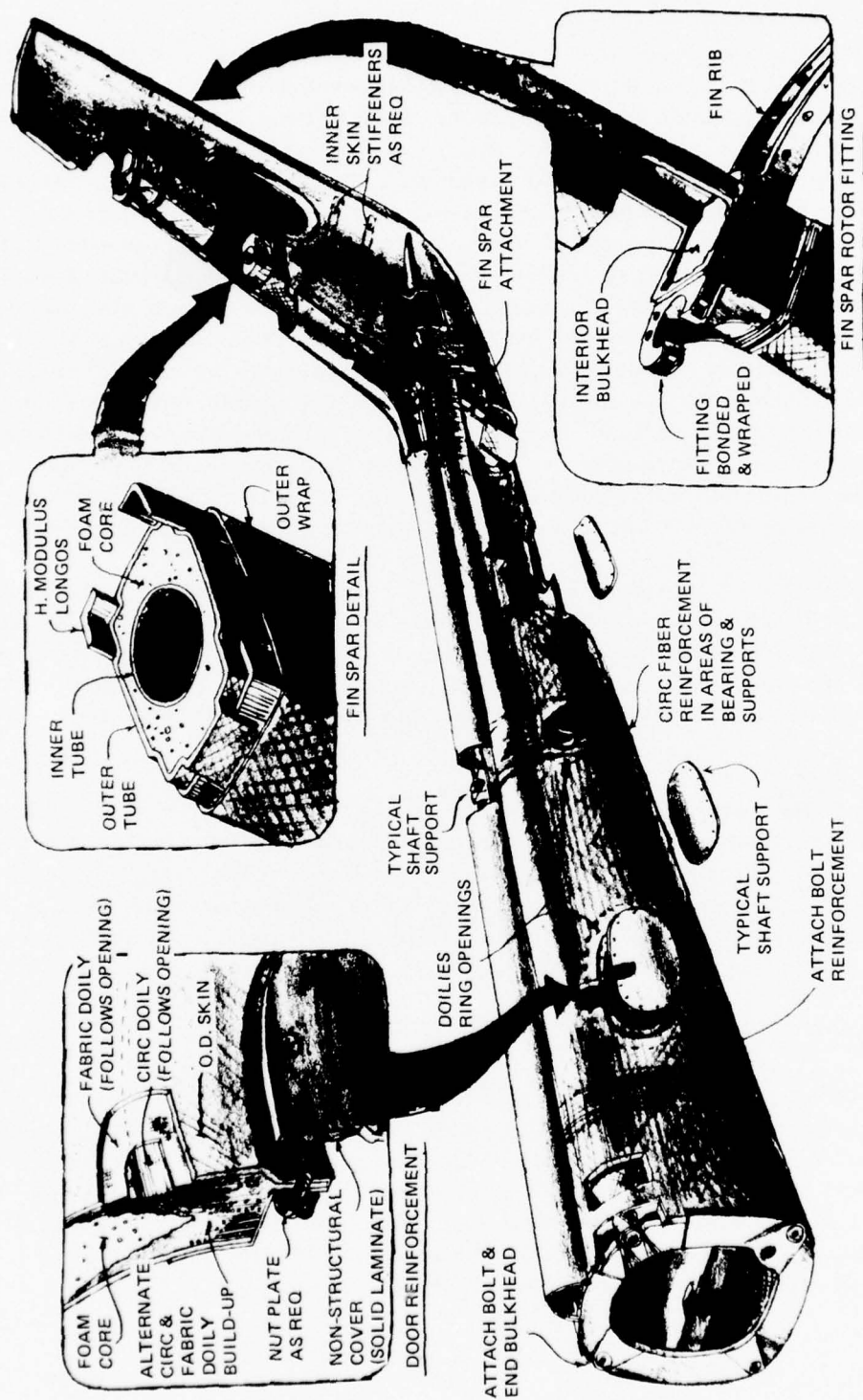


Figure 18. Composite Tail Boom Assembly.

INITIAL FABRICATION REVIEW

The first graphite outside skin was wound and cured using vacuum pressure. The unidirectional doubler was wound on a 5-foot-diameter drum; and while it was still in the uncured (wet) condition, it was transferred to the outside skin winding mandrel. Both ends of the unidirectional material were tied with hoop winds. The basic helical layer was then wound over the entire mandrel. Difficulty was experienced in winding the graphite bands on non-geodesic helical path. Slippage of helical winding occurred at approximately the mid-length of the mandrel at the start of the ± 25 -degree winding angle. Slippage of the hoop wind and the unidirectional doublers were also experienced; however, to a much lesser degree. Since there was no reason to maintain that tail boom, it was decided to static test the boom to failure by the method described in Appendix B. Even with the gross structural defects, including skin wrinkles and overlaps and large unbonded areas of skin to core, the tail boom sustained maximum design limit load and went to 7 percent over the limit load when failure occurred. The structural potential of the basic design approach using advanced composites was established.

The fin-spar skin was filament wound to the required ± 30 -degree helix with no problems. It was then placed in a female mold to the proper cross section and cured. When the skin was removed from the mold, a wrinkle was found on the left-hand surface, extending almost the full length of the spar. It was decided to repair it with fiberglass fabric and continue with the spar fabrication.

Polystyrene foam was originally selected to stabilize the spar skins. The fabrication sequence was to pour expandable beads of styrene between the skin and the inner S-glass tube. The result of the foaming experiment was unsatisfactory. Polyurethane foam was selected as a substitute with a stage foaming process being employed. Fabrication problems still existed as the foam varied in density and was generally overweight.

ATTACHMENT TEST TAIL BOOM

The tail boom skins were redesigned using combinations of geodesic winding patterns because of the band slippage problems encountered in fabricating the initial boom skin. The revised design includes nonsymmetrical sandwich faces and three different winding patterns. The previous concept had symmetrical inside and outside skins with only one helical winding pattern. Also, the revised design eliminated the use of prewound, hand lay-up, longitudinal fibers and added reinforcement in the forward attachment area.

The fabrication sequence for the attachment test tail boom is outlined below:

Outer Skin: The design of the outer skin of the second boom consisted of one helical layer $\pm 7\text{-}1/2$ degrees at Station 41.32, geodesic path, full length; one helical layer ± 45 degrees at Station 41.32 with geodesic path to Station 76.0, one circumferential ply, full length; and one extra circumferential ply from Station 41.32 to 59.45 and from Station 57.0 to 67.0.

The material was Thornel 300 graphite rovings impregnated with APCO 2434/2374 Epoxy resin. The skin was placed in the tail boom female mold and cured in the same manner as the initial boom outer skin.

Core: HRH 10/OX-3/16 - 3.0 (Nomex Honeycomb) was used as the core material throughout the entire boom structure. Bonding of the honeycomb core to the outer skin was easier than foam because of its flexibility, and eliminated the attachment of foam to honeycomb. The honeycomb panel was trimmed to the size of the flat pattern and bonded together to form a cone with 3M 2216 structural adhesive. A room temperature set resin system - APCO 2434/2340 mixed with Cab-O-Sil (thickening agent) - was applied to the inside of the outer skin by a paint roller. The honeycomb core was coiled up around a metal pipe and inserted into the outer skin. The honeycomb core was then uncoiled and positioned inside the outer skin. A vacuum bag was used to pressurize the honeycomb against the outer skin in the female mold. The assembly was cured at room temperature for 6 hours and at 200° F for 4 hours. The installation of the honeycomb core was very successful.

Inner Skin: The design of the inner skin of the second boom consisted of one helical layer ± 18 degrees at Station 41.32, geodesic path, full length, and one circumferential ply from Station 41.32 to 59.45 and from Station 47.0 to 61.0. The material was Thornel 300 graphite roving impregnated with APCO 2434/2347 resin. The inner skin, with its associated bleeder plies, vacuum bag, ASB bladder, etc., was inserted into the tail boom approximately three-fourths of its full length, in a horizontal position. The assembly was then raised vertically. The inner skin was slipped into position while a vibration force was applied to the boom female mold. The assembly was cured for 4 hours at 130° F, 2 hours at 180° F, and 2 hours at 200° F.

FABRICATION REVIEW

The attachment test tail boom was fabricated as previously described. A detailed inspection was performed on the completed tail boom. Two structural deficiencies were observed.

1. The skins bridged in the corners, resulting in unbonded areas between the skins and the honeycomb core.
2. The graphite filament rovings did not compress sufficiently to form a uniform bandwidth in the area where the helix (wrap) angle was less than 10 degrees. This resulted in gaps between adjacent bands.

The fabrication technique of wet filament winding the skin onto a cylindrical or conical mandrel and then inserting it into a female mold to be deformed and cured to the required contour will result in one of the following conditions:

- Bridging and free forming of the corners if the filament-wound perimeter is too small.

or

- Wrinkling or overlapping of the skin if the perimeter is too large.

It is undesirable structurally for skin wrinkles to exist. The wrinkles will cause a loss of strength and stiffness in the composite material. The bridging in the corners will not affect the structural properties of the composite. The bridged corners will not have the glossy mold finish produced where the composite contact the mold, but will have an acceptably smooth surface. The deviation from the mold contour can be maintained to an acceptable limit.

Wet filament winding consists of several rovings, wetted with resin, that wind onto the mandrel at the same time. A tension force is applied to the rovings as they wind on the mandrel. It is necessary that the mandrel exert a force against the rovings to spread the rovings to form an even band of filaments. The smaller the helix angle, the lower the force that is exerted by the mandrel against the rovings. For the tail boom skins, it was determined that the helix angle was required to be equal to or greater than 10 degrees.

FINAL BOOM FABRICATION

NEW FABRICATION CONCEPT

A new sandwich fabrication concept was developed that consisted of wet filament winding the inner skin, adding the honeycomb core, and wet filament winding the outer skin. This concept had two possible problems:

1. Wet filament winding over an open honeycomb core could possibly cause the honeycomb cells to fill with excess resin.
2. Transferring the wet-wound, conical shaped, sandwich structure to the female mold for shaping and curing to a final contour could cause a handling problem.

Fiber Science, Inc., was in production of a water tank constructed of sandwich walls for the commercial airlines. The water tanks were constructed of glass filament wound skins and PVC foam core.

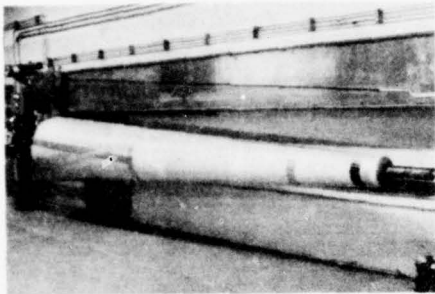
To test out the new fabrication concept and hopefully solve the immediate problems, a water tank was constructed using the same glass filament wound skins but using Nomex honeycomb core. The ends of the tank were removed and the center section was placed in the tail boom female mold in the area of the mold where the perimeter of the tank most closely fit the perimeter of the boom contour.

The result of the new fabrication concept was very successful and better than anticipated. The skins were smooth and uniformly bonded to the honeycomb core with a smooth filet of resin. There were no honeycomb cells filled or even partially filled with resin. The corners, where the tank structure did not fit the mold, free formed to produce a smooth, structurally acceptable sandwich structure.

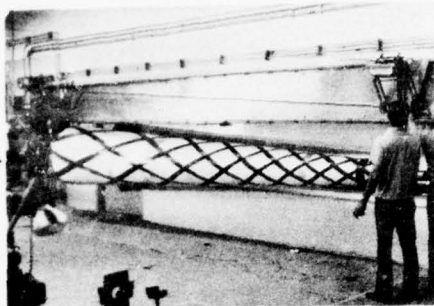
FABRICATION OF THE STRUCTURAL TEST TAIL BOOM

The technique for fabricating the structural test tail boom is dramatically changed from the initial fabrication concepts and is outlined below and shown pictorially in Figures 19 and 20.

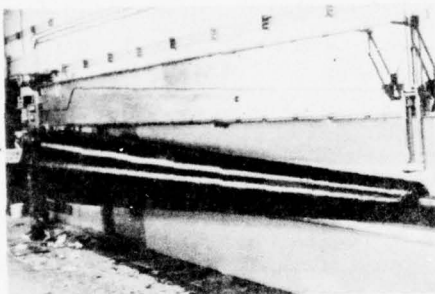
1. The inside skin was wet-filament-wound over the conical mandrel. The mandrel was stiffened to provide better tolerance control.
2. The 0.625-inch-thick Nomex honeycomb core was then formed over the outside surface of the inside skin. The core was bonded on the edges with Hardman epoxy adhesive so that it could not move.



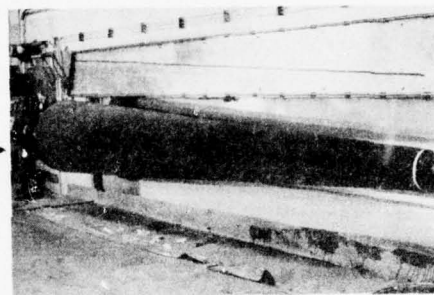
MANDREL



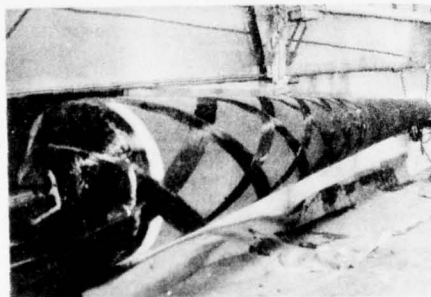
WINDING INNER SKIN



NOMEX (.625 IN.)



WINDING OUTSIDE SKIN



FINAL OUTSIDE SKIN

**READY TO BE FORMED
IN MOLD AND CURED**



Figure 19. Manufacturing Process for the Composite Tail Boom.

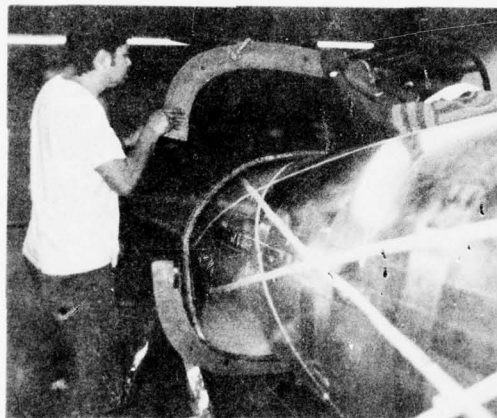
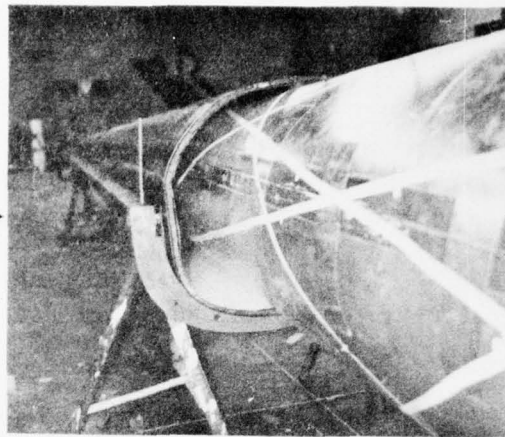
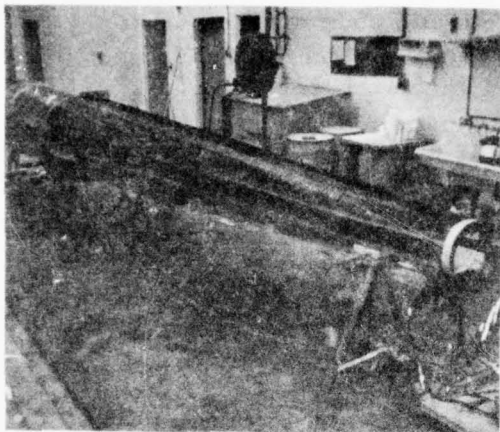


Figure 20. Forming in the Mold.

3. The outside skin was wet-filament-wound over the Nomex honeycomb core to obtain the outer skin windings and thickness and to complete the sandwich construction of the tail boom.
4. The end domes were removed and the entire assembly was placed in the master female mold. The inner mandrel was moved only the amount necessary to close the mold.
5. The inner skin, core, and outer skin were then vacuum bagged to the female mold as a unit, pressurized, and cured at an elevated temperature.

The inner and outer skin construction configurations were redesigned and are summarized below. The sandwich material remains the same - Thornel 300 graphite filaments with APCO 2434/2347 epoxy resin and HRH 10/OX-3/16-3.0 Nomex honeycomb, 0.625 inch thick.

Inner Skin

1. The filament winding angle begins with a winding angle of ± 17 degrees at Boom Station (BS) 41.32, continues in a geodesic path to BS 159, and then continues at a constant winding angle of ± 30 degrees to the end.
2. One complete circumferential ply for the full length of the boom.

Outer Skin

1. The first layer begins with a winding angle of ± 35 degrees at BS 41.32 with a geodesic path that terminates at BS 156 with a 1-inch scalloped edge.
2. The second layer starts with a winding angle of ± 12 degrees at BS 41.32 with a geodesic path throughout the full length of the boom.
3. The outer skin is finished with one complete circumferential ply for the full length of the boom.

The structural test tail boom consisted of the tail boom structure with the fin spar installed, reinforced access holes, and the following loading structure:

1. Tail rotor gearbox mounting bracket at Fin Station 5.08.
2. A simulated structural loading point at approximately the mid-section of the fin spar.

3. Fin spar to boom attachment structure.
4. Tail rotor drive angle gearbox support structure.
5. Tail skid support structure.
6. Elevator support structure.

FABRICATION OF THE FIN SPAR

The fin-spar construction was redesigned after the fabricating procedure for the tail boom proved to be successful. The redesign was a sandwich construction consisting of Thornel 300 graphite filaments and epoxy resin skins, unidirectional graphite fibers added in the four corners, and a 0.50-inch-thick Nomex honeycomb core. The inner skin consisted of one layer of material with the winding angle ± 45 degrees and one circumferential ply. The outer skin consisted of two layers of material with the winding angle ± 45 degrees and one circumferential ply. Refer to Figure 21.

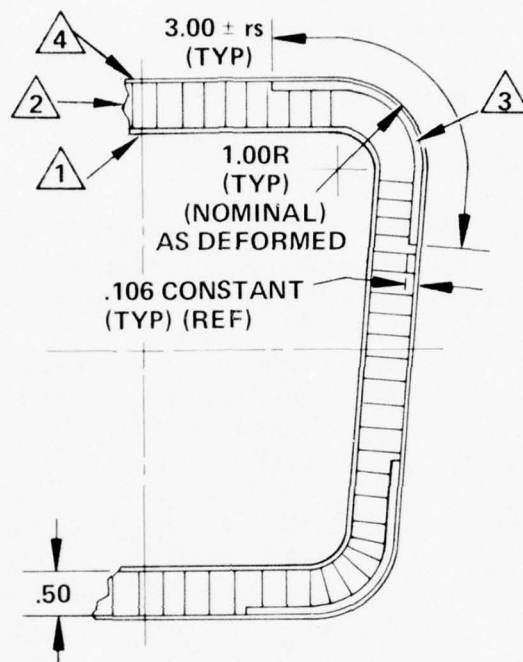
The method of fabrication was to wind the inner skin and form the Nomex honeycomb core over the outside of the inner skin; place four corner longos in the grooves that were previously cut in the honeycomb core; and then wind the outer skin over the honeycomb. The wound assembly, including the mandrel, was deformed in the spar mold. Tacks were placed over each end of the longos before winding the outer skin. The tacks were used as an alignment index to position the assembly in the spar mold. The inside of the mandrel was pressurized to 30 psi and cured at elevated temperature.

FABRICATION OF THE TAIL BOOM

Forward Bulkhead

The forward bulkhead is a sandwich construction using 3/16-inch-thick PVC foam as the core, and 181 fiberglass fabric as the skin faces. Additional cap plies of 143 fiberglass are added to form the inner bulkhead cap.

The forward bulkhead is trimmed to fit the inner skin mold line and metal inserts of the attachment fittings. Aluminum plates are added at each attachment fitting to distribute shear loads to the bulkhead. The bulkhead is bonded to the tail boom inner and outer skins with plies of 181 fiberglass and APCO 2450/2340 adhesive.



NOTES:

- ① Inner skin consists of one helical layer at $\alpha = \pm 45^\circ$ and one circumferential ply.
- ② Core is Nomex honeycomb (HRH 10/0X-3/16-3.0)
- ③ Corner angles are unidirectional graphite fibers. (longos)
- ④ Outer skin consists of two helical layers at $\alpha = \pm 45^\circ$ and one circumferential ply.
- ⑤ Skins and longo material is Thornel 300 graphite and epoxy resin. Fiber volume is 50 percent.

Figure 21. Final Fin Spar Configuration.

Door & Stabilizer Reinforcement

The door and stabilizer reinforcements consist of continuously hoop-winding Thornel 300 graphite rovings on a mandrel shaped to fit the opening of the door of the stabilizer and are called doilies. This construction results in a continuous graphite ring or frame that reinforces the cutout in the boom sandwich wall. See Figure 22.

The method of assembling the doilies consists of trimming back the inner skin and honeycomb to accept the doilies. Two doilies are fabricated for each opening and are installed with three plies of 181 fiberglass between the doilies. The overall thickness of the doilies and 181 fiberglass is equal to the thickness of the Nomex honeycomb core plus the inner skin. The honeycomb around the cutout is cleaned and filled with a syntactic foam consisting of a thixotropic mixture of APCO 2434/2340/glass microballoons to provide uniform transition from the doilies to the honeycomb. Three plies of 181 fiberglass are added that cover the doilies and extend over the inner and outer boom skins. The opening reinforcement is vacuum bagged and allowed to gel at room temperature.

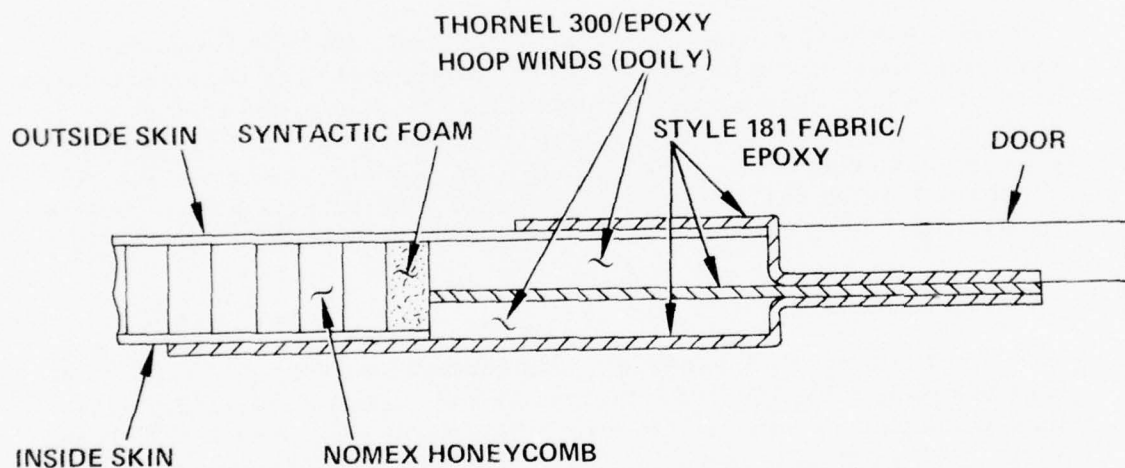


Figure 22. Typical Reinforcement Doily.

Fin Spar to Boom Attachment

The fin spar to boom attachment remains essentially the same as previously described. The spar extends from the lower inner skin of the boom through the upper boom sandwich structure. The spar is sandwiched between and bonded to two boom cant bulkheads. The

boom sandwich structure is reinforced with graphite doilies, similar to the door cutouts, in the area where it is pierced by the spar. There were only minor manufacturing changes from the initial fabrication concept. See Figure 16.

Gearbox Attachment Structures

The tail rotor gearbox mounting bracket is composed of four pieces, which are described below and shown in Figure 23.

- a. 10-ply 181 fiberglass fabric shoe
- b. 10-ply 181 fiberglass fabric web
- c. 6-ply 181 fiberglass fabric angle
- d. 7/8-inch-thick Aluminum plate.

The upper end of the fin spar (FS 5.08) is trimmed where necessary to accept the mounting bracket components. The shoe, web, angle and plate are bonded together and to the fin spar structure with APCO 2450/2340/Cab-O-Sil thixotropic adhesive. An aligning fixture is used to assure proper positioning of the gearbox mounting bracket.

The tail rotor drive angle gearbox is mounted with four 1/4-inch-diameter bolts on the upper boom structure forward of the intersection of the fin spar. The basic boom structure is reinforced inside the boom by adding partial bulkheads at the forward and aft ends of the gearbox mounting area. The outside skin is reinforced by adding a 0.060-inch-thick 6061-T6 aluminum plate, and the honeycomb core is locally filled with synthetic foam in the area surrounding each bolt.

Vertical Fin Aft Structure

The fin aft skins are a sandwich construction consisting of one ply of 181 fiberglass fabric for both the inside and outside skins and a 3/8-inch-thick Nomex honeycomb core. The resin system is APCO 2434/3240. The method of fabrication is hand lay-up in a female mold that is shaped to the airfoil contour. See Figure 24.

The fin ribs are fabricated by hand lay-ups of plies of 181 fiberglass fabric and APCO 2434/2340 resin. There are five ribs required at Fin Stations 5.08, 8.17, 18.5, 30.5 and 42.49 and two brackets. A trailing-edge strip is fabricated from unidirectional Thornel 300 graphite fibers and APCO 2434/2347 resin. The strip is triangular shaped with the area necessary to provide the required fin chordwise stiffness.

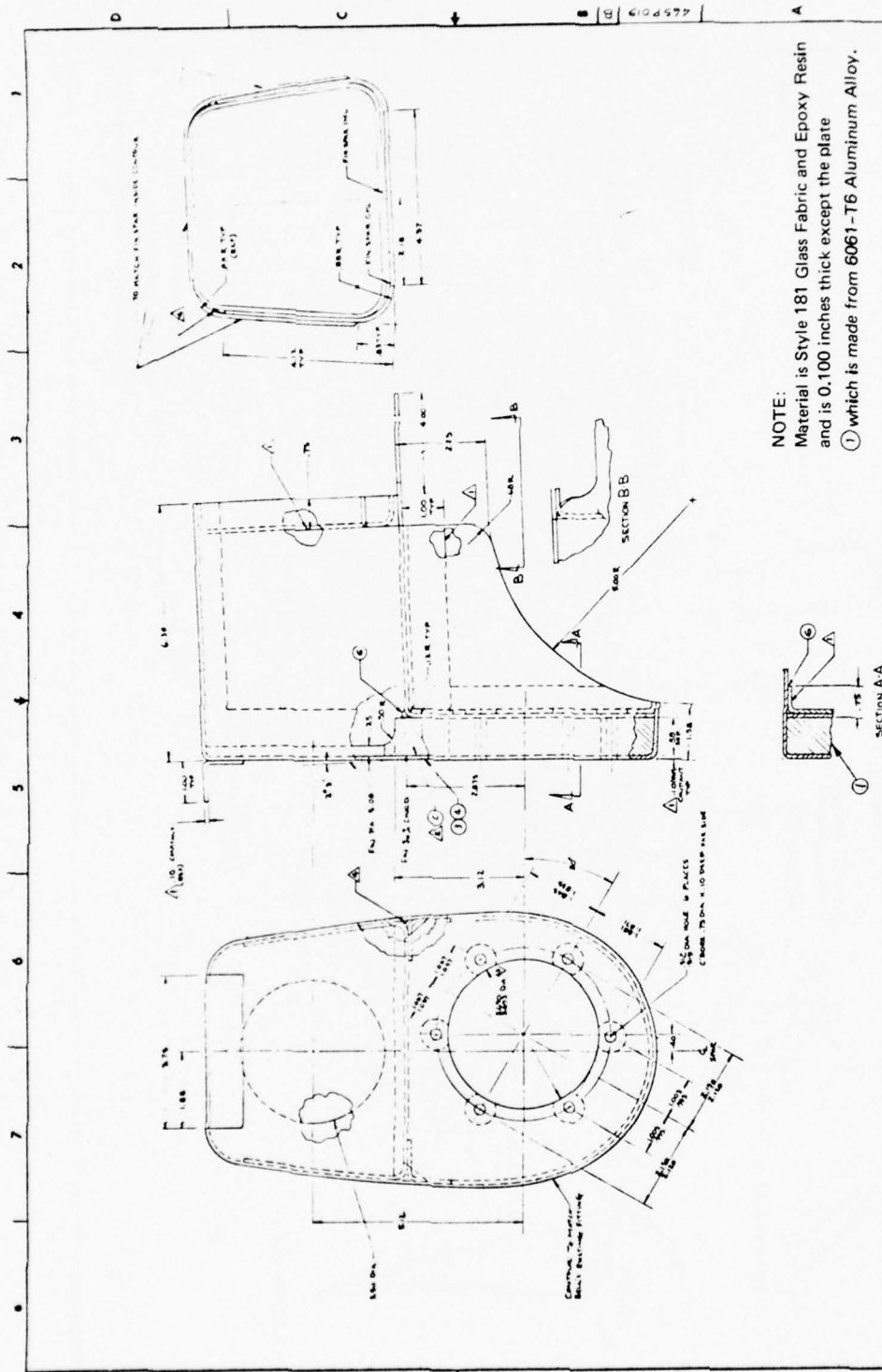


Figure 23. Tail Rotor Gearbox Mounting Bracket.

The fin ribs, brackets, and trailing-edge strips are bonded to the left-hand skin, which in turn is bonded to the spar. The control pulley brackets are located on and bonded to the structures. The right-hand skin is then bonded to the assembly.

Control System

The standard AH-1G synchronized elevator and attachment hardware were used. The scope of this program did not include designing and fabricating a new elevator from advanced composite material.

The control system to the tail rotor blades is essentially AH-1G hardware; however, it was necessary to reroute the cable system. The control cables are routed through the center of the fin spar for the present metal AH-1G tail boom. For the composite tail boom, it was necessary to route the control cables to the aft side of the fin spar.

This resulted in slightly longer control cables. It was required, because of the scope of the program, to use standard AH-1G pulleys, brackets, hardware, etc. The boom and fin structure required additional modification to accept the control system bracketry. This resulted in a weight penalty, in not being able to optimize the tail rotor control system.

FABRICATION OF FLIGHT TEST TAIL BOOM AND VERTICAL FIN

The fabrication of the flight test tail boom and fin spar was identical to that of the structural test tail boom. In addition, the following items were added to make the tail boom flightworthy:

1. Shelves for radio and electrical components
2. Attaching structure for drive shaft covers
3. Doors and attachments for all access holes
4. Installation of AH-1G sync elevator
5. Installation of tail rotor blade control system including supporting structures
6. Installation of drive system components
7. Complete vertical fin structure
8. Tail sting and support structure

The fabricated flight test tail section is shown in Figure 25, and the design details are shown in Figures 26 and 27.

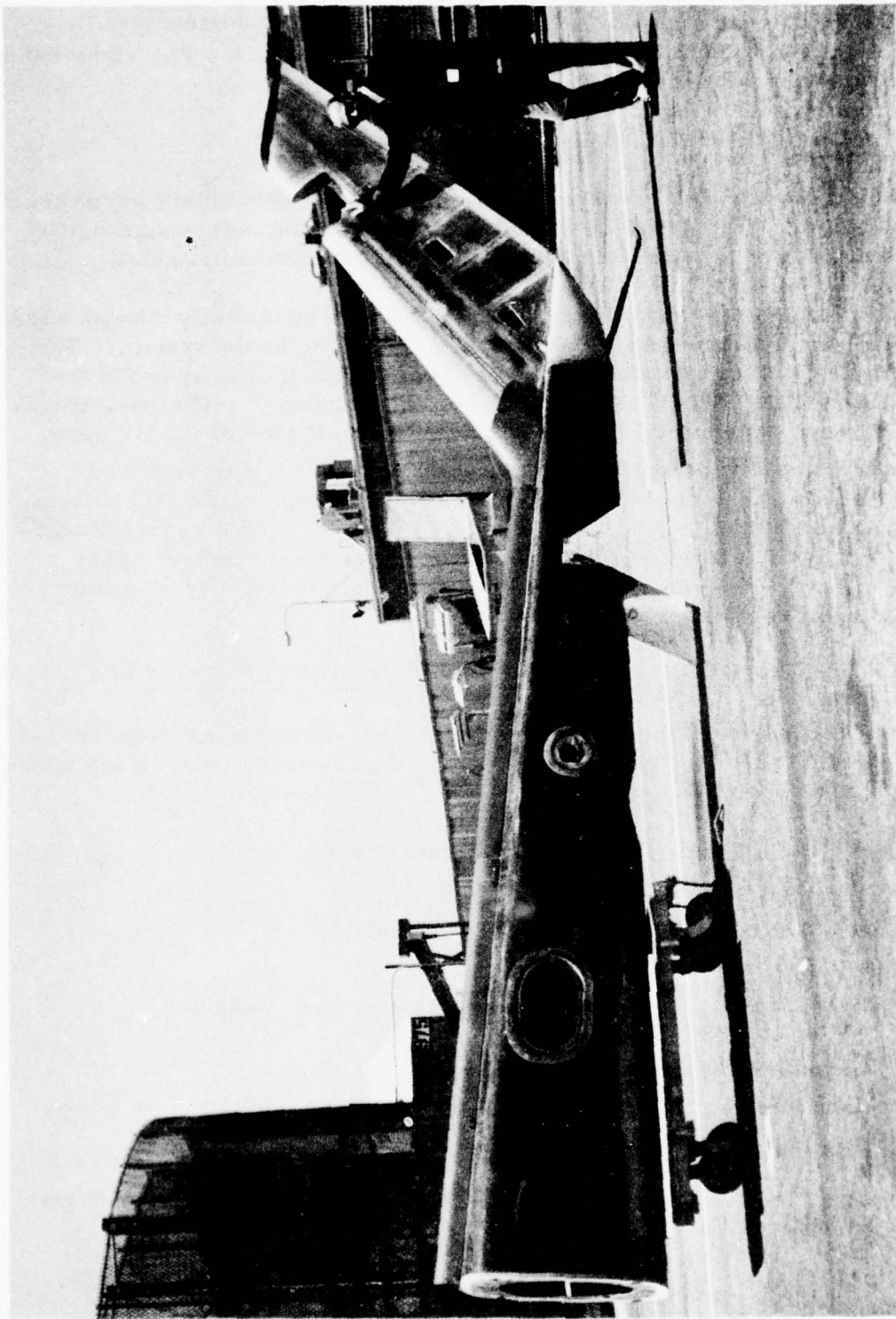
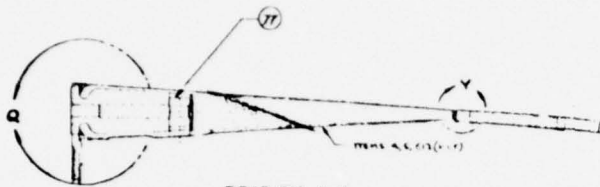
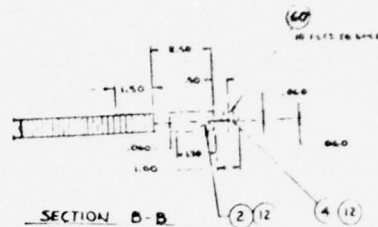


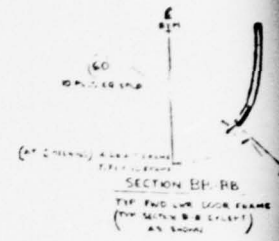
Figure 25. Flight Test Tail Section



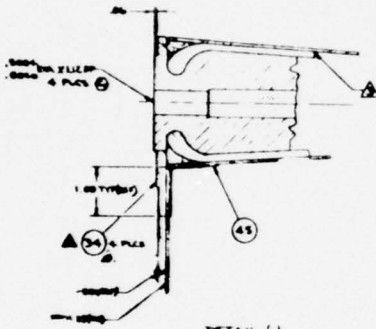
SECTION A-A
ROTATED 30° CW
SCALE HALF
TYP. & PLS



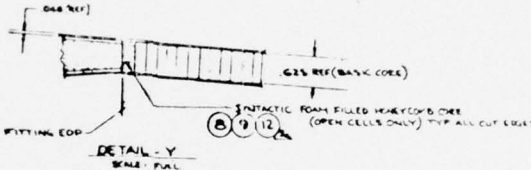
SECTION B-B
(TYP. ALL AROUND)
SCALE 1/2



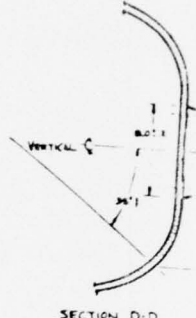
SECTION B-B
TYP. END VIEW LOOK FRAME
(TYP. SECTION B-B EXCEPT)
ALL SHOWN



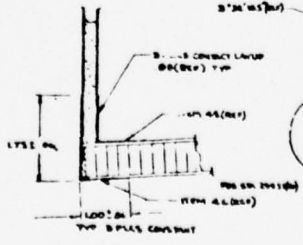
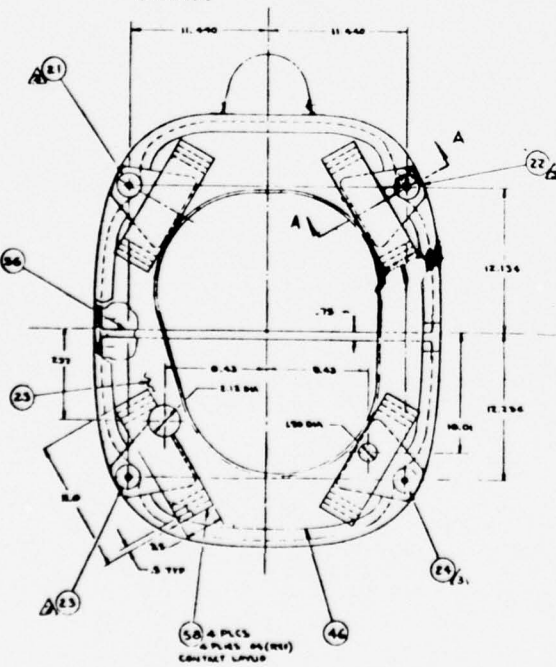
DETAIL V
FULL SCALE
TYP. & PLS



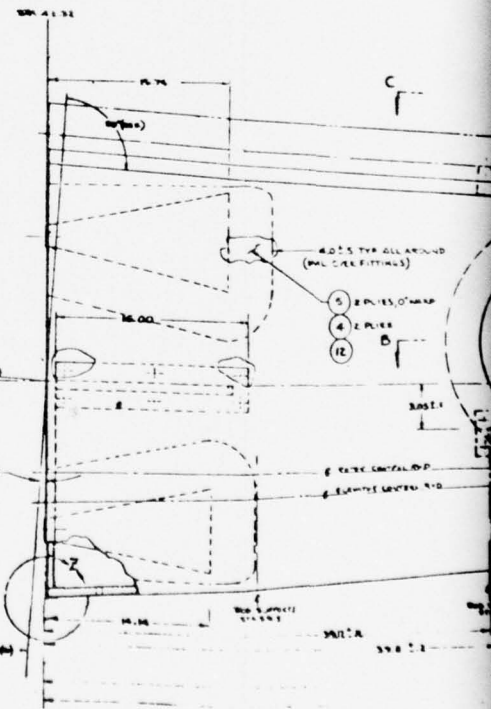
DETAIL Y
SCALE FULL



SECTION D-D



SCALE



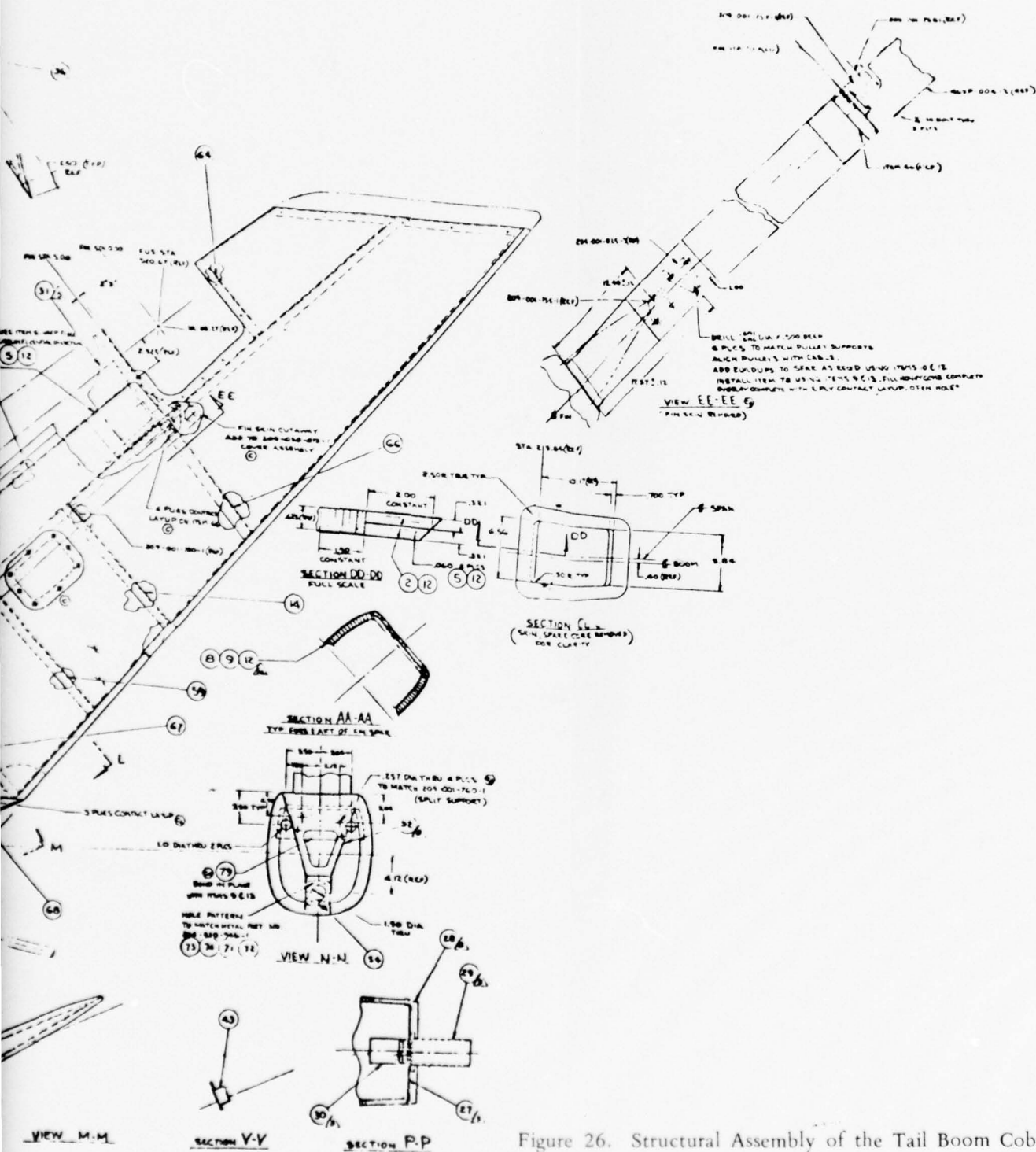


Figure 26. Structural Assembly of the Tail Boom Cobra AH-1G.

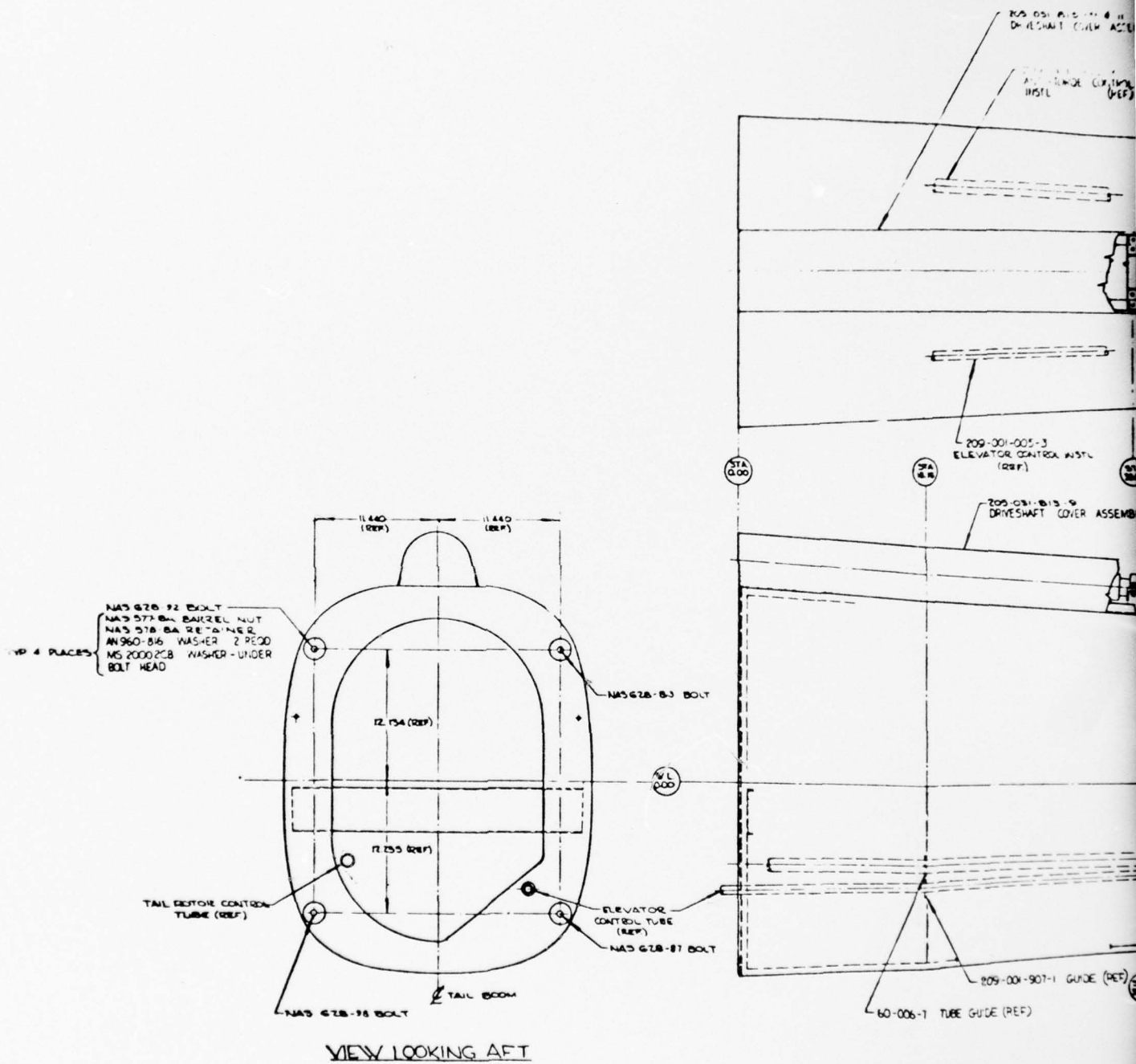
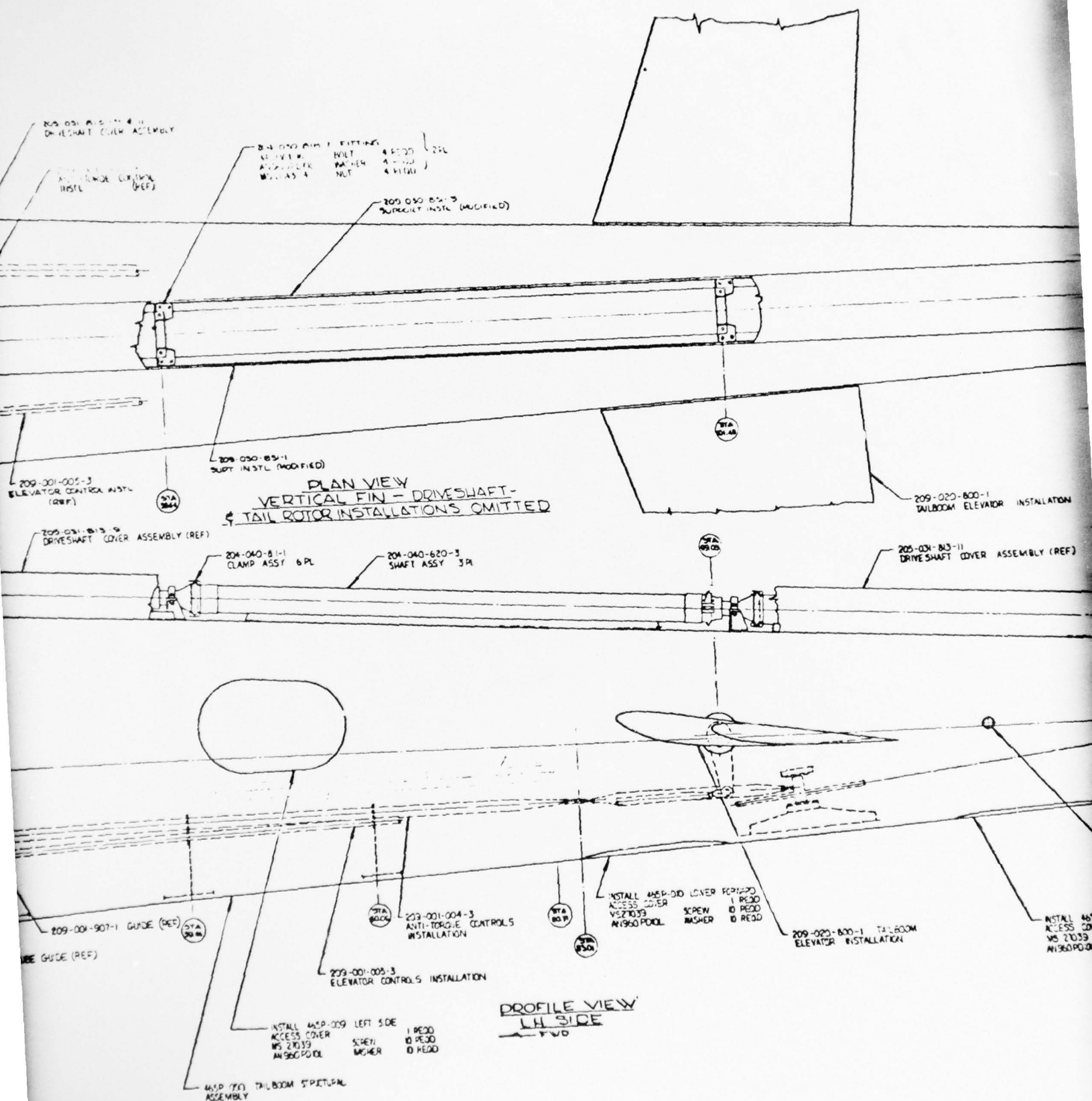
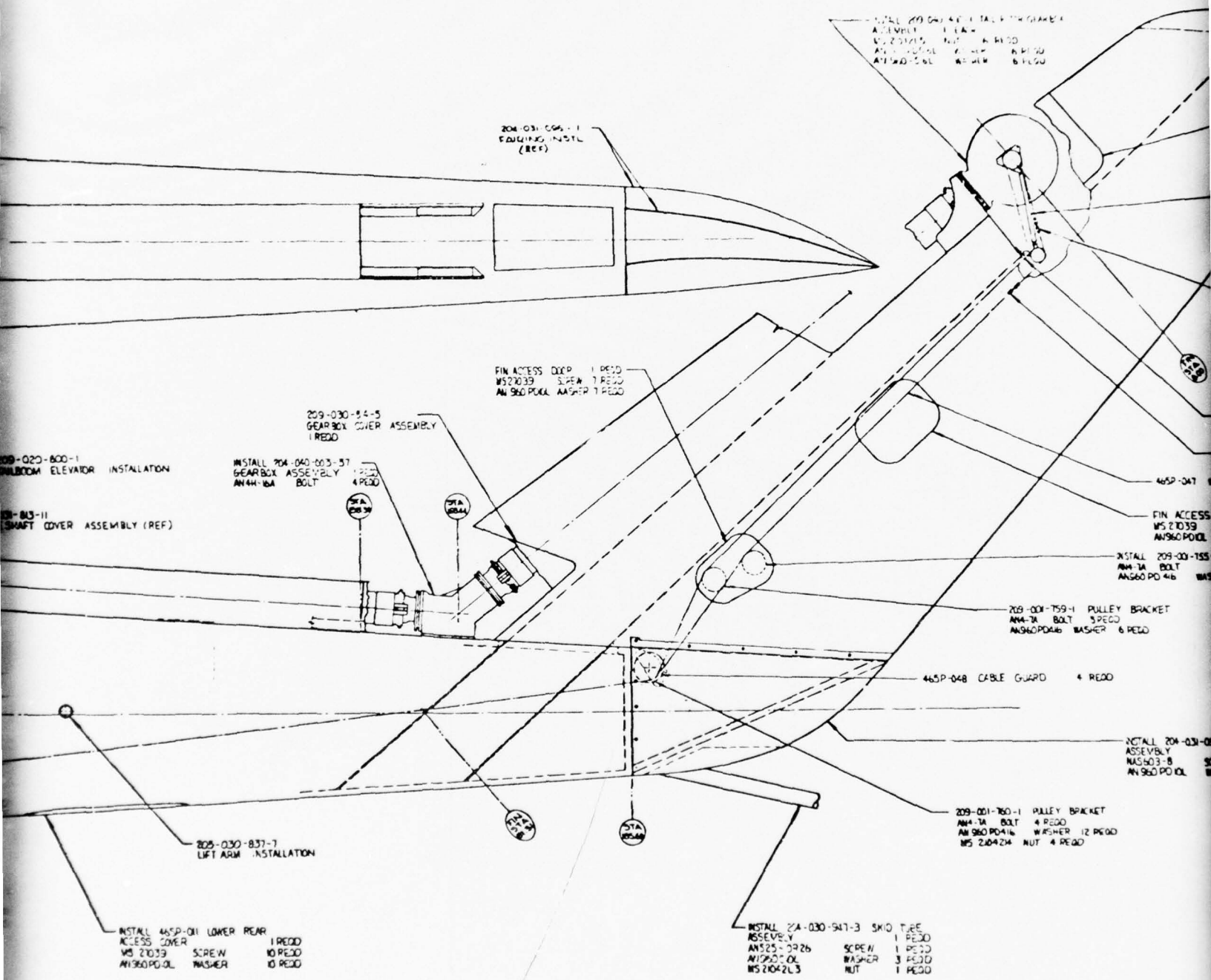
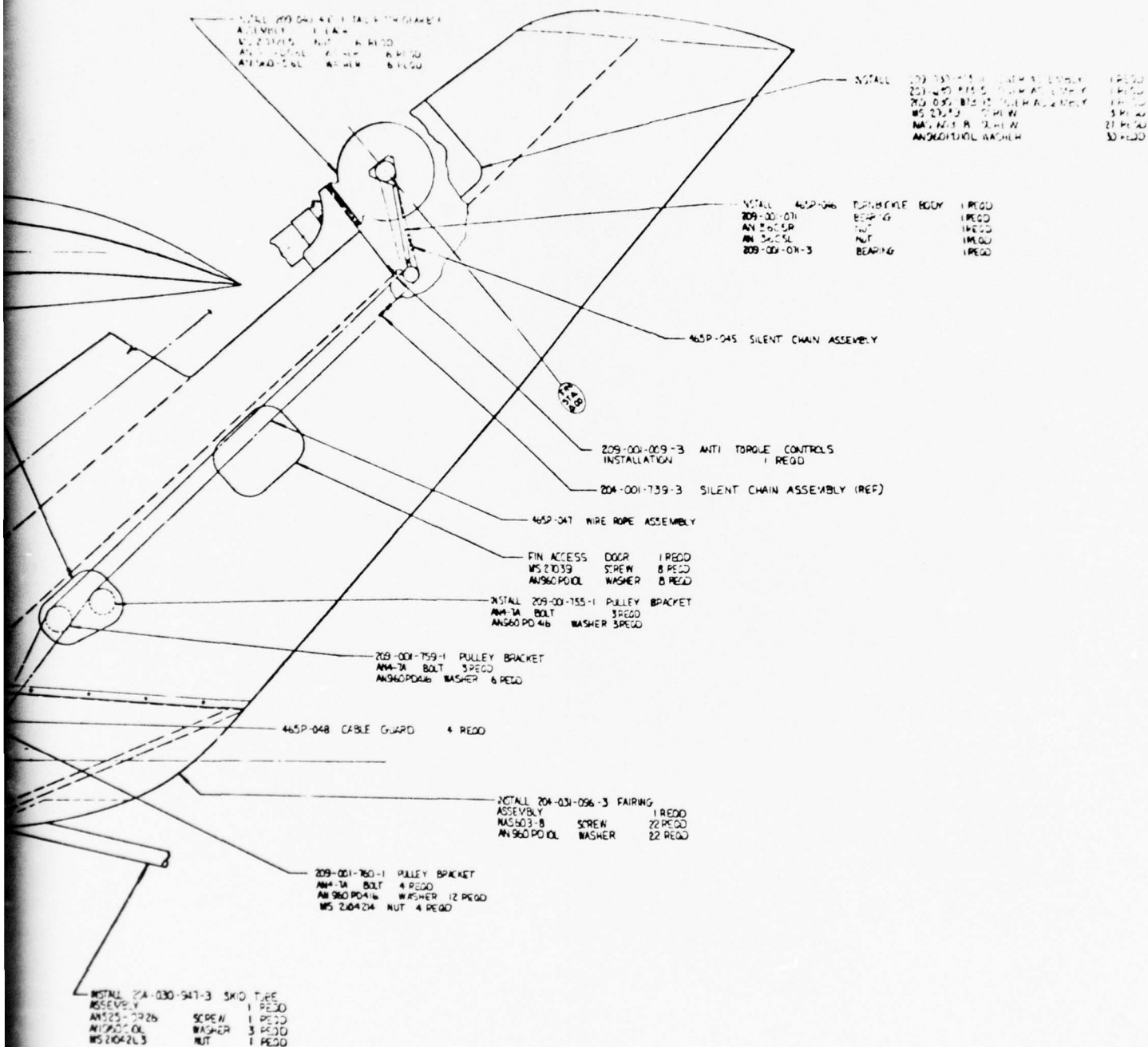


Figure 27. Tail Boom Assembly and Installation.







4

STRUCTURAL AND FLIGHT TESTS

DISCUSSION

The method used to structurally test the AH-1G composite tail boom was to attach the boom to a test fixture by the forward four attachment fittings and to apply the loads to the fin spar and boom. The magnitude of the loads and the location of the loading points were to match the design condition shears and moments as closely as possible using a minimal number of load application points. The three critical design conditions are: Cond. V, +15 degrees Yaw-recovery (Condition A), Cond. V, -15 degrees Yaw-recovery (Condition B) and Cond. XIV, Tail Down Landing (Condition C).

Figures 28, 29, and 30 show the comparison between the boom test bending moments and torques and the design limit moments for the most critical design condition (Cond. V, +15 degrees Yaw, Recovery). The comparison of test to design moments is similar for the other conditions tested. An unsymmetrical load was applied at the sync elevator attachment fittings (BS 140.3) to reduce the test torque to more closely approximate the design torque; however, the delta torque was applied to increase the boom torque, resulting in a conservative test.

As part of this program, it was required to fatigue test the composite tail boom and to estimate its fatigue life. This necessitated the establishment of a test fatigue load spectrum and the frequency of fatigue damaging load cycles. There were no reports available that contain measured steady and cyclic loads imposed on the AH-1G tail boom. There were neither estimated design fatigue loads nor measured loads from flight strain test programs.

The only fin/tail boom loads available were the maximum design limit loads for several critical flight conditions presented in Reference 11 (External Design Loads for the AH-1G Tactical Helicopter). These are the structural envelope design loads and are never expected to occur in service. They are also defined as "once in the helicopter lifetime loads."

The two highest design limit load conditions (Cond. V \pm 15 degrees Yaw-recovery) occurring on the tail boom were selected to establish the test fatigue load spectrum.

The conditions selected included the following parameters:

1. Critical helicopter gross weight (9500 pounds)
2. Maximum dive speed (222 knots)

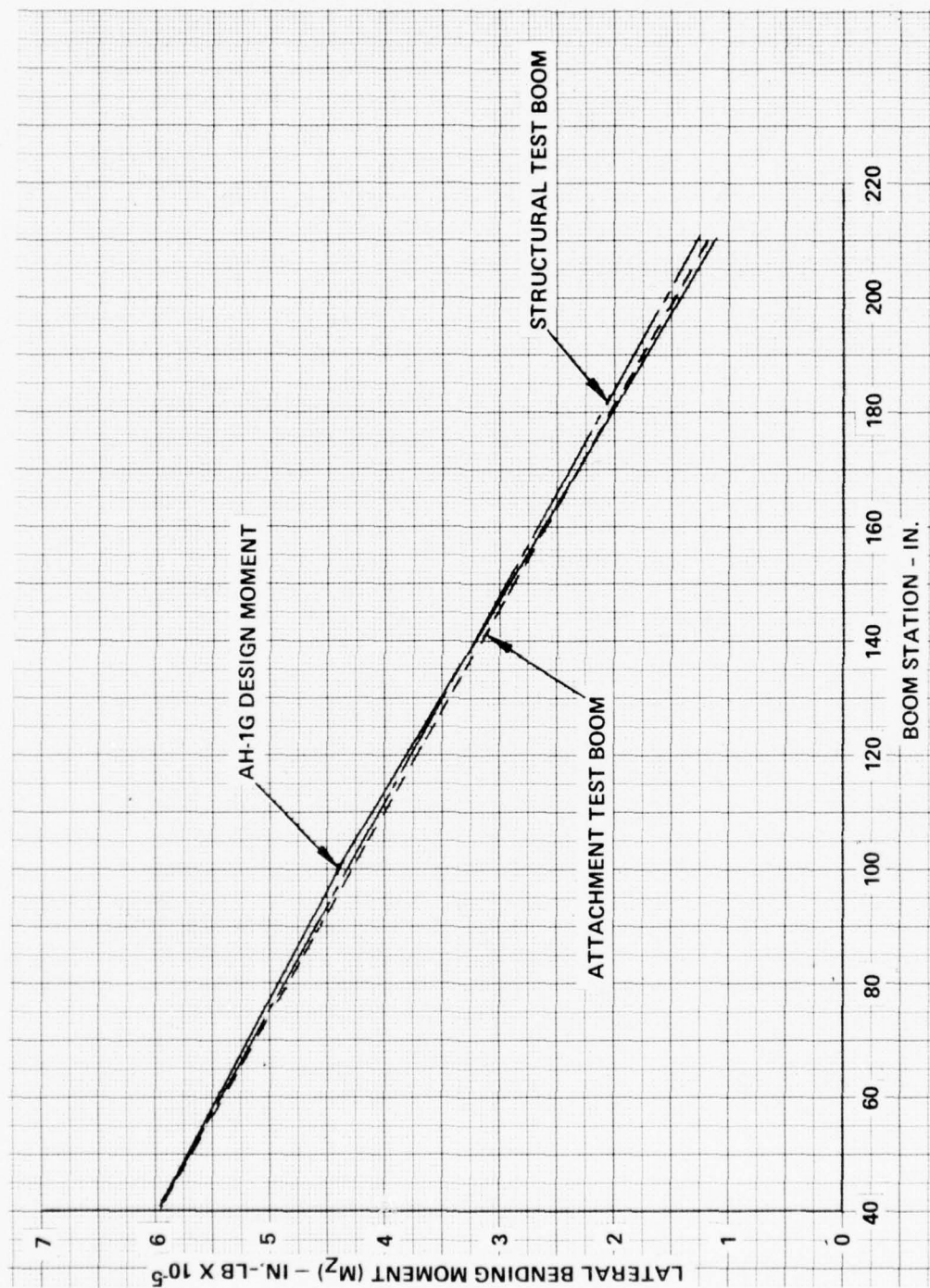


Figure 28. Comparison of Tail Boom Lateral Bending Moments (M_z) for Condition V, +15 degrees Yaw, Recovery.

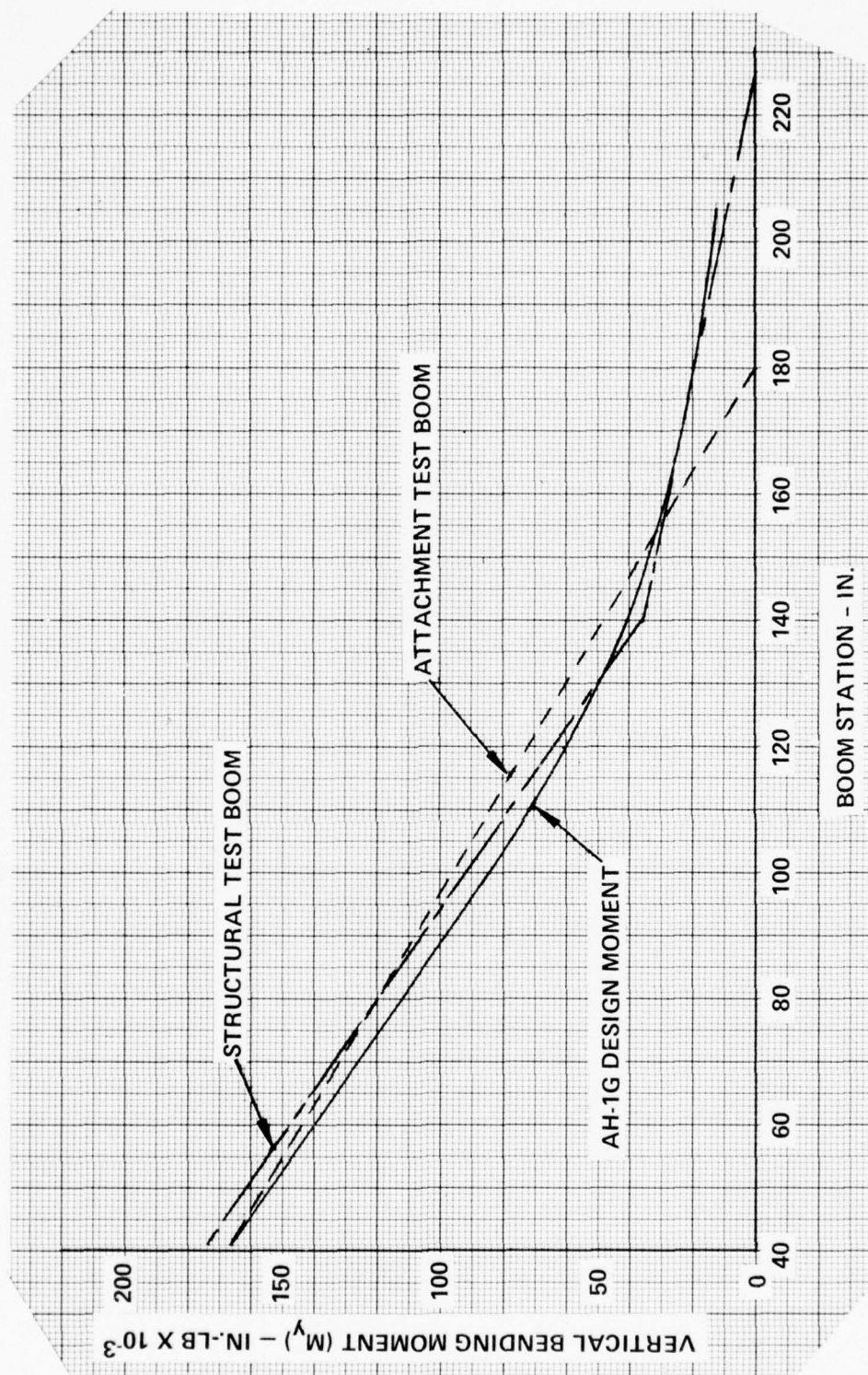


Figure 29. Comparison of Tail Boom Vertical Bending Moments (M_y) for Condition V, +15 degrees Yaw, Recovery.

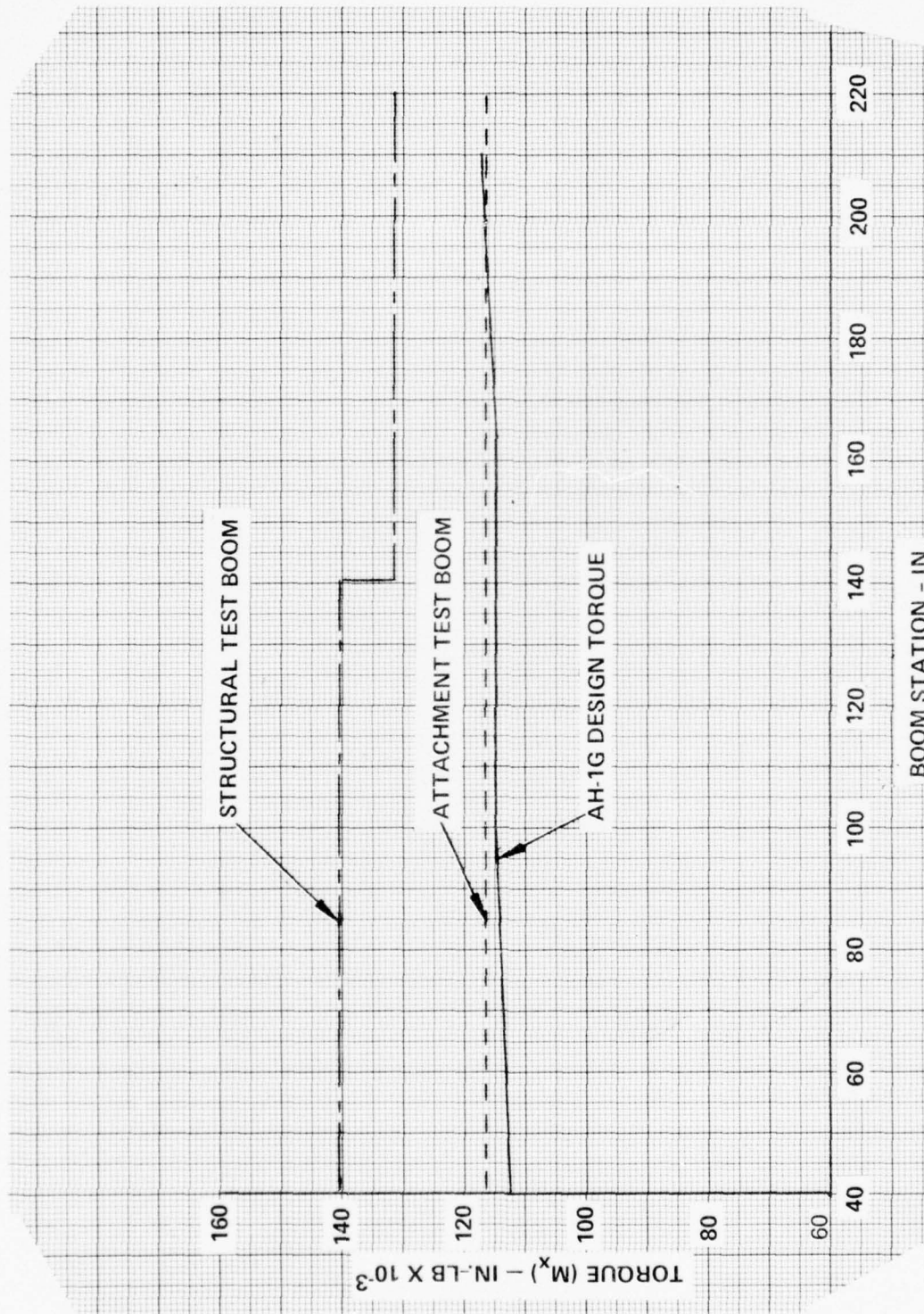


Figure 30. Comparison of Tail Boom Torque (Mx) for Condition V, + 15 degrees Yaw, Recovery.

3. Critical helicopter weight cg (forward)
4. 15 degrees yaw (right and left)
5. Instantaneous recovery.

Sixty percent of these design loads were selected as the test fatigue load spectrum. The tail boom moments are shown in Figure 31. It was assumed that these fatigue loads would occur on the AH-1G helicopter in service at a rate of three per flight hour. This frequency was derived from a comparison of the tail boom loads for other maximum design limit load conditions together with a review of the flight conditions flown to establish fatigue lives of other structural components (Reference 13).

TEST RESULTS OF TOOL-PROOF (SPECIMEN A) TAIL BOOM

The tool-proof tail boom (Specimen A) had not been originally scheduled to be tested and was included in the test program to obtain general strength and stiffness information. As previously described in this report under Fabrication, the tail boom had numerous and gross discrepant structural areas.

The boom failed at a resultant bending moment of $3195 \times 183.5 = 586,300$ inch-pounds or $-M_y = M_z = 586,300 \times .707 = 414,600$ inch-pounds at the forward attachment bolts. The following simplified method of analysis is used to compute bolt loads for comparing the applied test loading to the maximum design limit load. Using the bolt nomenclature and geometry of Table 2, the equations for the bolt axial loads are

$$P_2 = -0.0205 M_y - 0.0219 M_z$$

$$P_5 = 0.0205 M_y - 0.0219 M_z$$

$$P_7 = 0.0205 M_y + 0.0219 M_z$$

$$P_{10} = -0.0205 M_y + 0.0219 M_z$$

The bending moments for design Condition V, +15 degrees Yaw, Recovery are $M_y = -166,500$ inch-pounds and $M_z = 591,900$ inch-pounds. The resulting test and design condition axial bolt loads are

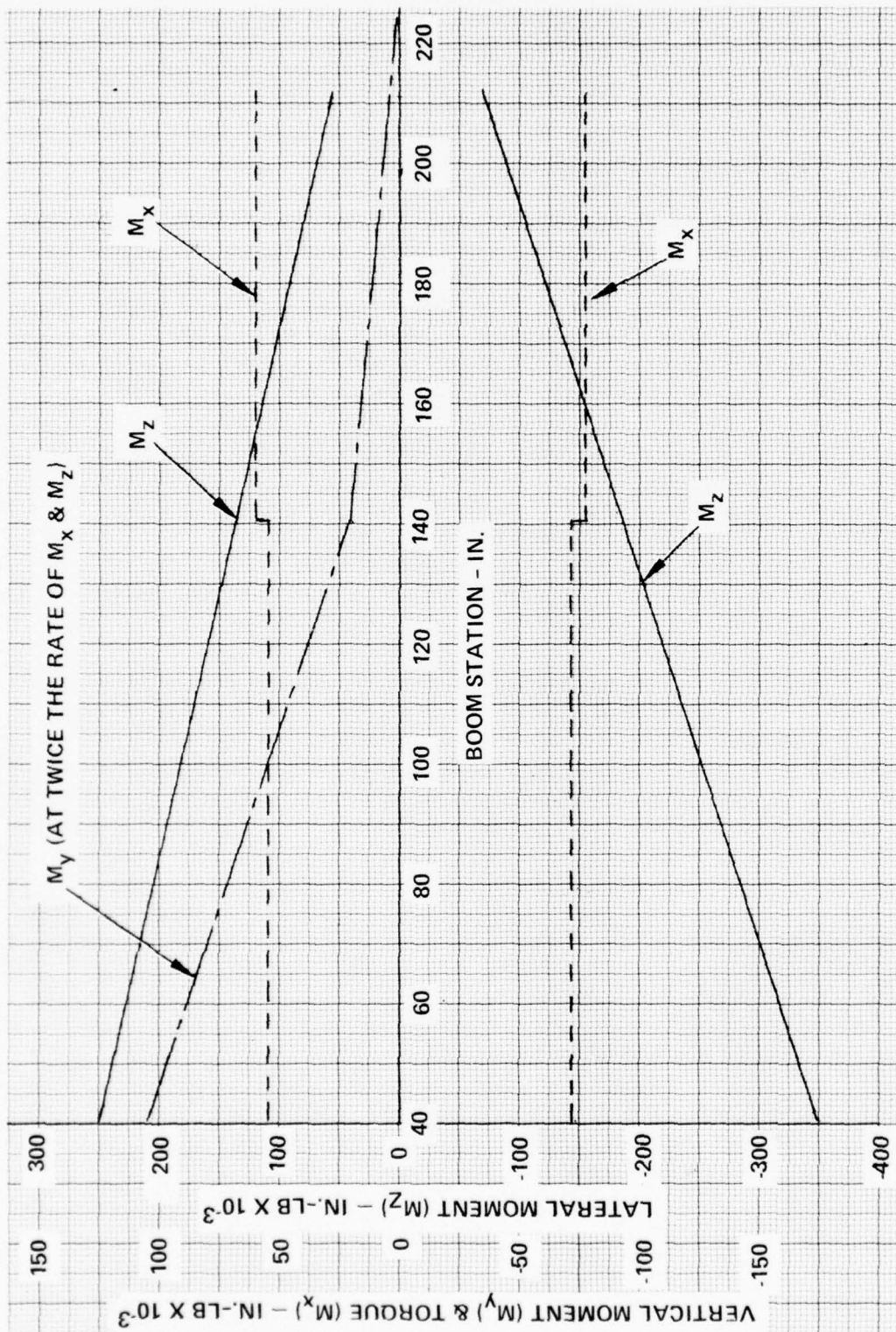


Figure 31. Structural Test Tail Boom Fatigue Loading.

Bolt	Condition V	Test
P ₂	-9520	-550
P ₅	-16350	-17570
P ₇	9520	550
P ₁₀	16350	17570

The tool-proof tail boom sustained a 7-percent higher loading than the maximum design limit condition. Refer to Appendix B for additional test information.

TEST RESULTS OF THE ATTACHMENT TEST TAIL BOOM

The attachment test tail boom was first loaded to the limit loads of Conditions A, B, and C. There were no failures or indications of yielding. The boom was then cyclic loaded to 60 percent of the limit loads of Conditions A and B. A total of 5000 cycles of vertical load (P_z) with 2500 cycles of lateral load (P_y) were applied to the boom specimen. Some outside skin fiber delaminations occurred on the compression side of the boom during the first 1300 (P_z) cycles. However, no additional delaminations or increase in the original delaminations were noted.

Design Load Condition A was selected for the failure test. The load was applied in the same manner and sequence as that for the limit proof load test. However, a failure of the fin spar corner longitudinal fibers occurred at the limit load after the load was held for approximately 2 minutes. The failure was compressive instability failure of the corner longitudinal graphite fibers. It was subsequently determined that a circumferential wrap of the spar had been inadvertently omitted, and this omission had caused the premature spar failure.

The spar was repaired by wrapping and bonding fiberglass fabric around the damaged area. Testing was then resumed to failure, which occurred at 150 percent of the limit load as a compression failure of the right and bottom sides of the boom outside the attachment test areas. The attachment test areas consisted of the four forward bolt fittings and boom supporting structure and the fin spar to boom attachment area. The strength of the attachment test areas was in excess of the design ultimate load; however, the actual strength of the attachments was not established. Refer to Appendix B for additional information, including photographs and measured strains and deflections.

TEST RESULTS OF THE STRUCTURAL TEST TAIL BOOM

STATIC TESTS

The design limit loads of Conditions A, B and C were applied to the structural test tail boom. Deflection, load, and strain gage readings were recorded for each test condition. Each design load condition was completed successfully, and no damage was noted during the subsequent inspections.

FATIGUE TESTS

The fatigue test loads were then applied to the tail boom by means of the closed-loop servomechanism system. The lateral loads, P_{y1} , P_{y2} and P_{y3} , were applied at a cyclic rate of 1.5 cps; and the vertical loads, P_{z1} , P_{z2} and P_{z3} , were applied at a cyclic rate of 3 cps. The sync elevator loads (P_{z1} and P_{z2}) were programmed in a "milking machine" manner. The P_{z1} load was applied during the first half cycle of the lateral loads and the P_{z2} load during the second half cycle of the lateral loads. The magnitude of the fatigue loads were 60 percent of the two highest design limit load conditions. After the completion of 267,310 cycles of lateral loads, fatigue testing was terminated. A final inspection of the test boom revealed no damage or change in stiffness.

SELECTIVE STATIC TESTS

The simulated bolt failure static test consisted of loosening the upper left-hand attachment bolt and applying loads that would produce a tension reaction at the loosened bolt. From Reference 1, it was determined that the maximum ultimate load used in structural substantiation of the metal AH-1G tail boom was equal to $17,511 \times 1.5 = 26,270$ pounds. The limit loads and moments of Condition A, when applied to the three-bolt configuration, result in a maximum compressive load equal to $(166,500/24.36) + (59,1940/22.88) = 32,700$ pounds. The test loads for the simulated bolt failure test were taken as $(26,270/32,700)$ or 80 percent of Condition A design limit loads. After completion of the test, an inspection of the tail boom revealed no damage.

The simulated bullet hole damage static test consisted of drilling two 0.50-inch-diameter holes through the side and through the top of the tail boom at a 45-degree angle with the vertical axis. The holes were located in an area of high tensile stress, the upper left-hand corner of the boom above the side access hole (see Figure C-6 Appendix C). The static loads of Condition A were applied, and no damage or increase in damage of the holes was noted.

The third selective static test consisted of dropping a 1-pound steel ball on the tail boom from the height of 6 feet. Only a very slight mark was noted in the impact area, but no indentation or damage to the tail boom was noted. Because of the lack of damage to the tail boom, static test loads were not applied.

Refer to Appendix C for additional information including photographs and measured strains and deflections.

PROOF LOADING OF THE FLIGHT TEST TAIL BOOM AND VERTICAL FIN SPAR

The objectives of proof loading the flight test tail boom were:

- To assist in the establishment of the structural integrity of the flight tail boom.
- To calibrate the strain gages for known applied loads and moments

Test loads were applied to the flight test tail boom and fin spar at five load points. The test loads were to produce as closely as possible the limit loads and moments of Conditions A, B and C. The test boom bending moments and torques are given in Figure 32. Each load condition was completed successfully, and no damage was noted during the subsequent inspections. For more detailed information on the results of proof loading of the flight test tail boom, see Appendix D.

A primary design requirement for the composite tail boom was to maintain the same lateral, vertical and torsional stiffnesses of the AH-1G tail boom structure. As previously stated, graphite (Thornel 300) fibers were used to meet this design requirement. The tail boom structure fabricated for flight testing proved to be 12 percent stiffer laterally, 14 percent stiffer vertically and 33 percent stiffer torsionally than the AH-1G metal tail boom structure.

The curves presented in Figures 33, 34, and 35 show the comparison of stiffness for the composite structure to the existing metal structure. The stiffness curves for the composite structure are based on the curve shapes derived from the cross-sectional properties computer program (Appendix A) and are adjusted to produce the deflections recorded during the proof loading of the flight test tail boom (Appendix D).

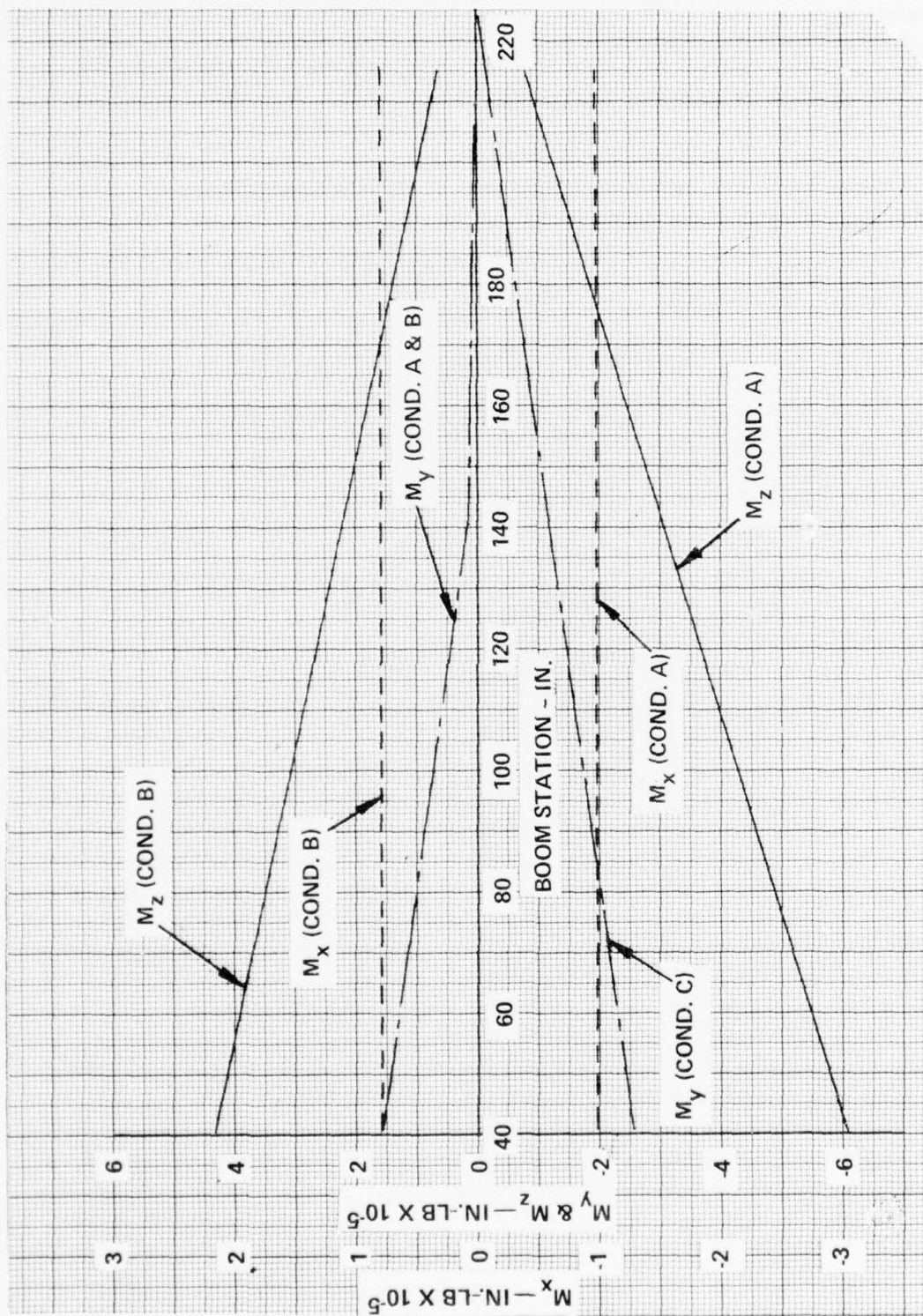


Figure 32. Proof Loading for Flight Test Tail Boom.

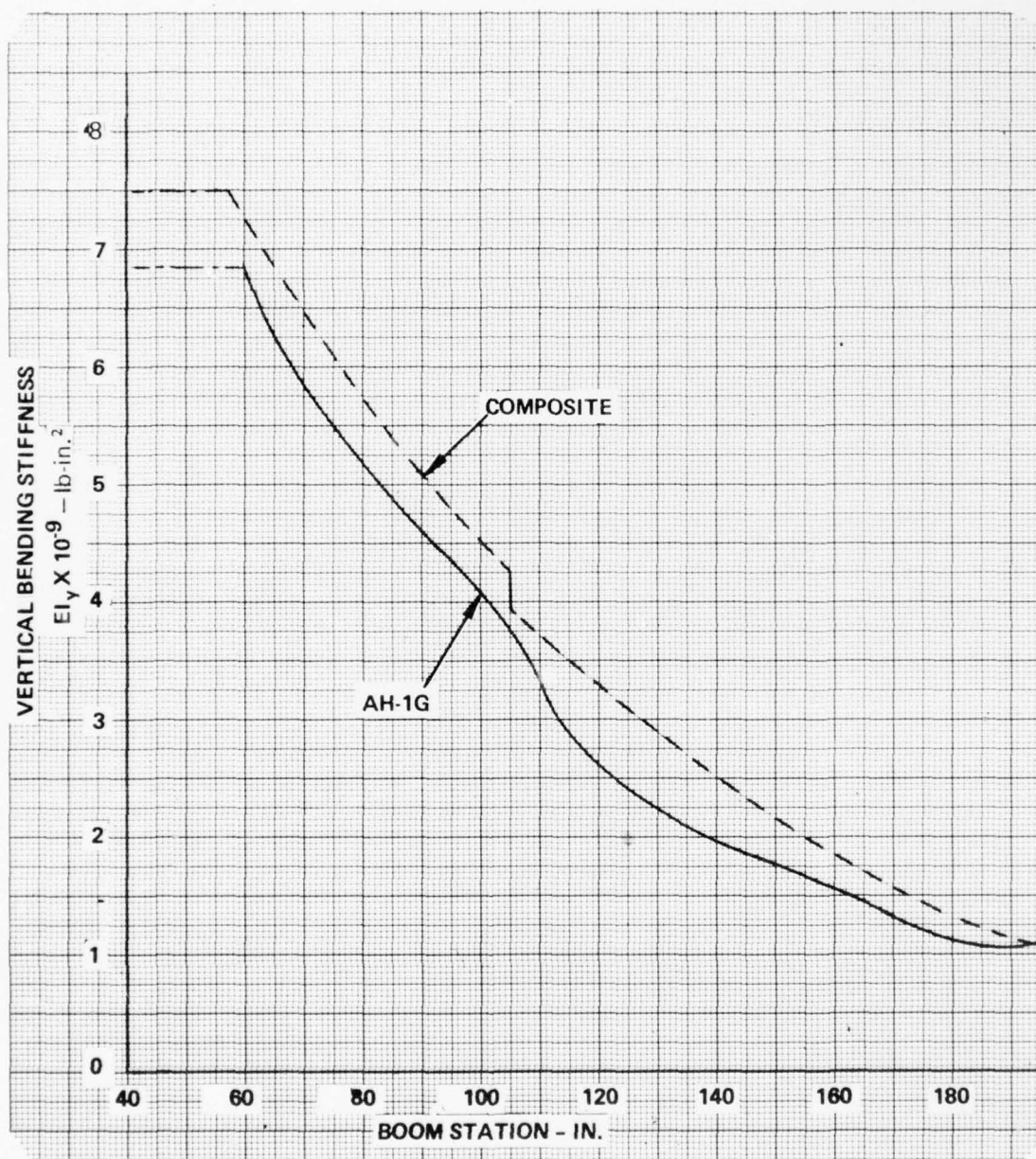


Figure 33. Comparison of Vertical Bending Stiffness of AH-1G Structure to Composite Structure.

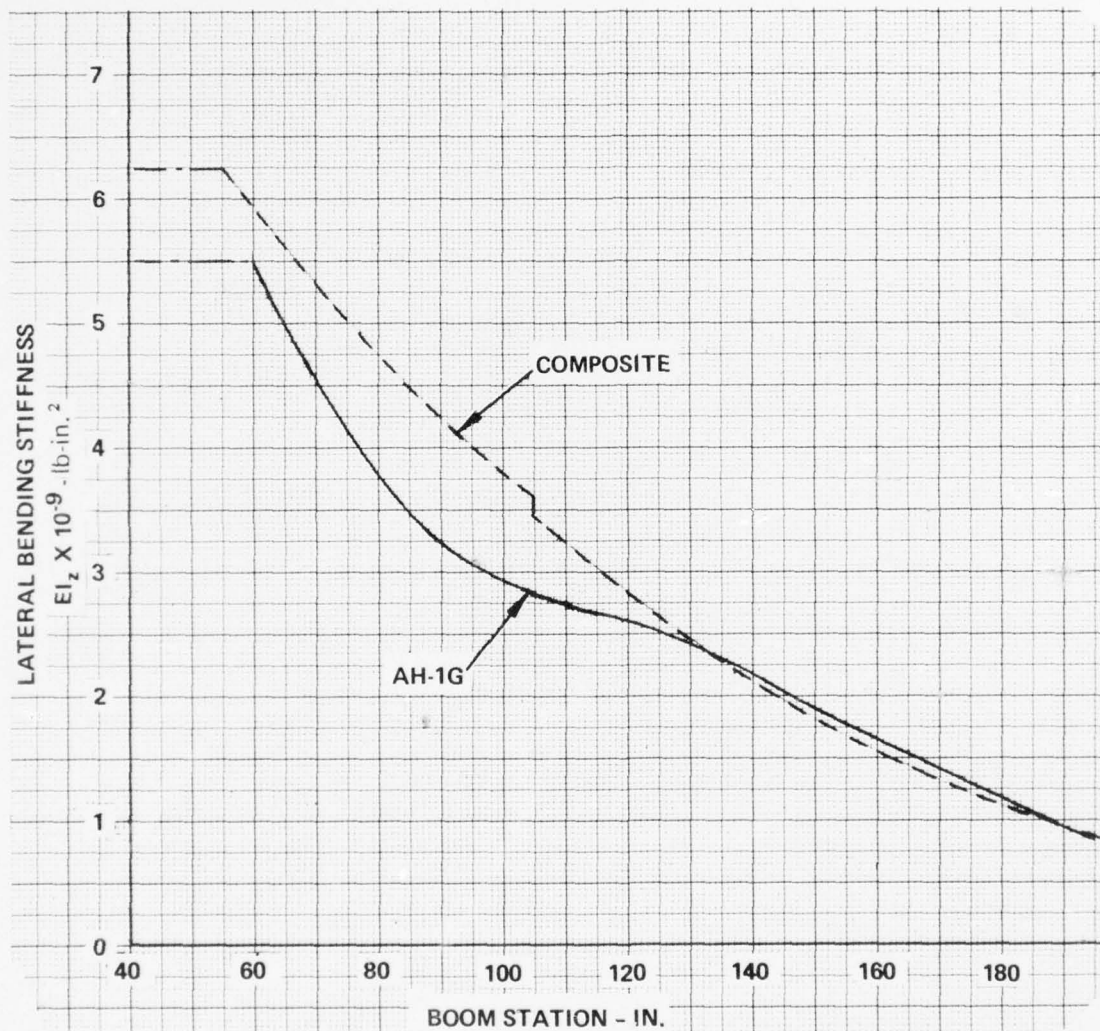


Figure 34. Comparison of Lateral Bending Stiffness AH-1G Structure to Composite Structure.

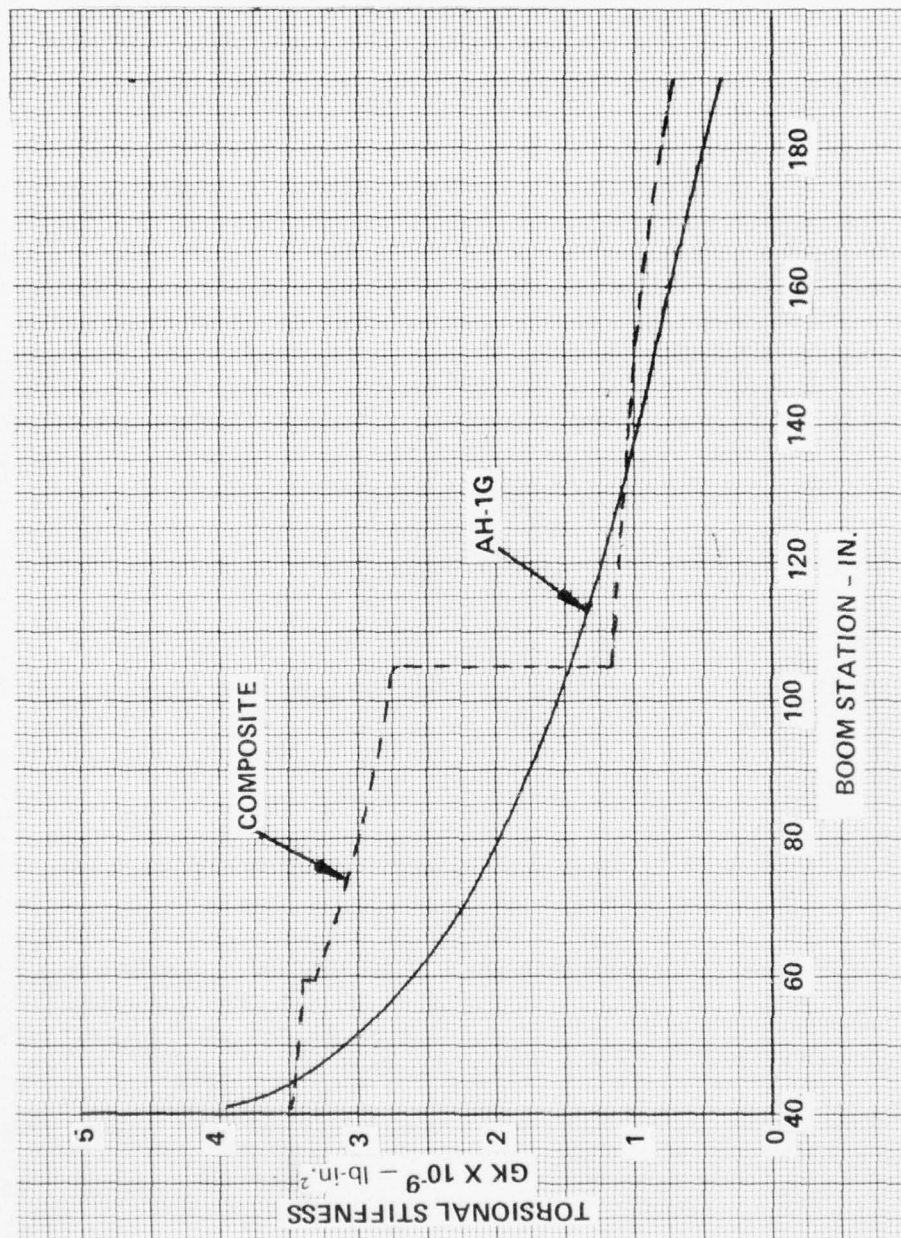


Figure 35. Comparison of Torsional Stiffness of AH-1G Structure to Composite Structure.

LATERAL CONTROL SYSTEM PROOF LOAD

The objective of this test was to establish the structural integrity of the lateral (tail rotor) control system. It was necessary to reroute a portion of the control system to make the system compatible with the composite vertical fin spar.

The specimen for this test consisted of the tail rotor control system of the AH-1G Cobra composite tail boom flight test vehicle from the pilot's pedals through the entire control system, excluding the two tail rotor blades and pitch links. The test load was applied at the pilot's tail rotor control pedals and reacted at the tail rotor pitch-link crossbeam. A maximum load of 225 pounds was applied to each pedal. A load of approximately 160 pounds was applied to each pedal during its full operational travel. The results of this proof and operation test revealed that the tail rotor control system sustained no structural damage, excessive deflections, or interference of moving parts during the test (Reference 14).

FLIGHT DEMONSTRATION

GENERAL

The composite AH-1G tail section was successfully test flown during the time period from October to late December, 1975. The AH-1G helicopter in flight with the composite tail section installed is shown in Figure 36. The flight demonstration envelope included the following:

1. IGE Maneuvers (Hover, turns, forward-sideward-rearward flight and control reversals)
2. Forward Level Flight (speeds to 190 knots)
3. Maneuvers (turns, pull-ups, push-overs and control reversals to speeds of 171 knots and a peak cg load factor of 3.42g)
4. Power Transitions (simulated power failures with power recovery and acceleration maneuvers)

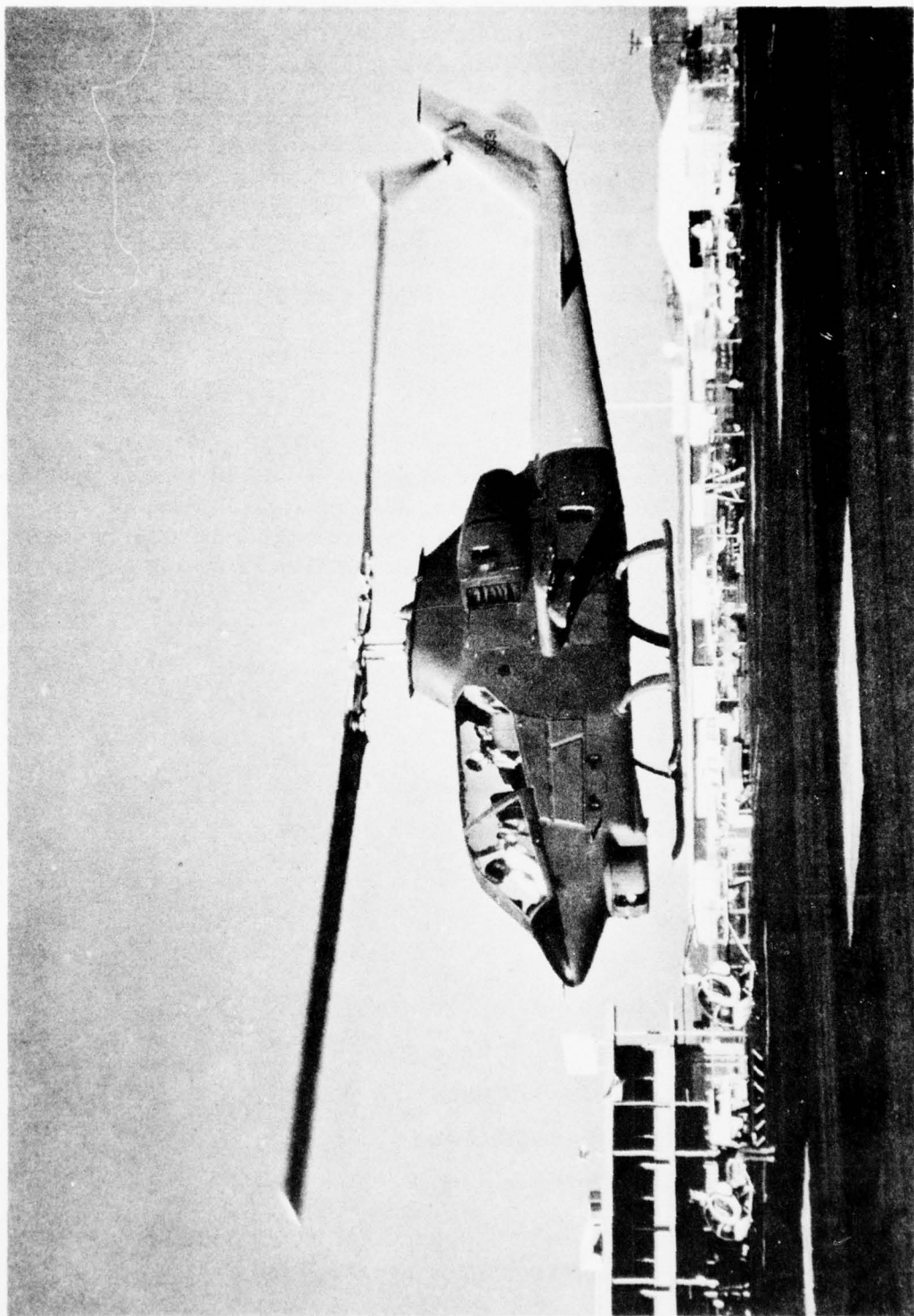


Figure 36. Composite Tail Section in Flight

The basic helicopter parameters for the demonstration flights were:

1. Takeoff gross weight = 8100 pounds minimum
2. Mid cg = Fuselage Station 196
3. Main Rotor Speed = 100% = 324 rpm
4. Density Altitude = 3000 feet
5. Vmax = 190 knots
6. Maximum cg G = 3.0

INSTRUMENTATION

The data acquisition system used on the composite AH-1G tail boom program consisted primarily of a 50-channel oscillograph, cockpit display of one strain gage parameter and tail boom surface temperature, necessary signal conditioning, and cockpit controls for the system. The following parameters were recorded:

1. Main Rotor rpm
2. Airspeed
3. Vertical acceleration at the cg
4. Vertical acceleration at the tail rotor gearbox
5. Lateral acceleration at the tail rotor gearbox
6. Pedal position before the SAS input
7. Pedal position after the SAS input
8. Fin spar strain, right hand
9. Fin spar strain, left hand
10. Tail boom strain, upper left hand
11. Tail boom strain, lower left hand
12. Tail boom strain, upper right hand
13. Tail boom strain, lower right hand
14. Bridge voltage
15. Tail boom skin temperature (hand recorded only)

The locations of the strain gages on the tail boom and the vertical fin spar are given in Figure D-5 of Appendix D. The output strains of the strain gages for applied loads to the fin and tail boom are given in Table D-1 of Appendix D.

Strain and acceleration data were read to determine the highest single cycle for each maneuver flown. That is, the highest peak and lowest valley, not necessarily coincident in time, were read. These strains and accelerations were tabulated along with condition information for each maneuver flown.

Primary interest on the tail rotor gearbox accelerations was vibration or cyclic acceleration. For that reason, gain on these accelerometers was set low so as to produce a legible oscillographic trace. No attempt was made to verify the exact accelerometer orientation at the time zeros were recorded (i. e., helicopter attitude on the skids). Small angles differences will affect the zeroes. The low gain setting compromises the ability to get accurate mean values which are dependent on zeroes. Therefore, the mean accelerations at the tail rotor gearbox are not reported.

Review of the data indicates a possible temperature effect (engine exhaust/downwash) on the tail boom strain gages during hover and low airspeed operation. In the beginning of the flight test program when, unfortunately, most of the low and slow flying was accomplished, the tail boom strain gages were exposed. The strain gages were left exposed so that their condition could be monitored. The gages were covered prior to Flight 5. The impact of the possible temperature effect on the data is to erroneously offset the mean values. Since the temperature change is relatively slow compared to the cyclic data read out, the cyclic data should not be affected. Only the mean values recorded by the fin spar strain gages are considered to be accurate for Flight 5 and subsequent flights. These strain gages are the most important gages for determining the severity of flight loads imposed on the vertical fin and tail boom during the flight demonstration.

Early in the test program, templates were put on the tail boom to monitor surface temperatures due to engine exhaust. Subsequently, it was decided to give the crew the capability to monitor tail boom surface temperatures in flight. Seven thermocouples were placed on the tail boom at the hottest spots indicated by the templates. These temperatures were read out by the crew in flight, using a selector switch and a standard temperature indicator.

ANALYSIS OF FLIGHT TEST RESULTS

Measured Strain Data

The maximum flight loads on the vertical fin and tail boom occurred during the pedal reversal flight conditions. Table 12 gives the measured strains and load factors for the pedal reversal flight condition that were recorded at various helicopter airspeeds. Also included in the Table are the strains for the highest measured helicopter cg load factors. The peak loading occurred for a pedal reversal at an airspeed of 150 knots and converts to the following fin spar bending moment:

From Appendix D, the applied bending moment at the fin spar strain gages equals 100,200 inch-pounds, resulting in the left-hand strain gage measuring a strain of 1490 μ inches and the right-hand gage measuring a strain of 1775 μ inches. The gage factors are:

$$R/H \text{ Factor} = 100,200/1490 = 67.2 \text{ in. -lb}/\mu \text{ inches}$$

$$L/H \text{ Factor} = 100,200/1775 = 56.6 \text{ in. -lb}/\mu \text{ inches}$$

The measured strains for the pedal reversal at 150 knots are:

$$R/H = 482 \pm 241 \text{ or Max} = 723\mu \text{ inches}$$

$$L/H = 680 \pm 312 \text{ or Max} = 992\mu \text{ inches}$$

which results in fin spar bending moments of:

$$R/H = 723 \times 67.2 = 48,510 \text{ in. -lb}$$

$$L/H = 992 \times 56.5 = 56,060 \text{ in. -lb}$$

or using the average moment (to account for probable unsymmetrical bending) results in a bending moment of 52,300 in. -lb at the strain gages.

The maximum design limit bending moment at the fin spar strain gage location (Reference Figure D-5 in Appendix D) is:

$$M_x = -113,500 \text{ in. -lb}$$

$$M_z = 101,000 \text{ in. -lb}$$

$$M_r = -113,500 \sin 44^\circ 3' - 101,000 \cos 44^\circ 3' = -151,500 \text{ in. -lb}$$

The maximum load imposed on the composite tail boom during the flight demonstration program was approximately 35 percent of the maximum design limit load.

TABLE 12. MEASURED FLIGHT STRAIN AND LOAD FACTOR DATA

TABLE 12. MEASURED FLIGHT STRAIN AND LOAD FACTOR DATA

Airspeed Knots	Fin Spar Strains		Cyclic Tail Boom Strains				cg Vertical Acceleration g	Cyclic Tail Gearbox Vert. Accel. Lat. Accel. g g	
	R/H μin.	L/H μin.	LL μin.	UL μin.	LR μin.	UR μin.			
① 0	* ±186	* ±215	±116	±84	±99	±120	1.03±0.18	±1.1	±5.1
① 0	* ±255	* ±247	±112	±99	±118	±121	1.08±0.15	±0.6	±4.7
① 70	* ±239	* ±306	±56	±58	±84	±164	1.11±0.27	±0.6	±6.1
① 90	-227±258	238±272	±141	±124	±143	±121	1.09±0.31	±0.9	±6.9
① 90	-233±343	269±407	**	±147	±166	±214	1.04±0.54	±1.5	±9.0
① 126	-281±295	356±338	**	±139	±141	±199	1.09±0.51	±3.0	±11.5
① 126	-234±276	463±321	±152	±98	±102	±165	1.00±0.56	±4.5	±13.2
① 150	-482±241	680±312	±159	±125	±136	±173	1.02±0.58	±6.4	±13.5
① 150	-350±294	489±368	±210	±142	±158	±239	1.09±0.86	±3.8	±13.3
① 170	-336±280	368±387	±270	±151	±250	±239	0.90±1.83	±4.9	±13.6
① 171	-469±189	690±177	±210	±106	±108	±209	1.39±1.74	±6.0	±13.5
① 170	-413±189	503±205	±210	±89	±117	±263	1.44±1.98	±4.5	±14.3

Notes:

① Flight condition - pedal reversal at various airspeeds

② Flight condition - pull-up at 171 knots

③ Flight condition - right turn at 170 knots

* Mean values were not considered to be accurate because of temperature effects

** Strain gage channel inoperative for one flight

Notes:

① Flight condition - pedal reversal at various airspeeds

② Flight condition - pull-up at 171 knots

③ Flight condition - right turn at 170 knots

* Mean values were not considered to be accurate because of temperature effects

** Strain gage channel inoperative for one flight

The maximum measured cyclic strains on the fin spar were during a pedal reversal flight condition at a helicopter airspeed of 90 knots. The measured strains are:

$$R/H = -223 \pm 343 \mu \text{ inches}$$

$$L/H = 269 \pm 407 \mu \text{ inches}$$

and the resulting fin spar bending moments are:

$$(R/H) M = (-233 \pm 343) 67.2 = -15,700 \pm 23,050 \text{ in.-lb}$$

$$(L/H) M = (269 \pm 407) 56.5 = 15,200 \pm 23,000 \text{ in.-lb}$$

The maximum cyclic moment is approximately 15 percent of the maximum design limit moment.

Skin Temperature Data

The initial tail boom temperature range for design was -65° to 120° F under maximum load, with a section of the upper boom surface from BS 44.3 to 81.0 to be designed for a maximum temperature of 300° F under a reduced loading condition. Templates were used to monitor the tail boom skin temperatures at the start of the flight demonstration program. The templates indicated boom skin temperatures to 260° F during the first ground runs and hover flights. Seven thermocouples were placed on the tail boom at the hottest spots indicated by the templates. The purposes of the thermocouples were to obtain more accurate temperature measurements and to give the crew the capability to monitor the tail boom skin temperatures in flight. Initially the thermocouples measured high and erratic temperatures, and it was concluded that they were measuring the temperature of the exhaust gas and not the boom skin temperature. The thermocouples were covered and temperature readings stabilized. The highest skin temperature observed during the flight demonstration was 195° F at BS 43 during a left turn at 150 knots. A summary of the highest and lowest skin temperatures (at each thermocouple location) observed during the flight demonstration is given in Table 13.

TABLE 13. SUMMARY OF OBSERVED SKIN TEMPERATURES					
Thermocouple		Max Temp (°F)	Flight Condition	Min Temp (°F)	Flight Condition
No.	BS				
1	43	195	150 Kn Left Turn	74	Ground Idle
2	57	101	150 Kn L/R Turn	46	126 Kn Rt Turn
3	71	126	Hover-Tail into Wind	59	90 Kn Lt Turn
4	86	183	Hover-Tail into Wind	56	"
5	101	188	Hover-Tail into Wind	57	126 Kn Rt Turn
6	121	194	20-Foot Hover	62	126 KN L/R Turn
7	141	169	10/20-Foot Hover	60	90 Kn Lt Turn
Note: The thermocouples were located on the upper surface of the boom, approximately 7 inches from the centerline on the right hand side					

Tail Gearbox Cyclic Accelerations

The primary purpose of measuring the cyclic accelerations at the tail rotor gearbox was to obtain a dynamic comparison between the standard metal AH-1G tail boom and composite tail boom. The lateral cyclic accelerations ranged from ± 2 to ± 20 g's at the gearbox for the conditions flown. The cyclic accelerations increase with speed and with maneuvers at low speeds. There were essentially no differences in the magnitudes of the cyclic accelerations between the composite tail boom and the metal tail boom. Table 14 gives the comparison of measured accelerations for several flight conditions.

The structural design criteria for the vertical fin did not indicate the high cyclic accelerations being imposed on the upper fin structure. The criteria gave only low aerodynamic loads on the fin structure above the gearbox attachment and for the fin trailing airfoil structure. The vertical fin fairing structure was not reinforced at an edge left by a clearance cutout of the fairing skin. The high vibration environment resulted in cracks developing in the fin skin above the tail rotor gearbox at this nonreinforced edge. Only a minor reinforcement in fin airfoil structure was required to provide adequate strength for the high vibratory environment. This structural change has subsequently been made.

TABLE 14. COMPARISON OF GEARBOX ACCELERATIONS

Flight Condition	Composite Tail Boom				Metal Tail Boom		
	cg Vertical	Gearbox Cyclic		cg Vertical	cg Vertical	Gearbox Cyclic	
		Vertical	Lateral			Vertical	Lateral
Ground Idle	1.00±0.07	±1.90	±1.07	1.04±0.13	±1.91	±2.87	
100% Flat Pitch	1.00±0.09	±1.50	±3.85	1.02±0.19	±1.36	±6.66	
Level 70 Kn	1.05±0.23	±1.08	±6.70	1.07±0.34	±1.91	±9.80	
Level 90 Kn	1.11±0.35	±5.38	±7.50	1.03±0.49	±2.18	±12.54	
Level 126 Kn	1.17±0.47	±2.63	±8.61	1.11±0.53	±2.99	±12.54	
Level 150 Kn	0.91±0.69	±6.38	±14.06	1.13±0.97	±3.54	±13.32	
Pedal Reversal at 126 Kn	1.00±0.56	±4.50	±13.20	1.15±0.60	±3.54	±12.28	
Pedal Reversal at 150 Kn	1.09±0.86	±3.80	±13.30	1.18±1.14	±3.54	±13.32	
Left Turn - 126 Kn	1.20±0.70	±2.63	±8.61	1.05±0.66	±2.18	±11.36	
Right Turn - 126 Kn	1.12±0.51	±2.63	±9.04	1.02±0.58	±2.73	±11.88	
Left Turn - 150 Kn	1.09±1.04	±6.75	±12.48	1.36±1.38	±4.91	±13.19	
Right Turn - 150 Kn	1.03±0.60	±6.75	±13.35	1.18±1.06	±5.18	±13.32	
Left Turn - 171 Kn	1.18±1.69	±4.80	±14.20	1.12±1.61	±4.50	±20.60	

Pilot Flight Evaluation

As part of the flight demonstration program, the pilot made a qualitative evaluation of vibration levels, stability and controllability for both the AH-1G standard configuration and the composite tail boom configuration. The pilot's evaluation was that no significant difference existed between the two configurations in these areas. The vibration levels were very high at speeds of 150 knots and above for both configurations, making a comparative evaluation very difficult. The high vibration level is substantiated by the high cyclic accelerations recorded at the tail rotor gearbox.

REVIEW OF DESIGN OBJECTIVES

GENERAL

A primary objective of the composite tail boom program was to design and manufacture a composite tail boom that would have a lower life-cycle cost than the present AH-1G metal tail boom. Two important parameters in establishing life-cycle costs are the initial cost and weight. Two study programs had been performed by Boeing Vertol and Kaman on fuselage advanced structural concepts (References 2 and 12). Both studies used the AH-1G tail boom as the model to apply design concepts. The studies indicated that a semi-monocoque sandwich structure was the optimum design concept and should produce a tail boom with a lower weight and initial cost, resulting in a lower life-cycle cost. The results of the study programs established the basic tail boom construction. HH used the wet filament winding technique for the fabrication of the sandwich inner and outer skins. This method was selected over the more prevalent fabrication techniques of hand or tape lay-up of prepreg material because of the potential cost savings in reducing the labor required. Both of the above studies established that graphite fibers should be used in the composite material to meet the stiffnesses of the metal AH-1G tail boom.

The composite tail boom met or exceeded the structural design criteria. The fatigue strength of the primary structure was exceptionally high, resulting in essentially an unlimited service life. The composite tail boom stiffnesses, lateral, vertical and torsional, were greater than the metal tail boom, which would allow the use of lower cost, lower modulus graphite fibers or the use of less graphite fibers that were used. The composite tail booms that were fabricated for structural testing and the flight demonstration had a higher initial cost and weight; the reasons for the weight and cost increases are discussed in detail in the subsequent paragraphs.

WEIGHT

A design objective was to fabricate the tail boom using simplified tooling and fabrication processes. The simplest method of wet filament winding is to impregnate the dry graphite rovings with the epoxy resin by feeding the rovings through a resin bath and then winding them directly on to the mandrel. Excess resin is to be removed, and the resulting composite should have a fiber volume of 50 percent. However, coupons removed from the tail boom indicated that the fiber volume varied from 42 to 47 percent (an average of 45 percent). This resulted in a weight penalty in the fabrication of the tail boom and the fin spar skins. The volume of the tail boom

inner and outer skins is 1080 cubic inches with a fiber volume of 50 percent. The composite fiber content is a fixed quantity and averages 45 percent of the volume of the actual composite; therefore, the actual volume of the skin composite was equal to $540/0.45 = 1200$ cubic inches or 120 cubic inches of excess resin. The density of resin is 0.0412 pound per cubic inch, and the weight penalty is $120 \times 0.0412 = 5.0$ pounds. The fin spar skin and the longo computed volume are 241 cubic inches, and the actual volume is 268 inches, resulting in 27 cubic inches of excess resin. The weight penalty is 1.1 pounds. A new, simple method was developed to control the impregnation of the dry roving with resin to produce a composite with the fiber volume varying from 50 to 54 percent and averaging 52 percent. Using the new fiber impregnation technique to fabricate the tail boom would save over 8 pounds of weight without reducing the structural integrity or stiffness of the tail boom.

The standard AH-1G pulleys, brackets, and hardware were used to install the tail rotor control system. This resulted in a weight penalty in the supporting structure which mounted the pulleys and brackets.

A review of the composite tail section shows several areas where additional weight could be reduced by design changes without sacrificing structural integrity or adding to the fabrication costs. Some of these design changes are described in the following section. The weight of the composite tail section is compared to the metal tail section in Table 15, also included in Table 15 is the anticipated weight of the advanced composite tail section.

COSTS

The wet-filament-winding technique proved to be a very cost-effective method to fabricate the skins for the tail boom sandwich wall construction. Filament winding is an automated fabrication method using a minimum of labor hours. Wet filament winding also uses composite materials at their lowest cost versus tape or hand lay-up that require the use of preimpregnated composite materials. The cost of prepreg material is two and one-half to three times the cost of dry composite filaments and resin purchased separately.

The two major items that increased the composite tail boom costs above the initial predicted costs were the price of the material and the labor costs involved in the installation of the reinforcements for the access holes, the sync elevator support, and the vertical fin spar support. The cost of Thornel 300 graphite fibers averaged 55 dollars a pound during the fabrication of the structural test and flight demonstration composite tail booms. The present price of Thornel 300 is approximately 42 dollars a pound, depending on the quantity purchased, and is expected to reduce in price to 20 dollars a pound by 1980. The fabrication method used to install the

AD-A034 457

HUGHES HELICOPTERS CULVER CITY CALIF

F/G 1/3

DESIGN, FABRICATION, AND TESTING OF ADVANCED COMPOSITE AH-1G TA--ETC(U)

NOV 76 J F NEEDHAM

DAAJ02-73-C-0079

UNCLASSIFIED

HH-76-50

USAAMRDL-TR-76-24

NL

2 OF 2
ADA034457



END

DATE
FILMED
2 - 77

TABLE 15. TAIL SECTION WEIGHT COMPARISON

Item	Composite Section Weight (lb)	Metal AH-1G Section (lb)	Advanced Design Approx. Wt. (lb)
Basic Boom Shell	91.3	-	75.3
Fin Spar	17.2	-	15.0
T/R Attach Fitting	6.5	-	4.5
Fwd. Attach Fittings	13.6	-	8.5
Bulkheads	9.5	-	7.0
Hole Reinforcements	24.8	-	22.3
Fin Aft Structure	21.5	-	20.5
Shelves	16.4	-	13.1
Drive Cover Attach Angles	13.6	-	10.9
Doors - Covers	15.5	-	14.0
Miscellaneous	16.8	-	10.8
	246.7	234.7*	203.0
*Measured weight of metal AH-1G tail section S/N 68-15031			

reinforcements for the access holes and sync elevator consisted of cutting the holes in the cured tail boom shell, removing the honeycomb core and inner skin to fit the reinforcement, adding fiberglass inner and outer doublers, and vacuum bagging and curing the installation. A new fabrication technique has been developed to fabricate the tail boom shell to its final contours on the winding mandrel. This will allow the access hole reinforcements to be incorporated with the honeycomb core and be placed together on the winding mandrel and cocured. The labor required to install the reinforcements will be grossly reduced and secondary curing operations will be eliminated. Additional cost and weight savings for the next-generation composite tail booms are discussed in the following section.

As previously stated, the initial cost of the composite tail boom was higher than projected. The composite tail boom is still competitive with the metal AH-1G tail boom if the accepted 85 percent learning curve is used to predict the cost at the 1000th tail boom. The projected cost of the tail boom would be \$9,470. (Refer to Figure 38.)

An advanced configuration utilizing several recommended changes and simplifications discussed in the following section would result in a tail boom projected cost of \$6,016 for the 1000th unit. (See Figure 38).

ADVANCED TAIL BOOM DESIGN

DISCUSSION

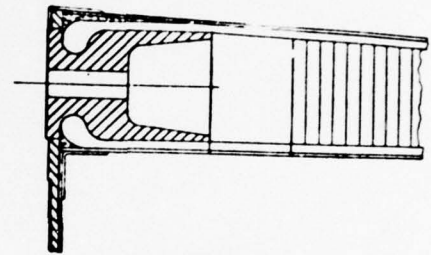
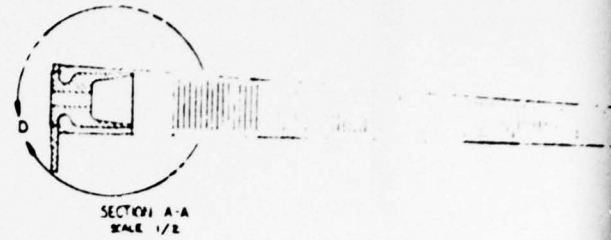
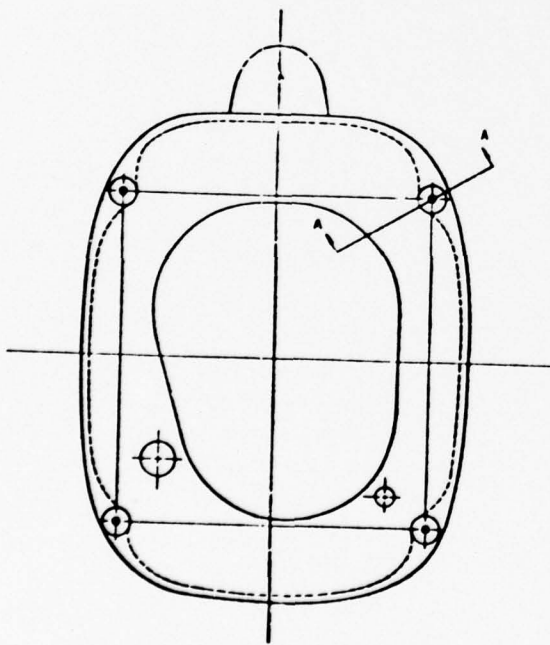
The composite tail boom fabricated for structural and flight testing successfully met the initial design criteria and design objectives. This program was the first helicopter program to design, fabricate and flight test a primary fuselage structural component. The design approach for the tail boom construction was very conservative, to assure that the strength and stiffness design requirements were met. This led to overly conservative designs in several areas of the boom and vertical stabilizer structure. In reviewing the final composite tail boom configuration, several design refinements or modifications, in addition to more emphasis on cocuring discussed in the preceding section, could be accomplished that would reduce the fabrication costs and/or the weight. The advanced tail boom design would continue to meet or exceed the structural and stiffness design requirements. The proposed design refinements and modifications to the composite tail boom are discussed in subsequent paragraphs. Figure 37 illustrates the major proposed design changes.

COMPONENT REDESIGN

Two areas of concern during the initial design phase of the composite tail boom were the forward four bolt attachments that attach the tail boom to the AH-1G aft fuselage and the attachment of the fin spar to the boom. Weight and costs may be saved in both areas by redesign.

The present composite boom retained the barrel nut configuration of the metal tail boom, which resulted in an oversized aluminum fitting for the composite tail boom (see Figure 16 & 26). By redesigning the end fittings to a hollow configuration and using standard nuts and washers a weight saving would be realized at no increase in cost (see Figure 37). Aluminum plates were added to the forward bulkhead to redistribute shear loads from the end fittings. The plates could be replaced by locally reinforcing the forward bulkhead with composite structure. The reinforced bulkhead would provide ample strength and would result in a net weight saving.

The fin spar is redesigned to a constant diameter tube that will provide several fabrication advantages. It eliminates the requirement for a female forming mold. The present support structure for the gearbox is composed of four separate components that are required to be fitted and bonded to each other and to the fin spar (refer to Figure 23). By using a constant diameter tube, a single aluminum support fitting for the gearbox could be attached to the spar while still on the winding mandrel (see Figure 37). The fin spar



DETAIL D
FULL SCALE

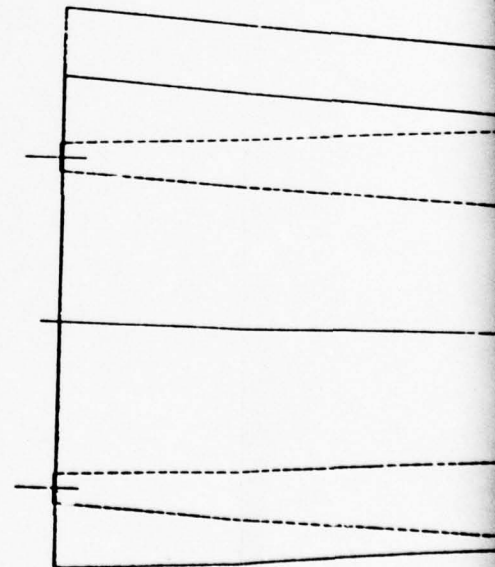
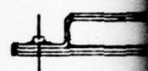
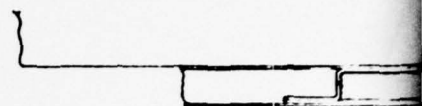
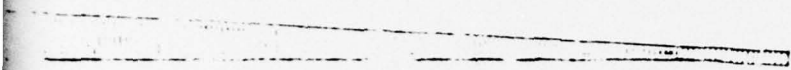
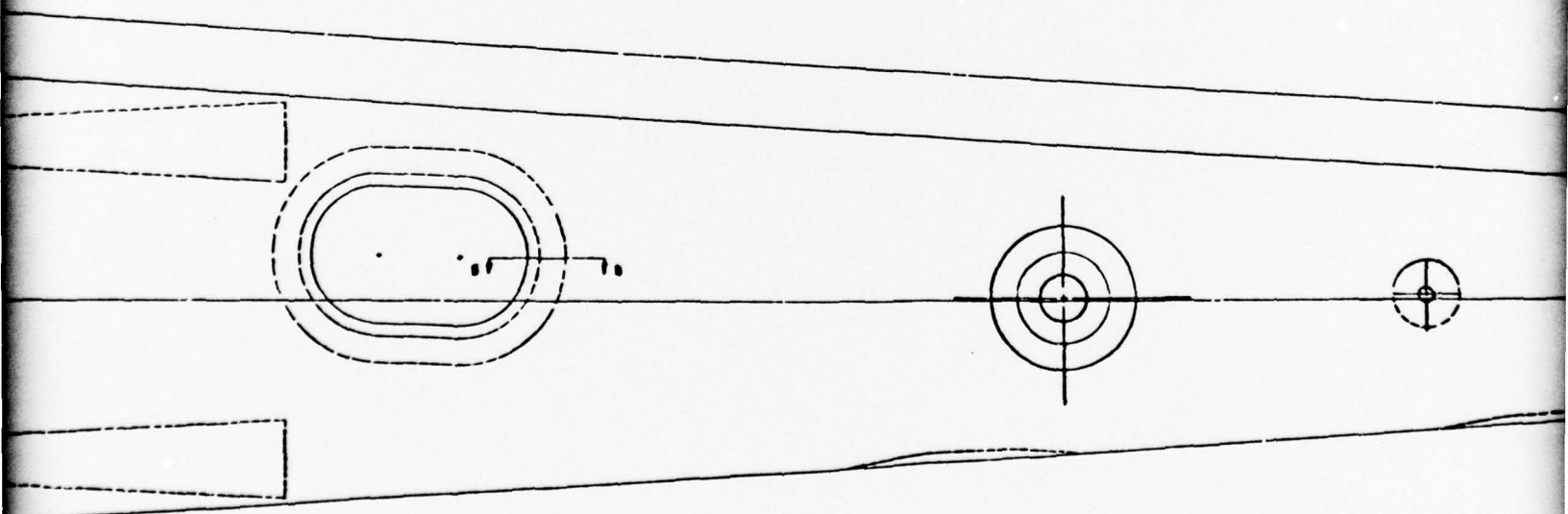


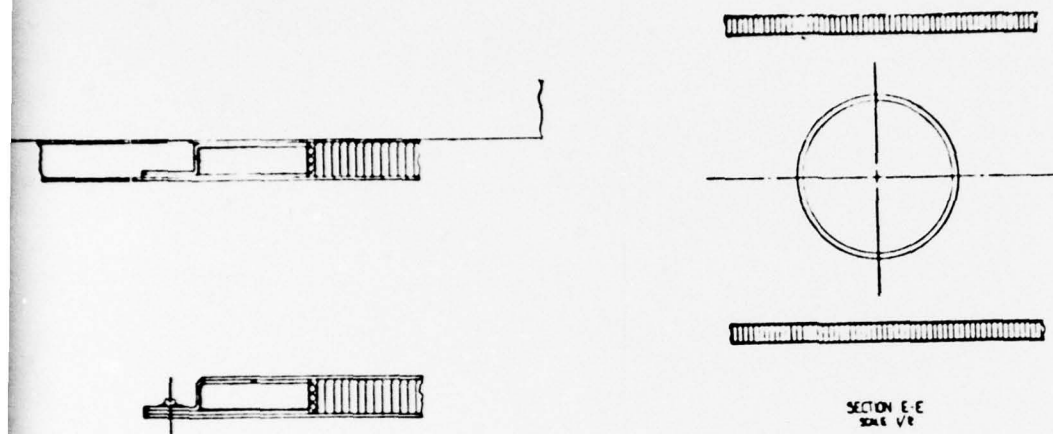
Figure 37. Advanced Tail Boom Design.



SECTION B-B
SCALE 1/2

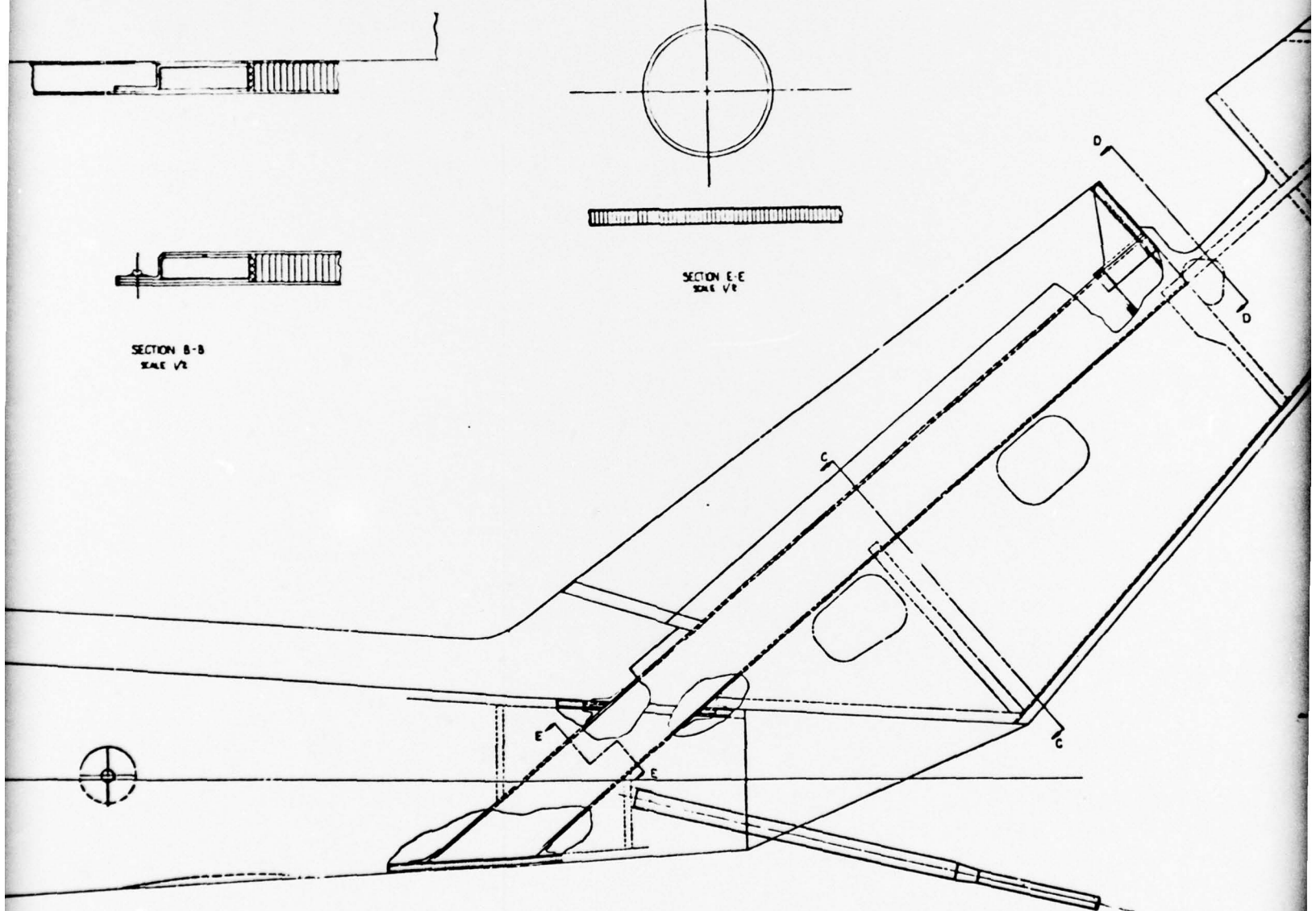


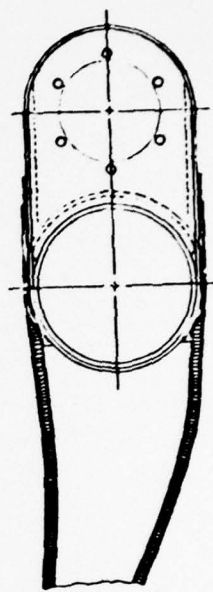
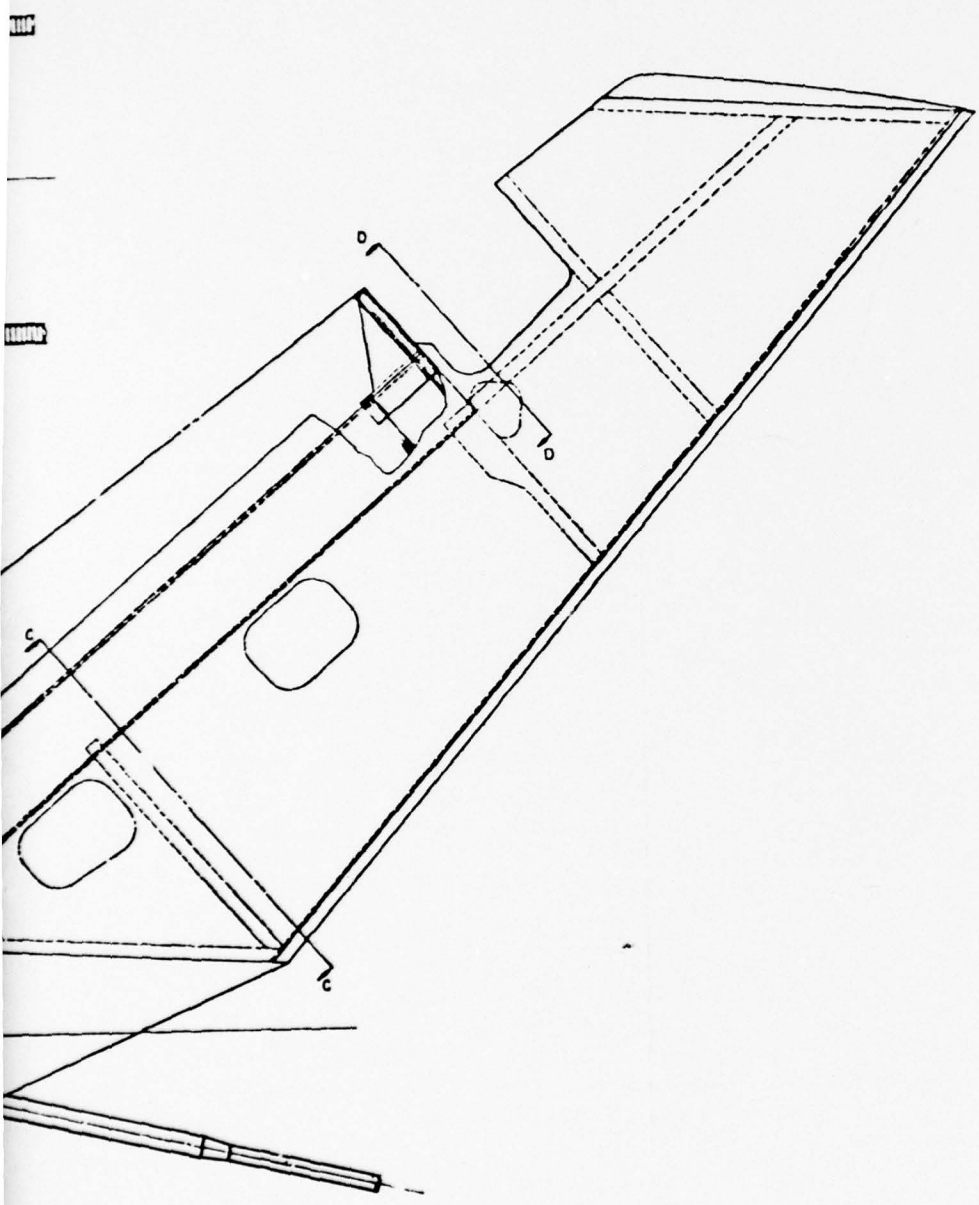
2



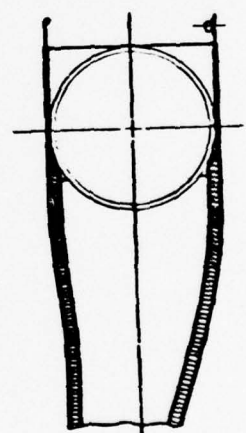
SECTION B-B
SCALE 1/2"

SECTION E-E
SCALE 1/2"





SECTION D-D
SCALE 1/2"



SECTION C-C
SCALE 1/2"

and support fitting would then be cured as a unit, resulting in a reduction in fabrication time. The constant outside diameter would simplify the design, fabrication and installation of the fin ribs, skins and control bracketry. The assembly would have a minimal weight reduction.

Eliminating the forward and aft cant bulkheads that are used in attaching the fin spar to the boom would save both weight and cost. In reviewing the vertical fin loads and the results of the boom structural tests, adequate strength could be obtained by attaching the fin spar to only the upper and lower boom structure. The main parameters contributing to the lateral stiffness at the tail rotor are the lateral and torsional stiffness of the tail boom and the fin spar stiffness. The present composite tail boom has excess stiffness both laterally and torsionally when compared to the metal AH-1G tail boom (refer to page 75). The redesigned structure would satisfy the initial stiffness design criteria to be within ± 10 percent of the metal tail boom stiffnesses.

TAIL BOOM CONSTRUCTION COST ESTIMATE

A production unit cost estimate was prepared for manufacturing the composite tail boom in production quantities. Two different approaches were taken in determining the probable unit cost. The first approach was to estimate the amount of time, and the number of people directly needed to perform each of 10 process steps required to fabricate the advanced design tail boom. This estimate data, called "touch-times" was prepared by HH/FSI engineering personnel and is presented in Table 16. The estimated times were based on the S/N 10 unit. Along with the touch-time labor estimate, an estimate was made of the materials needed for each process step, and the tools and fixtures required. Each of these items were priced, using both actual and projected cost data. For example, the 1974 graphite fiber price of \$55/lb incurred for the R&D tail booms was projected to be \$20/lb for future year production quantities. The advanced design manufacturing costs were determined by the extension of the estimated S/N 10 labor hours and material costs as shown in Table 17.

The second approach to determining production unit cost was to extend the measured unit cost of the R & D tail boom (Table 18) to production quantity units using standard 85 percent learning curve projection technique to determine labor hours. This cost estimate data, identified as "present design" on Figure 36, also included an adjustment for quantity purchase price and G&A/profit factors appropriate for manufacturing production. The measured initial unit cost of \$45,675 for the current design was determined from cost accounting records. This data established labor hours for the initial unit to be 1800 hours at \$15/hr burdened, with material costs of \$4500. The G&A and profit for this R&D fabrication added 45 percent to the

TABLE 16. PRODUCTION UNIT COST ESTIMATE -
ADVANCED DESIGN

Item	Tooling \$*	Material \$**	Labor Man-Hours Touch Time**
1. Boom Shell	64,000		
• Mandrel			16
• Honeycomb		300.00	40
• Winding		1400.00	16
2. Attach Fittings	12,000	110.00	24
3. Main Bulkhead	7,500	60.00	8
4. Door Doilies	10,000	100.00	16
5. Vertical Fin Spar	4,500	200.00	4
6. Assembly Fixture	5,500	-	8
7. Drive Shaft Covers	1,500	200.00	16
8. Miscellaneous Layups	60,000	100.00	88
9. Finishing	12,000	20.00	46
10. Miscellaneous	24,000	10.00	10
11. Preproduction Engineering and Planning	100,000	-	-
Totals	300,000	2500	292
*Estimated for a 48-month/1000 unit requirement			
**Estimated for S/N-10.			

TABLE 17. ADVANCED DESIGN-UNIT PRODUCTION
COST ESTIMATE CALCULATION TABLE

	S/N-1	S/N-10	S/N-100	S/N-1000
Material ①	3,500	2,500	2,500	2,000
Labor Hours ②	900	525*	305	180
At \$15.00/hr Burdened	13,500	7,875	4,590	2,700
G & A/Profit Factor ③	4,760	2,905	1,985	1,316
Totals - Dollars	21,760	13,280	9,075	6,016

① Per Table 16 (approximated for unit cost quantity)

② From 85% learning curve passing through 525 hrs for S/N-10

③ Factor equals 28% (18% G & A and 10% profit)

* Touch-time man-hours times realization factor equals production labor hours. Based on touch-time estimate (Table 16) of 292 m/hrs times 1.8 (realization factor that includes QA and scrap) equals 525 hrs for S/N-10

TABLE 18. INITIAL FABRICATION COSTS		
	Material (Dollars)	Labor (Man-Hours)
Boom Shell	2600	126
Attachment Fittings	86	144
Bulkheads	62	216
Door Reinforcements	714	450
Vertical Fin Spar	486	54
Fin Aft Structure	172	252
Shelves - Doors	197	126
Control Supports	86	198
Miscellaneous	97	234
	$\Sigma = 4500$	1800
Total Cost = $[1800 \times 15.00 + 4500] \times (G/A / \text{Profit Factor}) = \$45,675.00$		

basic labor and materials costs. From this data, the labor hours were extended on a serial unit basis using an 85 percent learning curve projection. The material costs were approximated on a unit cost basis following a decreasing cost pattern; the same as used for the advanced design. A G&A and profit factor of 28% was used for the projected production quantities.

Figure 38 presents a comparison of estimated manufacturing unit costs for both the current design and the advanced design. An additional cost must be added to each unit cost to cover the nonrecurring production costs associated with engineering, tooling and planning of the production unit. These costs which total \$300,000 must be allocated based upon a set of assumed conditions for production such as total quantity ordered, span time for producing these units, facilities used, etc. Based upon an order quantity of 1000 units, this would add approximately \$300 to each unit cost shown.

For comparison with the present metal AH-1G boom shell, quoted by the Army to be \$17,000, the unit cost of S/N 1000 of the current design composite tail boom would be \$9,470, and the unit cost of S/N 1000 of the advanced design composite tail boom would be \$6016.

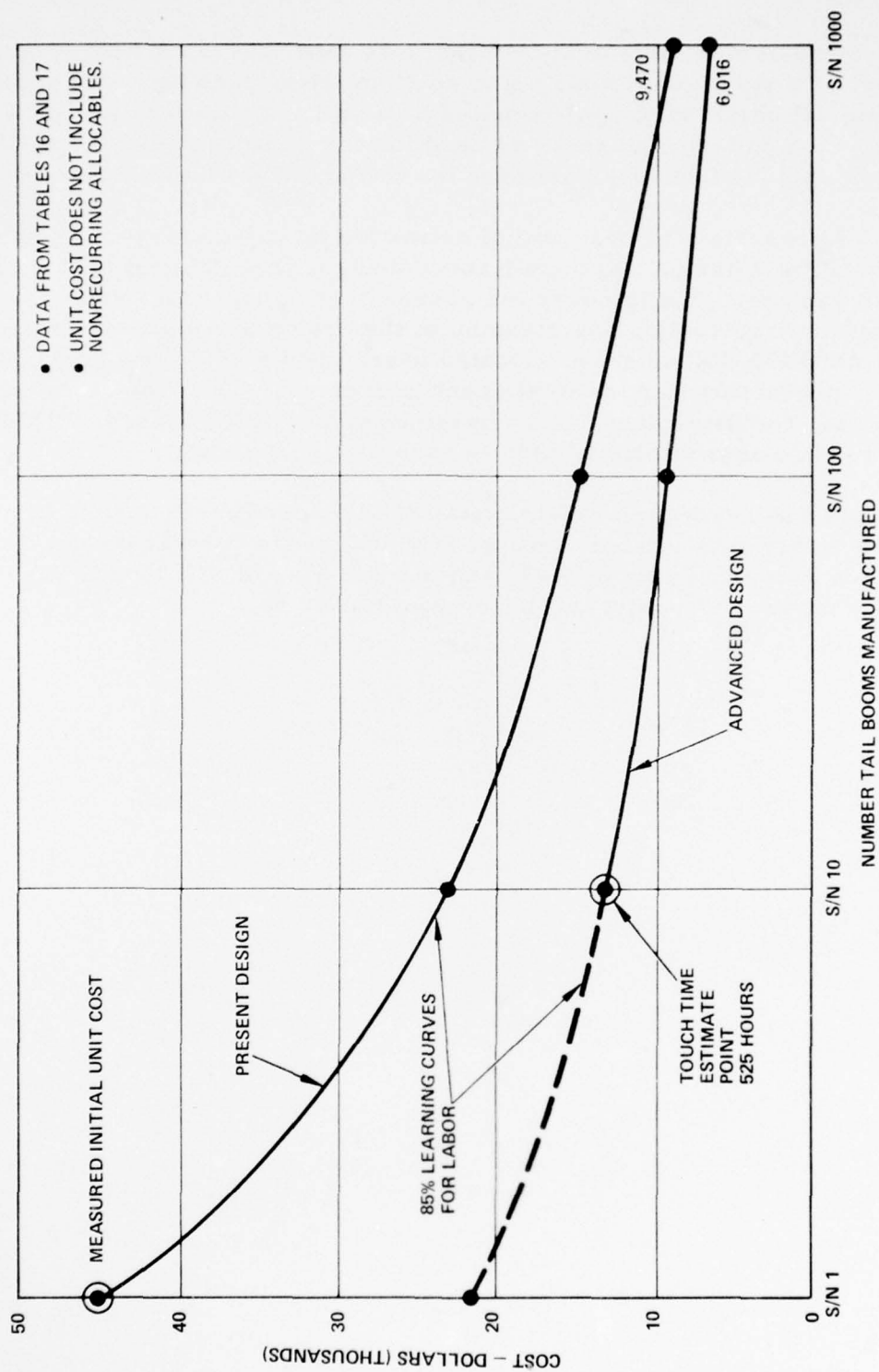


Figure 38. Manufacturing Unit Cost Estimates - Composite Tail Boom.

RECOMMENDATIONS

It is recommended that:

1. A failure mode and effect analysis (FMEA) be performed on the advanced tail boom design. This analysis should include, but not be limited to, predictions of mean time between failures, removal rate, replacement rate, scrap rate and repair rate.
2. The maintainability characteristics of the advanced tail boom design be determined. As a minimum, the mean time to repair, maintenance man-hours per flight hour, maintenance level, and personnel skill level required should be estimated.
3. The limits of repairability be determined, types of materials to be used, repair techniques be established for the advanced tail boom design. A prototype repair list(s) would be developed along with detailed description of different types and locations where realistic repairs could be incorporated.
4. Approximately ten tail booms of the advanced design be fabricated. The tail boom would incorporate any modifications and/or refinements to improve reliability and/or maintainability determined under items 1, 2, and 3.
 - a. Use two of the tail booms for additional structural and flight testing. Included in the structural testing would be induced simulated field damage such as foreign object impact, ballistic impact, rough handling, etc. Utilizing the repair techniques and materials developed in item 3, make repairs to all damaged areas. The full-scale structural tests would be repeated and the test results compared to the undamaged test data.
 - b. Install the remaining eight composite tail booms on AH-1G helicopters to obtain in-service data. The collected data would include maintainability, reliability, repairability, repair rates, types of field damage and environmental effects on composite tail booms.

REFERENCES

1. Ambrose, E., Clarke, D., TAIL BOOM, VERTICAL FIN AND HORIZONTAL STABILIZER STRUCTURAL ANALYSIS, MODEL 209 (AH-1G), Bell Helicopter Company, Technical Report 209-099-056, January 23, 1967.
2. Mayerjak, R., Smyth, W., INVESTIGATION OF ADVANCED STRUCTURAL CONCEPTS FOR FUSELAGE, Kaman Aerospace Corp., USAAMRDL Technical Report 73-72, Eustis Directorate, U.S. Army Air Mobility Research and Development Laboratory, Fort Eustis, Virginia, October 1973, AD773597.
3. HANDBOOK OF FIBERGLASS AND ADVANCED PLASTIC COMPOSITES, VanNostrand-Reinhold Company, August 1969.
4. STRUCTURAL SANDWICH COMPOSITES, Department of Defense, MIL-HDBK-23A, December 30, 1968.
5. Gerard, G., HANDBOOK OF STRUCTURAL STABILITY, Part 1 - 'Buckling of Flat Plates', NACA TN-3781, July, 1957.
6. PLASTICS FOR FLIGHT VEHICLES, Part I - Reinforced Plastics, Department of Defense, MIL-HDBK-17, November 5, 1959.
7. COMPOSER PROGRAMS PROP II, STRENGTH AND BUCK, Fiber Science Incorporated, Gardena, California.
8. Francis, P., Ko, W., SURVEY OF THE LITERATURE ON STRENGTH CHARACTERIZATION OF FIBER REINFORCED COMPOSITE MATERIALS, AFOSR Scientific Report, AFOSR-TR-71-2437, November 1970.
9. Roark, R.J., FORMULAS FOR STRESS AND STRAIN, McGraw-Hill Book Company, Fourth Edition.
10. Johnson, J.W., AERODYNAMIC COEFFICIENTS AND LOADS, MODEL 209 (AH-1G) Report No. 209-099-053, Bell Helicopter Company, January 1967.
11. Bronstad, M., EXTERNAL DESIGN LOADS FOR THE AH-1G TACTICAL HELICOPTER, MODEL 209 (AH-1G) Bell Helicopter Company, Report No. 209-099-054, January 1967.

12. Swatton, S., STUDY OF ADVANCED STRUCTURAL CONCEPTS FOR FUSELAGE, The Boeing Vertol Co., USAAMRDL Technical Report 73-69, Eustis Directorate, U.S. Army Air Mobility Research and Development Laboratory, Fort Eustis, Virginia, October 1973, AD772708.
13. Adaska, W., QUALIFICATION LOAD LEVEL SURVEY FOR IMPROVED MAIN ROTOR BLADES ON THE MODEL AH-1G HELICOPTER, Bell Helicopter Company, Report No. 209-099-305.
14. Quinn, J.R., CONTROL SYSTEM LOAD AND OPERATION TEST AH-1G (Bell) COBRA COMPOSITE TAIL BOOM FLIGHT TEST VEHICLE, Hughes Helicopters Report No. 150-BT-2004, October 1975.

APPENDIX A
SECTION PROPERTIES COMPUTER PROGRAM "SECPRO"

A computer program was developed to calculate the bending and torsional stiffness of closed structures made of sandwich wall construction. The program was developed by Fiber Science, Inc. and is entitled "SECPRO." The computer program nomenclature is given in Figure A-1. Typical elements of a cross section are given in Figure A-2. Typical input data for the structure cross section are given in Table A-1 and the resulting output data are given in Table A-2.

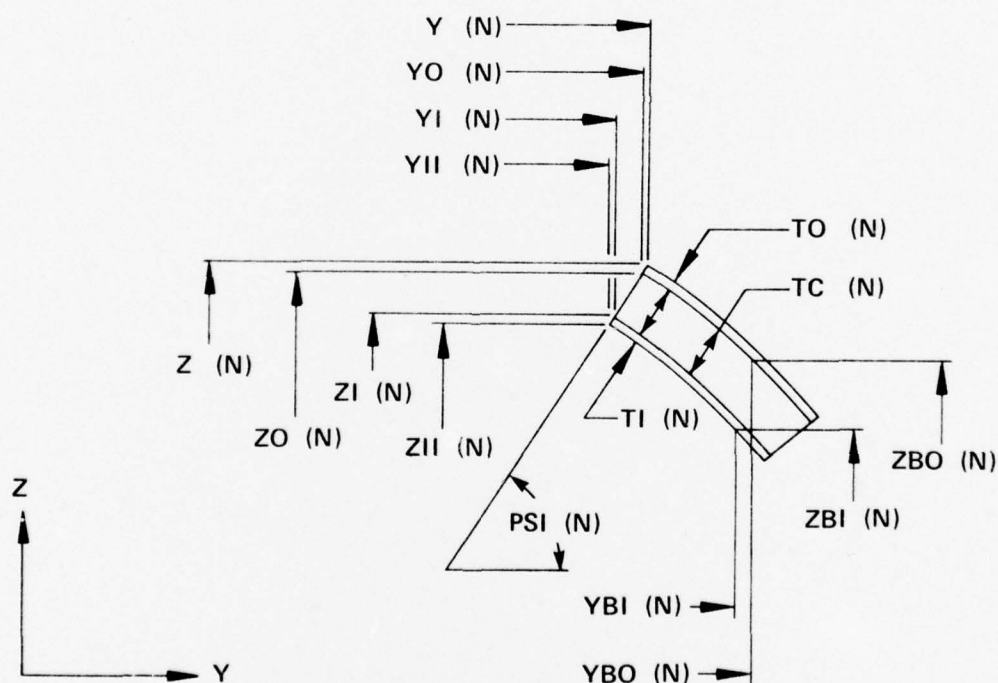


Figure A-1. Computer Program "SECPRO" Nomenclature.

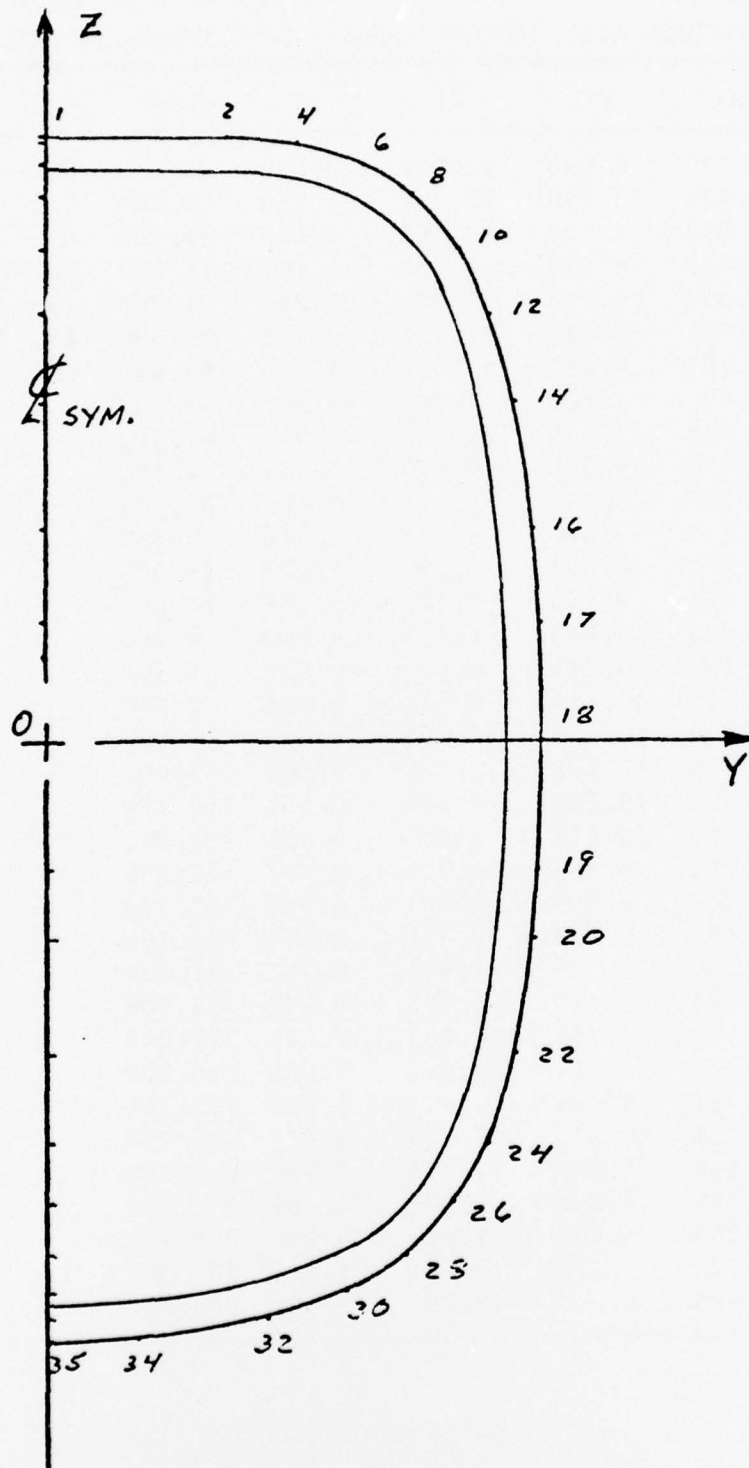


Figure A-2. Section Elements BS 122.33.

TABLE A-1. INPUT DATA - TAIL BOOM BS 122.33

N	ZO	YO	ZI	YI	PSI		
1	12.970	0.000	12.280	-0.000	90.000	TO	0.0320
2	12.970	3.750	12.280	3.750	90.000	TO	0.6250
3	12.950	4.500	12.262	4.442	85.200	TI	0.0330
4	12.845	5.238	12.168	5.103	78.750	EO	1.082E+07
5	12.655	5.954	12.000	5.737	71.700	GO	1.309E+06
6	12.393	6.645	11.768	6.352	64.900	EI	8.726E+06
7	12.155	7.080	11.572	6.710	57.600	GI	2.071E+06
8	11.694	7.669	11.180	7.208	48.100		
9	11.340	8.033	10.883	7.516	41.500		
10	10.533	8.630	10.170	8.046	32.200		
11	9.835	8.990	9.586	8.368	25.700		
12	9.185	9.290	8.941	8.645	20.750		
13	8.240	9.592	8.056	8.927	15.500		
14	7.264	9.830	7.123	9.155	11.800		
15	6.042	10.045	5.944	9.362	8.200		
16	4.548	10.215	4.482	9.528	5.500		
17	2.550	10.354	2.619	9.665	2.600		
18	0.000	10.415	0.000	9.725	0.000		
19	-2.768	10.355	-2.732	9.666	357.000		
20	-4.264	10.238	-4.194	9.552	354.200		
21	-5.512	10.078	-5.408	9.396	351.300		
22	-6.735	9.845	-6.583	9.172	347.250		
23	-7.708	9.593	-7.501	8.935	342.500		
24	-8.655	9.240	-8.375	8.609	336.100		
25	-9.316	8.915	-8.981	8.312	331.000		
26	-9.960	8.515	-9.563	7.950	324.900		
27	-10.552	8.054	-10.081	7.549	317.000		
28	-11.070	7.514	-10.545	7.066	310.500		
29	-11.524	6.915	-10.947	6.537	303.250		
30	-11.893	6.270	-11.277	5.959	296.750		
31	-12.190	5.585	-11.543	5.346	290.250		
32	-12.493	4.636	-11.825	4.463	284.400		
33	-12.750	3.400	-12.069	3.291	279.100		
34	-12.920	1.912	-12.231	1.867	273.700		
35	-12.975	0.000	-12.285	0.000	270.000		

TABLE A-2. OUTPUT DATA - TAIL BOOM BS 122.33

N	Element Area and Arc Length				Cross-Sectional Properties	
	AO	AI	LO	LI		
2	0.1200	0.1237	3.7500	3.7500	ZB =	0.2450
3	0.0240	0.0229	4.4989	4.4439	AO =	2.5549
4	0.0238	0.0221	5.2426	5.1135	AI =	2.4985
5	0.0236	0.0217	5.9814	5.7715	A =	5.0534
6	0.0236	0.0218	6.7185	6.4306	AIC =	429.9223
7	0.0158	0.0135	7.2123	6.8407	AOC =	481.0126
8	0.0238	0.0210	7.9576	7.4771	LO =	79.8404
9	0.0162	0.0142	8.4635	7.9074	LI =	75.7118
10	0.0319	0.0294	9.4607	8.7980	EA =	4.945E+07
11	0.0238	0.0221	10.2046	9.4673	EIYO =	2.512E+09
12	0.0243	0.0232	10.9648	10.1707	EIYI =	1.790E+09
13	0.0317	0.0307	11.9554	11.1011	EIY =	4.302E+09
14	0.0321	0.0317	12.9589	12.0622	EIZO =	1.795E+09
15	0.0397	0.0395	14.1987	13.2606	EIZI =	1.252E+09
16	0.0481	0.0486	15.7016	14.7826	EIZ =	3.047E+09
17	0.0641	0.0650	17.7036	16.7013	GKO =	4.856E+08
18	0.0816	0.0832	20.2536	19.2215	GKI =	6.674E+08
19	0.0886	0.0902	23.0214	21.9549	GK =	1.153E+09
20	0.0480	0.0484	24.5212	23.4225	WC =	0.26480
21	0.0402	0.0404	25.7786	24.6466	WF =	0.11827
22	0.0398	0.0395	27.0225	25.8440	WA =	0.03204
23	0.0321	0.0313	28.0263	26.7933	W =	0.41512
24	0.0323	0.0309	29.0351	27.7288		
25	0.0235	0.0223	29.7703	28.4054		
26	0.0242	0.0227	30.5267	29.0919		
27	0.0239	0.0217	31.2748	29.7494		
28	0.0239	0.0222	32.0213	30.4214		
29	0.0240	0.0220	32.7709	31.0878		
30	0.0237	0.0220	33.5122	31.7545		
31	0.0238	0.0221	34.2570	32.4248		
32	0.0319	0.0306	35.2525	33.3532		
33	0.0403	0.0396	36.5124	34.5524		
34	0.0479	0.0473	38.0086	35.9866		
35	0.0612	0.0617	39.9204	37.8559		

APPENDIX B

AH-1G COBRA TAIL BOOM

FOUR BOLT AND VERTICAL FIN ATTACHMENT TEST

PHASE II

OBJECTIVES

The objectives of this program are:

1. To substantiate the static strength of the forward attachment fittings and the local structure containing these fittings.
2. To substantiate the static and fatigue strength of the fin spar attachment to the tail boom.

SUMMARY OF RESULTS

Two tail boom sections (Specimens A and B) were tested under various loading conditions. The failures encountered were not in the areas of the boom under test, so that the actual strength of the forward attachment fittings and the fin spar to boom attachment could not be established. However, Specimen B failed at the design ultimate load, indicating that the strength of the attachments was in excess of the design ultimate load.

TEST SPECIMEN

Test Specimen A was used to determine the static strength of the forward attachment. This was a scrap part, which had been used by the manufacturer, Fiber Science Incorporated, as a tool check part. Test Specimen B was fabricated specifically for these static and fatigue attachment tests.

The test specimens consisted of a fuselage tail boom and vertical tail fin assembly. The tail boom section consisted of a double shell, filament-wound, composite fiber sandwich type monocoque structure composed of Thornel-300 type graphite fiber and a Nomex honeycomb core. The vertical tail fin assembly consisted of a filament-wound skin and a deformed filament-wound spar. The fuselage section and vertical tail fin assembly were permanently attached.

TEST LOCATION

These tests were conducted at the Hughes Helicopters Structures Test Laboratory, Culver City, California, during the period of 14 May 1974 through 24 June 1974.

TEST SETUP

Each tail boom section (Specimens A and B) was mounted to the test fittings by means of a tension bolt fastened into a barrel nut contained in each of the four attachment fittings. These bolts were torqued to 1,100-1,300 inch-pounds.

Each test load train contained a hydraulic actuator and load cell. For the static tests, the actuators were hydraulically activated by means of hand-pumps. The load cells, read out by a strain indicator, were used to monitor the load.

Fatigue loads were applied to Specimen B by utilizing servo valve controlled load actuators. A continuous trace of load versus cycles was recorded.

For the static tests, deflection wires were strung from the test specimens either to spring loaded dial indicators or over a pulley system which routed each wire across a sheet of graph paper mounted to a wooden frame. A weight was fastened to the end of each wire to eliminate sag. Metal tabs were clamped to the wires for use as pointers. During testing, pointer travel, which indicated specimen movement, was marked on the graph paper at each increment of load.

The Specimen A tail boom section was mounted in the fixture as shown in Figure B-3. Test load and deflection locations are indicated in Figure B-1. Local reinforcement of the skin at the loading station was required. This was accomplished by bonding a wooden block on the inside of the boom using fiberglass layup. A nylon sling was wrapped around the boom at this station and secured to the loading cylinder.

The Specimen B tail boom section was mounted in the test fixture as shown in Figure B-5. Vertical load was introduced to this specimen through a nylon sling arrangement similar to that of the Specimen A static test. The lateral loading system was pin connected to a plate bonded to the fin spar. The loading stations and the location and type of instrumentation required for Specimen B are shown in Figure B-2. Axial strain gages were bonded to this specimen and their locations are also shown in Figure B-2. During the static tests, the output of these gages was recorded by means of a strain indicator. The static and fatigue load requirements for Specimen B are given in Table B-1.

TEST PROCEDURE AND RESULTS

1. Specimen A. Static load was applied to the specimen, in the increments shown in Figure B-1, and deflections were recorded. Failure occurred at an applied load of 3,195 pounds. The failure, shown in Figure B-4, is located at about Station 64 on the compression sides of the boom (bottom and right side, looking forward). The test data is shown in Figure B-1.
2. Specimen B.
 - a. Natural Frequency Tests. Before each load test, the vertical and lateral natural frequencies of the test specimens were determined by applying a sharp enough blow ("banging") to the specimens to record its natural frequency in a particular direction. An accelerometer was located on the boom in the spar area and a brush recorder was used to record the accelerometer trace. No significant changes of the vertical or lateral natural frequencies of the test specimen were noted.

- b. Limit Proof Tests. For the limit proof tests, load was applied incrementally to the limit load. The P_z load increment was applied first and then the P_y load increment. Deflections and strain gage readings were recorded at each load level. Test loading conditions A and B were completed successfully, and the deflections and strains for 100 percent limit load are tabulated in Table B-2.
- c. Fatigue Test. The cyclic P_z fatigue loads were applied at a rate of 1 cps, which was twice the rate of application of the cyclic P_y fatigue loads. A total of 5,000 cycles of P_z loads and 2,500 cycles of P_y loads were applied to the specimen. Some fiber delamination occurred on the compression side of the boom during the first 1,300 cycles. However, after these early cycles, no other damage or increase in the original damage was noted.
- d. Failure Test. Load Condition A was selected for the failure test. Load was applied in the same manner and sequence as for the limit proof test. However, failure of the spar occurred at limit load after sustaining it for about 2 minutes. The origin of failure was approximately 13 inches up from the top of the boom on the right or compression side.

It appeared that shearing of the fiber bonding agent precipitated fiber instability failure. Figure B-6 shows the spar failure. It was subsequently determined that a circumferential wrap of the spar had been inadvertently left off and this omission had caused the premature spar failure.

The spar was repaired by wrapping and bonding fiberglass fabric around the damaged area. Testing was then resumed to failure, which occurred at 150 percent limit load. The right and bottom sides of the boom failed in compression. The damaged area ran from Station 36 on the right side and spiraled around to the tension or left side of approximately Station 48. Figure B-7 shows the failed boom.

TABLE B-1. TEST LOADING CONDITIONS,
TAIL BOOM SPECIMEN "B"

1. Static

Load Condition	Limit Load ~ Pounds	
	P_y	P_z
"A" Yaw +15° Recovery	-2800	1200
"B" Yaw -15° Recovery	2000	1200

P_y Loads are positive, acting to left looking forward

P_z Loads are positive, acting down

2. Fatigue Spectrum

A. Loads

$P_y = -240 \pm 1440$ pounds for 2500 cycles

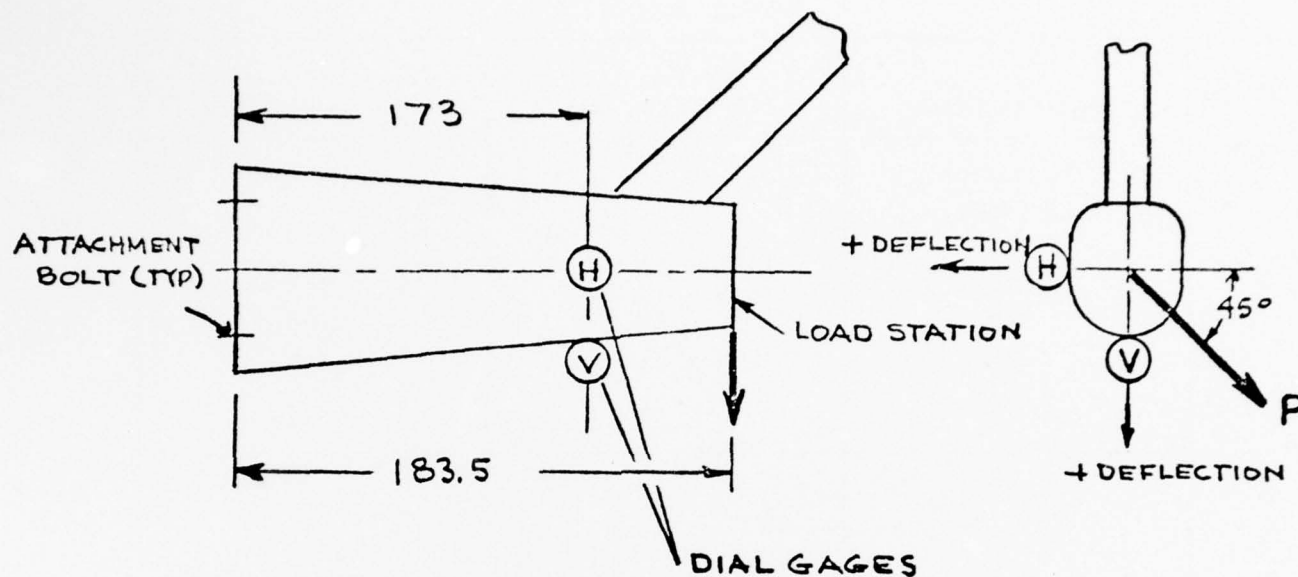
$P_z = 360 \pm 360$ pounds for 5000 cycles

B. Phasing

Load Identification	Load ~ Pounds		
	Max	Mid	Min
Lateral P_y	-1680	-240	1200
Vertical P_z	720	360	0

TABLE B-2. TEST RESULTS AT 100 PERCENT LIMIT LOAD,
TAIL BOOM "B"

Test Condition	A +15° Yaw, Rec	B -15° Yaw, Rec
Deflection Inches		
A	-5.30	3.68
B _T	-2.29	1.62
B _B	-1.91	1.37
C	.53	.53
Strain* μ-in./in.		
1	1300	-510
2	-825	1150
3	970	-1155
4	-1620	600
5	2850	-2200
6	-2830	2250
<p>*Positive strains are tension. Deflection and strain gages are identified in Figure B-2.</p>		



TEST LOAD P (LBS)	DEFLECTION ~ INCHES	
	H	V
0	-	-
500	0	0
1000	-.21	.34
1500	-.47	.52
2000	-.69	.90
2500	-.92	1.15
2700	-1.02	1.26
3000	-1.18	1.42
3195	FAILURE	

TEST DATE 5-14-74

Figure B-1. Test Load and Deflection Locations and Test Results, Tail Boom Specimen 'A'.

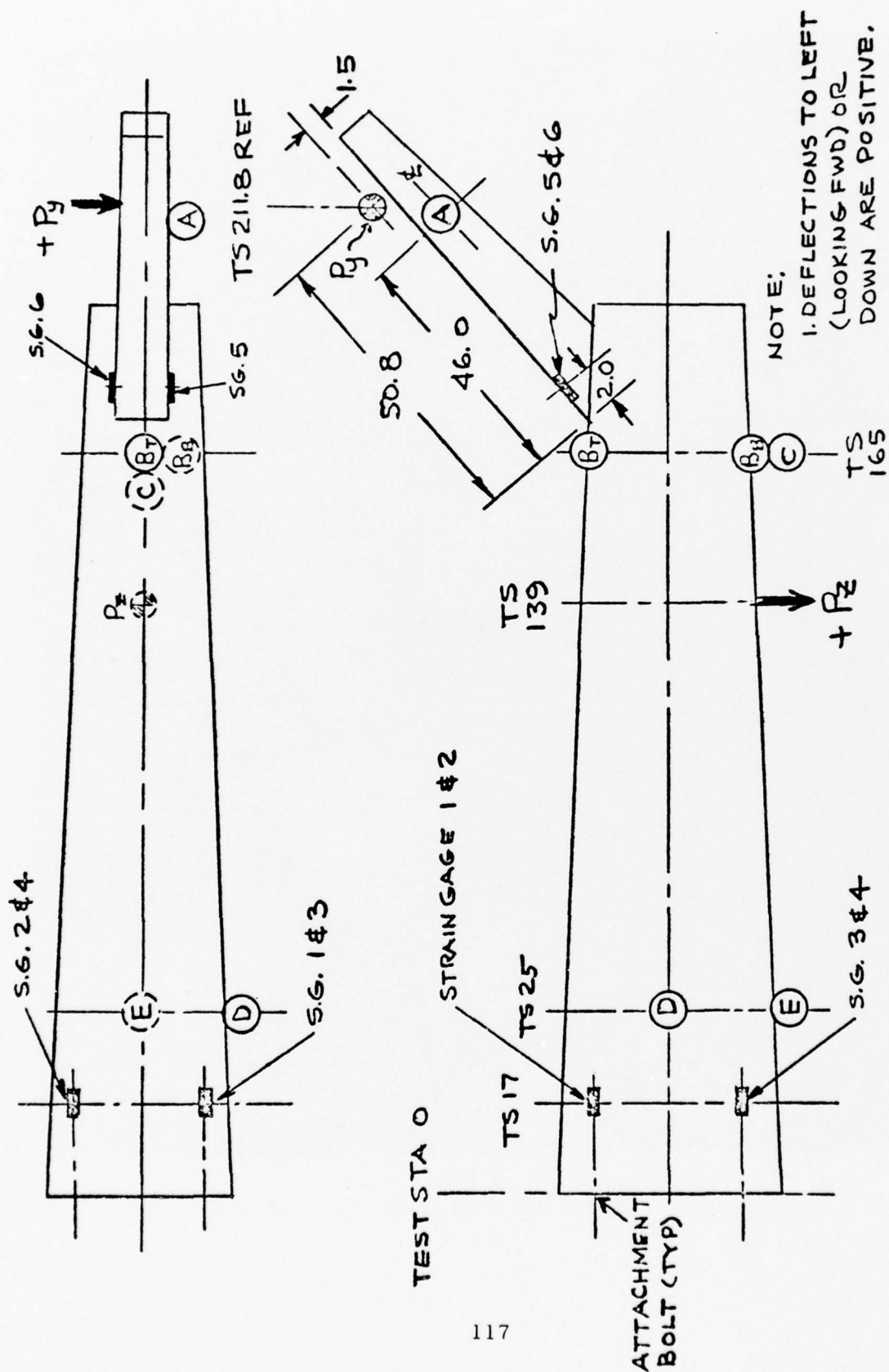


Figure B-2. Load Stations and Instrumentation, Tail Boom Specimen "B".

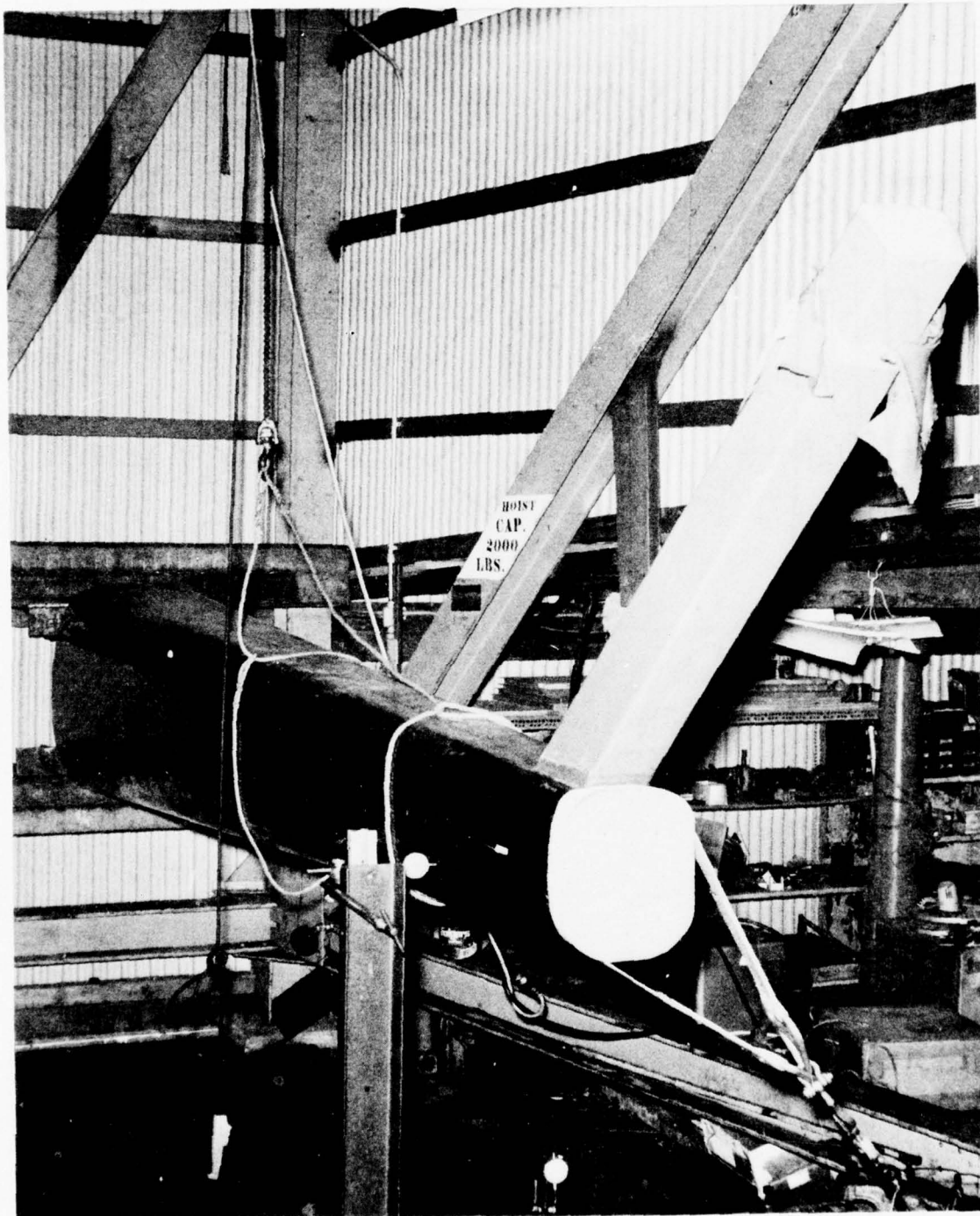


Figure B-3. Test Setup Tail Boom Specimen A.



Figure B-4. Failure Tail Boom Specimen A.

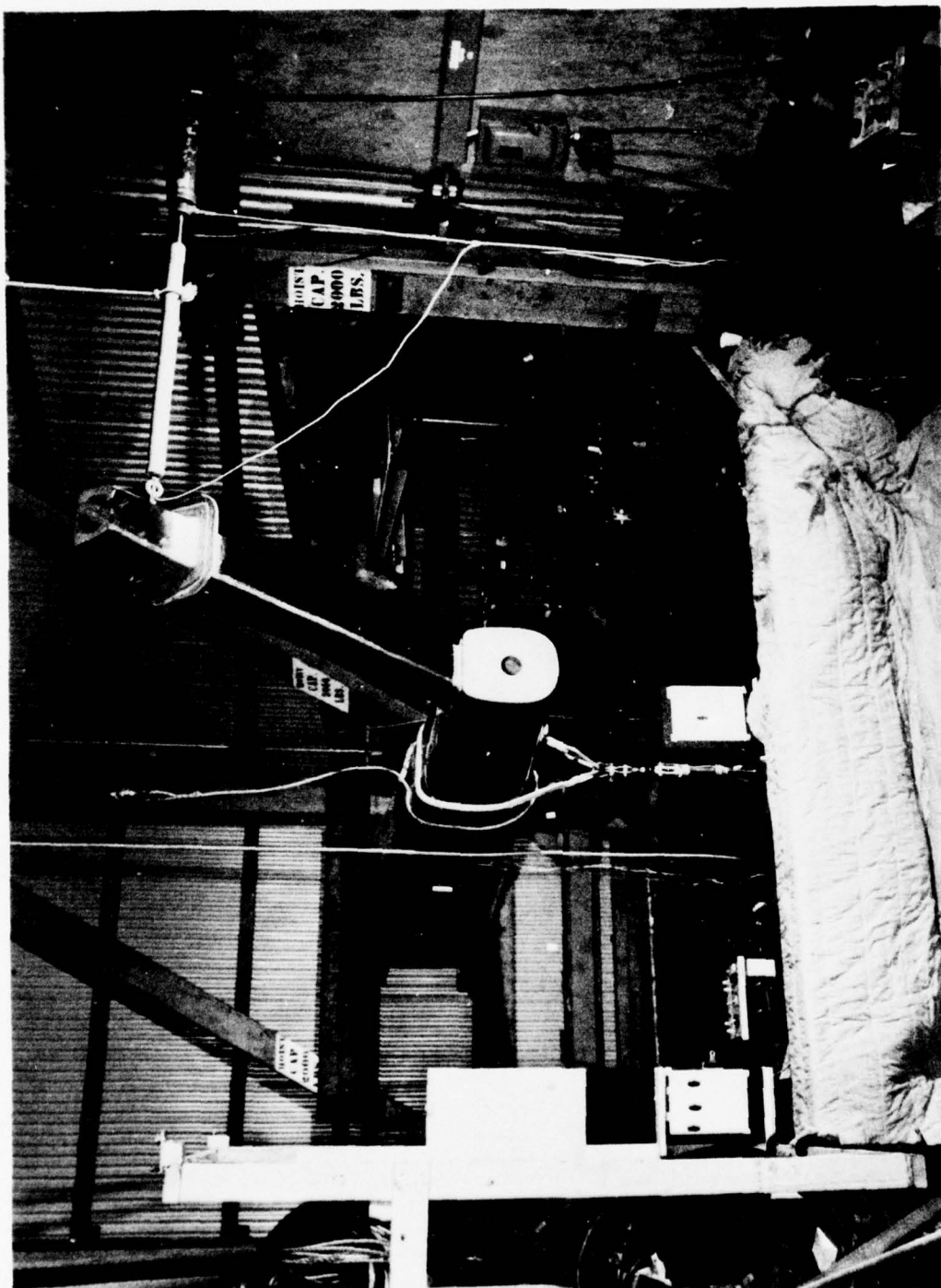


Figure B-5. Test Setup, Tail Boom Specimen B.



Figure B-6. Spar Failure, Right Side.

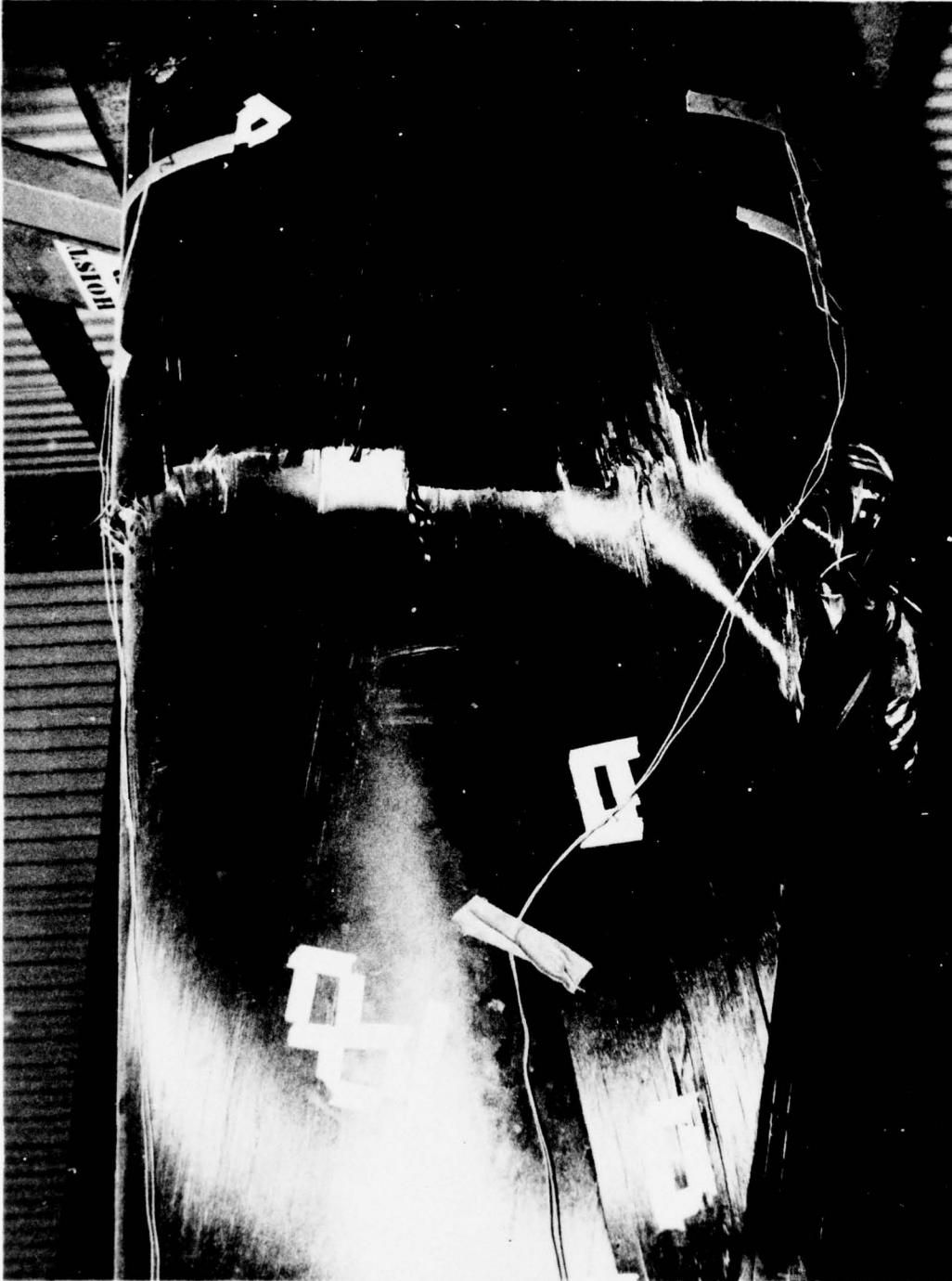


Figure B-7. Boom Failure, Right Side.

APPENDIX C

AH-1G COBRA TAIL BOOM

STRUCTURAL TEST AND EVALUATION

PHASE III

OBJECTIVES

The objectives of this test program are:

- To determine the structural integrity of the composite tail boom for static and fatigue loading conditions.
- To determine the bending and torsional boom stiffness.

INTRODUCTION

As per Contract No. DAAJ02-73-C-0079 and in accordance with Engineering Test Request No. AH-BT-01, one 465P-050 basic tail boom test specimen was subjected to a series of static and fatigue loads and dynamic natural frequency tests. These tests were conducted at the Hughes Helicopters Structures Test Laboratory, Culver City, California, during the period 8 October 1974 through 3 December 1974.

SUMMARY

One basic composite tail boom test specimen was subjected to a series of design limit load static tests, dynamic natural frequency ("bang") tests, a fatigue test, and a series of selected static tests, which included a simulated bolt-failure test, a simulated bullet-hole damage test, and a steel ball damage test. During the fatigue test, some localized movement was noted between the lower left-hand and lower right-hand attachment fittings and the tail boom structure. No apparent damage was noted while conducting the fatigue tests or during the other tests. The basic tail boom test specimen was still capable of carrying the test loads when testing was terminated following completion of all the tests. Table C-1 presents a summary of the complete test program.

DISCUSSION

TEST SPECIMEN

The test specimen, Part No. 465-050, consists of the basic fuselage tail section (tail boom and vertical tail fin assembly) - less doors, drive shaft, tail skid, elevator and tail rotor controls, fairings, and cover installations. Door cut-outs, however, were constructed in the specimen. The tail boom section is constructed of a double-shell, filament-wound composite fiber sandwich-type monocoque structure composed of Thornel 300 graphite fiber in an epoxy material and a Nomex honeycomb core. The vertical tail fin is also a sandwich construction consisting of graphite/epoxy skins and Nomex honeycomb core with longitudinal graphite fibers on the four corners of the spar. The fuselage section and vertical tail fin assembly are permanently attached.

A 1.31-inch-diameter aluminum tube (0.25 inch wall) was installed in the fuselage section to simulate the stabilizer support installation and was used to apply the stabilizer loads. Fittings were attached to the specimen at particular locations to apply the other test loads.

A schematic of the test specimen, with the location of these fittings and load points, is presented in Figure C-3.

TEST SETUP

1. General. The tail boom test specimen was mounted to a load reaction fixture by means of four NAS 628 attachment bolts. Each bolt was installed through the reaction fixture and into a barrel nut attachment in the test specimen. Each bolt was torqued to 1100-1300 inch-pounds.

Loads were applied to the specimen by means of six load trains that contained a hydraulic actuator and a load cell in each train. The sync elevator loads (P_{z1} and P_{z2}) were applied by two load trains, each attached to one end of the sync elevator support tube. The vertical and horizontal aft inertia loads (P_{z3} and P_{y3} , respectively) were applied by two load trains installed at the aft end of the tail boom specimen. The fin pressure loads (P_{y2}) and tail rotor thrust loads (P_{y1}) were applied by two load trains installed on the tail fin assembly. The location of these six load trains is schematically shown in Figure C-3.

2. Static Tests. For the design limit load and selective static tests, the actuators were hydraulically activated by means of an Edison Load Maintainer. The load cells, read out by a strain indicator, were used to monitor the test loads. Deflection wires were attached to the test specimen either from spring loaded dial indicators or over a pulley system which routed each wire across a sheet of graph paper mounted to a wooden frame. A weight was fastened to the end of each wire to eliminate sag. Metal tabs were clamped to the wires for use as pointers. During testing, pointer travel, which indicated specimen movement, was marked on the graph paper at each increment of load. These deflection measuring devices are shown in Figures C-1 and C-2, and their locations are schematically shown in Figure C-4.

Axial strain gages (micromeasurements; No. MA-13-250 BG; 120 ohm; 2.09 gage factor) were bonded to the test specimen in the locations shown schematically in Figure C-5. The output of these strain gages was recorded by means of a Baldwin SR-4 strain indicator, during the design limit load static tests.

3. Fatigue Test. Each actuator was hydraulically activated by a MTS closed-loop servomechanism system. The action of the actuators was controlled by load cells, which were also used to continually monitor the fatigue test loads on Gould Brush Strip Chart Recorders.

TEST PROCEDURE AND RESULTS

1. Dynamic Natural Frequency Tests. After the test specimen was installed on the load reaction fixture, dynamic natural frequency tests were conducted in the lateral and vertical directions. An accelerometer was mounted to the aft end of the specimen, and a sharp blow ("banging") was applied in the proper direction. The output of the accelerometer was simultaneously recorded on a Gould Brush Strip Chart Recorder.

These dynamic tests were again conducted at selected intervals of the test program. Before these tests were conducted, the six load trains were detached from the specimen. These test intervals are as follows:

- Before fatigue test start
- After application of 6000 cycles of fatigue test
- After completion of fatigue test.

No significant change was noted in the natural frequency of the test specimen.

2. Design Limit Load Static Tests. After completion of the first set of dynamic natural frequency tests, the six load trains and the deflection devices were attached to the specimen. The +15-degree yaw condition (Condition "A") of the design limit load static test was applied to the test specimen in 20-percent incremental load steps to 80 percent, then in 10-percent incremental load steps to 100 percent. Deflection, load, and strain gage readings were recorded at each incremental step. The tail down landing condition (Condition "C") and the -15-degree yaw condition (Condition "B") were then applied, respectively, in the same manner as Condition "A." Again, deflection, load, and strain gage readings were recorded at each incremental load step. After completion of each load condition, a visual inspection of the test specimen was conducted.

Each load condition was completed successfully, and no damage was noted during the subsequent inspections. The maximum applied loads (100 percent) are given in Table C-2 together with the resulting deflections and strains.

3. Fatigue Test. After completion of the second set of dynamic natural frequency tests, the six load trains were attached to the specimen. The fatigue test loads were then applied to the specimen by means of the closed-loop servomechanism systems. The horizontal loads [aft inertia load (P_{y3}), fin pressure load (P_{y2}), and tail rotor thrust load (P_{y1})] were applied at a cyclic rate of 1.5 cps. The vertical loads [sync elevator (P_{z1} and P_{z2}) and the vertical aft inertia load (P_{z3})] were applied at a cyclic rate of 3 cps. The sync elevator loads were programmed in a "milking machine" manner. The left sync elevator load was applied during the first half cycle of the aft inertia load, and the right stabilizer load was applied during the second half cycle of the aft inertia load. After completion of 6000 cycles of horizontal loads, the load trains were detached from the specimen to conduct the third set of dynamic frequency tests. After completion of these dynamic tests, the load trains were again attached to the specimen. Fatigue testing continued in the same manner as described above.

At the 50,000 cycle interval for the horizontal loads, the cyclic rate of the horizontal loads was increased to 2 cps and the cyclic rate of the vertical loads was increased to 4 cps. At the 102,000 cycle interval, a "squeaking" noise was noted at the attachment area of the

vertical fin with the tail boom. However, no damage to the specimen could be seen. Testing continued. At the 106,000 cycle interval, slight movement was noted between the lower left attachment fitting and the basic tail boom structure; and at this same interval, slight movement was also noted between the lower right attachment fitting and the basic tail boom structure. In both cases, this movement amounted to approximately 0.020 inch. As fatigue testing continued, no damage was noted, and there was no change in the previously noted movement between the two attachment fittings and tail boom structure.

After completion of 267,310 cycles of horizontal loads, fatigue testing was terminated. A final visual inspection of the test specimen revealed no damage, and the specimen was still capable of carrying the fatigue test loads. The applied fatigue test loads are given in Table C-3, and a brief summary of the fatigue test program is presented in Table C-4.

The load trains were detached, and the fourth and final set of dynamic natural frequency tests was conducted. No significant changes of the lateral or vertical natural frequencies of the test specimen were noted during the four dynamic tests.

4. Selective Static Tests.

- a. Simulated Bolt Failure Static Test. The upper left attachment bolt was loosened until a gap of 0.265 inch was measured between the bolt head and the reaction frame. As a result of this bolt loosening, a gap of 0.020 inch was noted between the upper left attachment fitting and the reaction frame. The load trains were then attached to the specimen. A series of static loads was applied to the specimen in 20-percent incremental load steps to 100 percent. At the 60-percent incremental step, the gap between the bolt head and the reaction frame was measured and found to be 0.128 inch (the gap between the boom and the reaction frame was now 0.157 inch). After completion of the test, a visual inspection of the specimen revealed no damage.
- b. Simulated Bullet Hole Damage Static Test. The upper left attachment bolt was retightened and torqued to 1100-1300 inch-pounds. Two 0.50-inch-diameter holes were drilled through the side and through the top of the specimen in a 45-degree angle with the vertical axis. The location of these holes is

shown in Figure C-6 and schematically represented in Figure C-7. The static loads of Condition A were applied to the specimen in incremental steps. After completion of this test, a visual inspection of the specimen was conducted. No damage was noted.

- c. Steel Ball Damage Test. A steel ball, weighing 0.97 pound and measuring 1.87 inches in diameter, was dropped from a height of 71 inches above the top of the specimen. The location of the path the steel ball traveled is shown schematically in Figure C-7. A very slight mark was noted in the impact area, but no indentation or damage to the specimen was noted. Because of the lack of damage to the specimen, static test loads were not applied.

Periodically during the test program, the four bolts that attach the tail boom to the reaction frame were checked for loss of torque. No loss of torque was found at any time.

TEST WITNESSES

These tests were witnessed all or in part by the following personnel:

Jim Needham	Hughes Helicopters
Herb Lund	Hughes Helicopters
George Deveau	Hughes Helicopters
Guido D'Agostino	Hughes Helicopters
Mr. Tom Mazza	Eustis Directorate

TABLE C-1. TEST PROGRAM SUMMARY,
AH-1G BASIC TEST TAIL BOOM

Test Title	Date Complete	Remarks
Dynamic Natural Frequency Tests	11-13-74	No significant changes noted in natural frequency.
Design Limit Load Static Tests	10-10-74	No damage.
Fatigue Test	11-13-74	Two bottom attachment fittings "breathing." No damage was noted.
Simulated Bolt Failure Static Test	11-20-74	No damage.
Simulated Bullet Hole Damage Static Test.	11-27-74	No damage.
Steel Ball Damage Static Test	12-3-74	No damage.

TABLE C-2. MAXIMUM APPLIED LOADS,
DEFLECTIONS AND STRAINS

Condition	A +15° Yaw, Rec.	B -15° Yaw, Rec.	C Tail Down Land.
Loads, lb ^①			
P _{y1}	-1259	1212	-
P _{y2}	-2188	1175	-
P _{y3}	786	-648	-
P _{z1}	43	934	-
P _{z2}	954	40	-
P _{z3}	388	395	-1847
Deflections - in. ^②			
A	-4.92	3.64	-
B _T	-2.19	1.55	-
B _B	-1.79	1.26	-
C	0.56	0.64	1.36
D	-0.05	0.02	-
E	0.01	0.01	-
Strains μ- in./in. ^③			
F ₁	2925	-2300	-
F ₂	-2795	2080	-
G _{1F}	-405	320	-135
G _{1A}	915	-735	60
G _{2F}	510	-385	-120
G _{2A}	-975	700	60
H ₁	335	-485	-30
H ₂	-475	245	10

TABLE C-2. Continued			
Condition	A +15° Yaw, Rec.	B -15° Yaw, Rec.	C Tail Down Land.
J ₁	1260	-525	-570
J ₂	1080	-1250	610
J ₃	-845	935	-640
J ₄	-1470	530	600
NOTES:			
① See Figure C-3 for location and direction of loads.			
② See Figure C-4 for location and direction of deflections.			
③ See Figure C-5 for location of strain gages - positive indicates tensile strain.			

TABLE C-3. APPLIED TEST LOADS, AH-1G
BASIC TEST TAIL BOOM

FATIGUE TEST					
Load ID	Applied Loads		Total Cycles Applied	Cyclic Rate	
	Mean Lb	Cyclic Lb		(2) CPS	(3) CPS
P _{Y1}	0	±720	267,310	1.5	2.0
P _{Y2}	-300	±1050	267,310	1.5	2.0
P _{Y3}	+45	±405	267,310	1.5	2.0
P _{Z1}	+30	±540 (4)	267,310	3.0	4.0
P _{Z2}	+30	±540 (4)	267,310	3.0	4.0
P _{Z3}	0	±240	534,620	3.0	4.0
<p>NOTES:</p> <ol style="list-style-type: none"> 1. See Figure 3 for location and direction of loads. 2. Cyclic rate for first 50,000 cycles of horizontal (P_Y) Loads. 3. Cyclic rate for the remaining 217,310 cycles of horizontal (P_Y) loads. 4. P_{Z1} cycle applied during first half of P_{Z3} cycle and P_{Z2} cycle applied during second half of P_{Z3} cycle. 					

TABLE C-4. FATIGUE TEST SUMMARY
AH-1G BASIC TEST TAIL BOOM

Date	<u>Test Duration</u>		Remarks (1)
	Start Cycle (3)	Stop Cycle (3)	
10-29-74			Test started at 1.5 cps.
10-30-74	0	6,000	Test stopped to run third dynamic frequency test. Test restarted at 1.5 cps.
11-4-74	6,001	50,000	Cyclic rate increased to 2.0 cps.
11-5-74	50,001	102,000	"Squaking" noise noted at attachment of vertical fin to tail boom. No damage noted.
11-5-74	102,001	106,000	Movement of approximately 0.020 in. noted between lower left attach fitting and tail boom and between lower right attach fitting and tail boom.
11-13-74	106,001	267,310	Test terminated. No further damage noted.
NOTES:			
1. Occurrences in remarks refer to stop cycle duration.			
2. Applied loads given in Table C-2.			
3. Cycle count is for horizontal (P _Y) load application.			

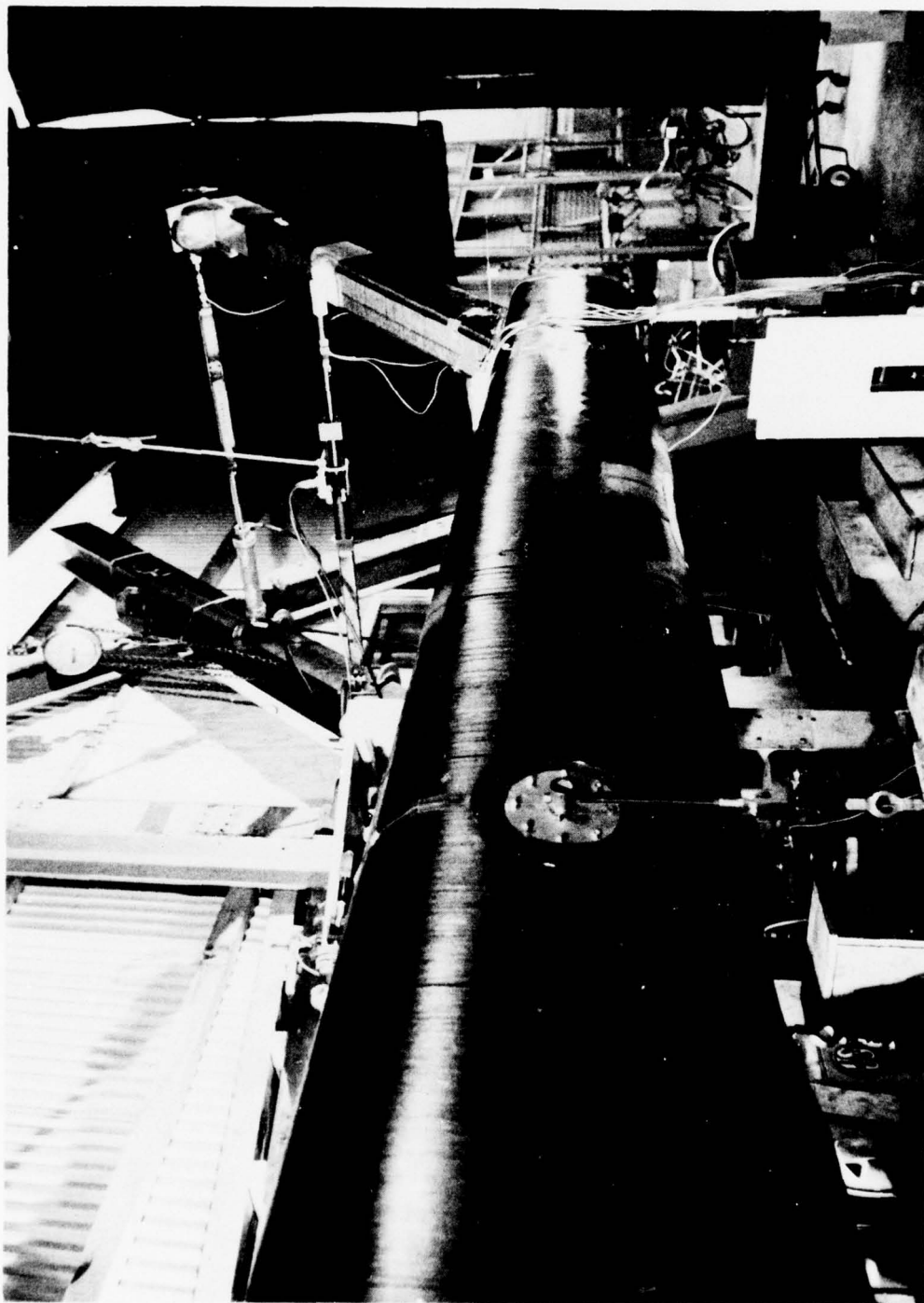


Figure C-1. View of Test Setup of AH-1G Basic Test Tail Boom
(Configuration II) Structural Tests.

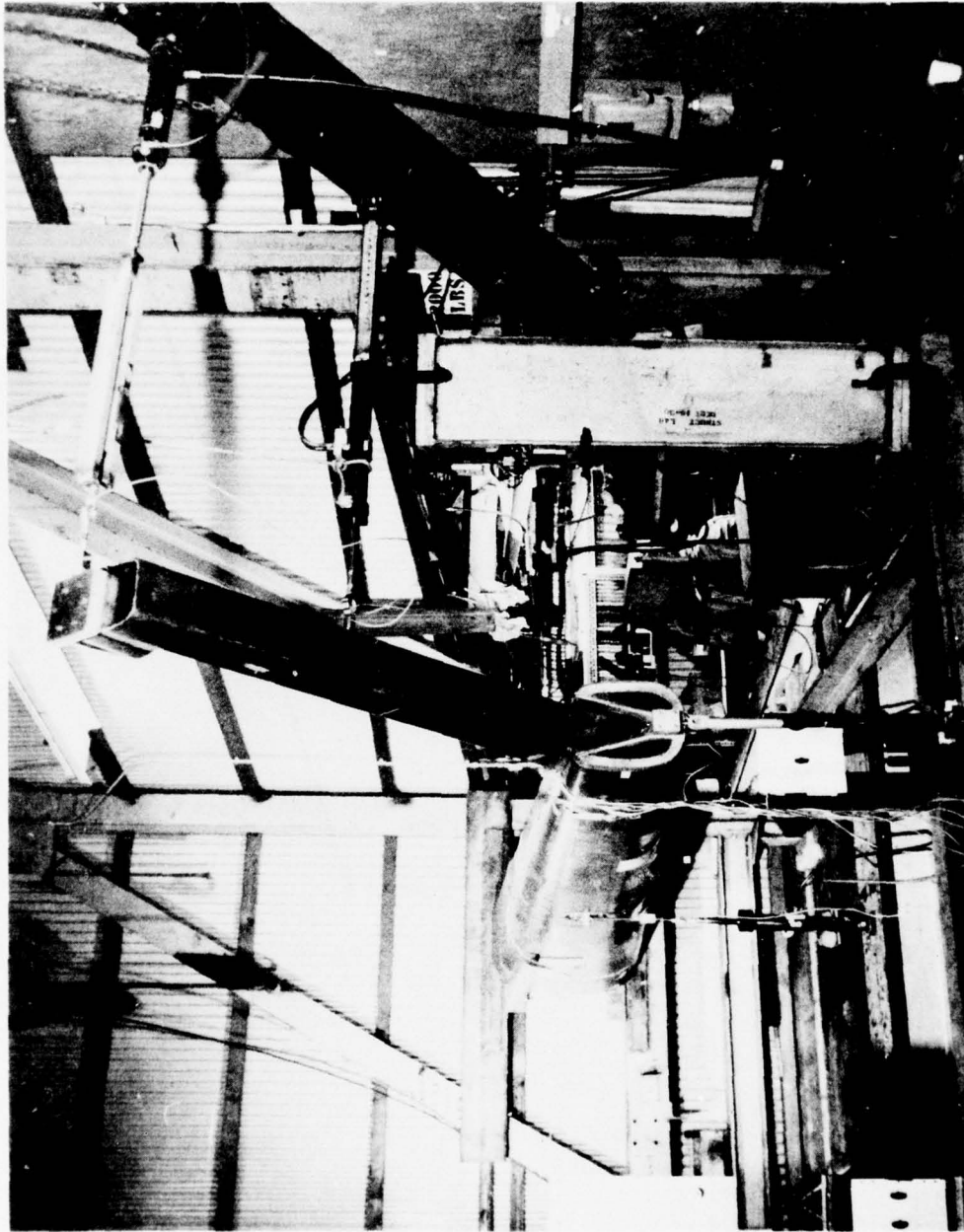


Figure C-2. View of Test Setup of AH-1G Basic Test Tail Boom
(Configuration II) Structural Tests.

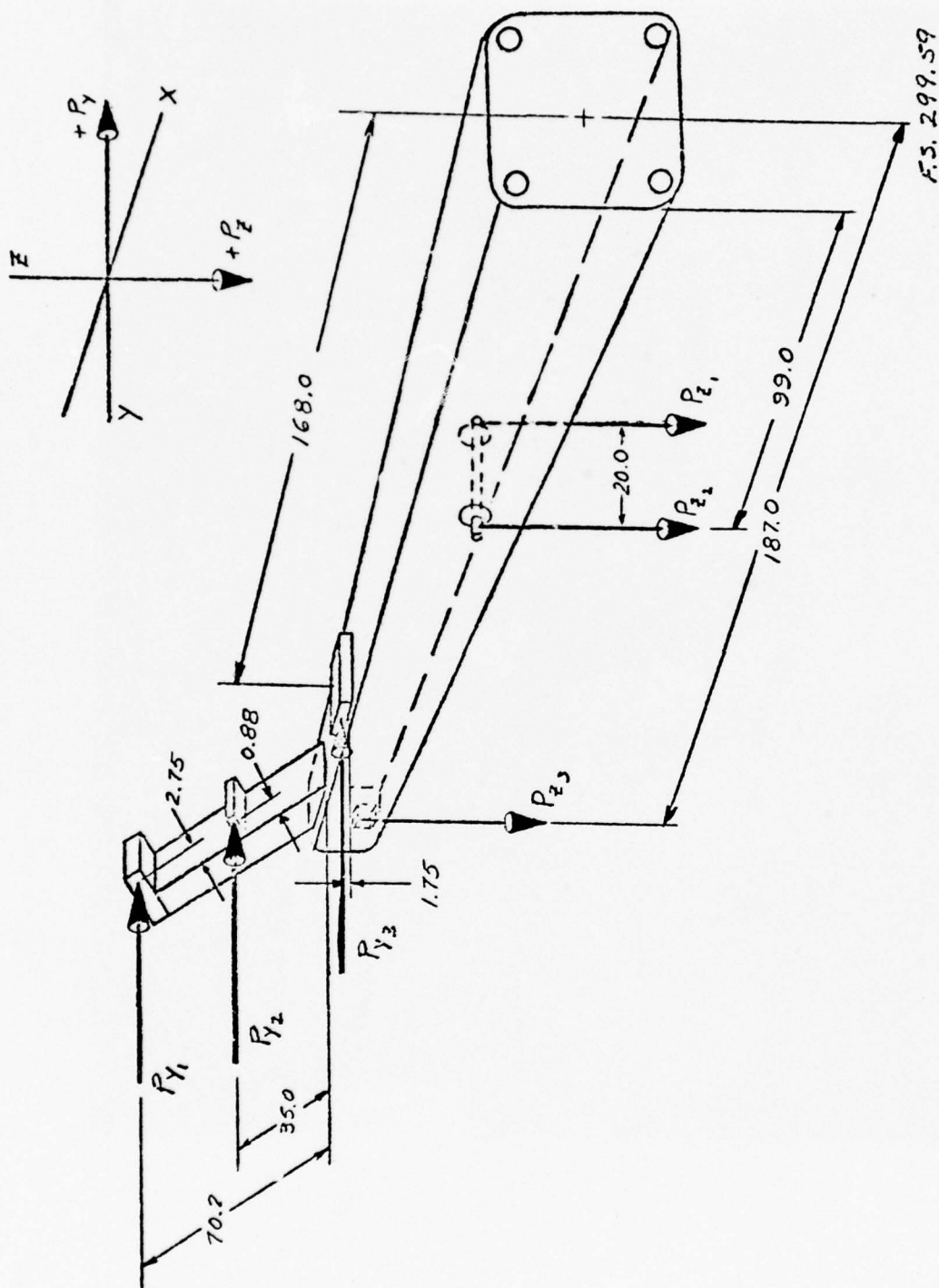


Figure C-3. Schematic Representation of Load Point Locations and Load Direction for the AH-1G Basic Test Tail Boom Structural Tests.

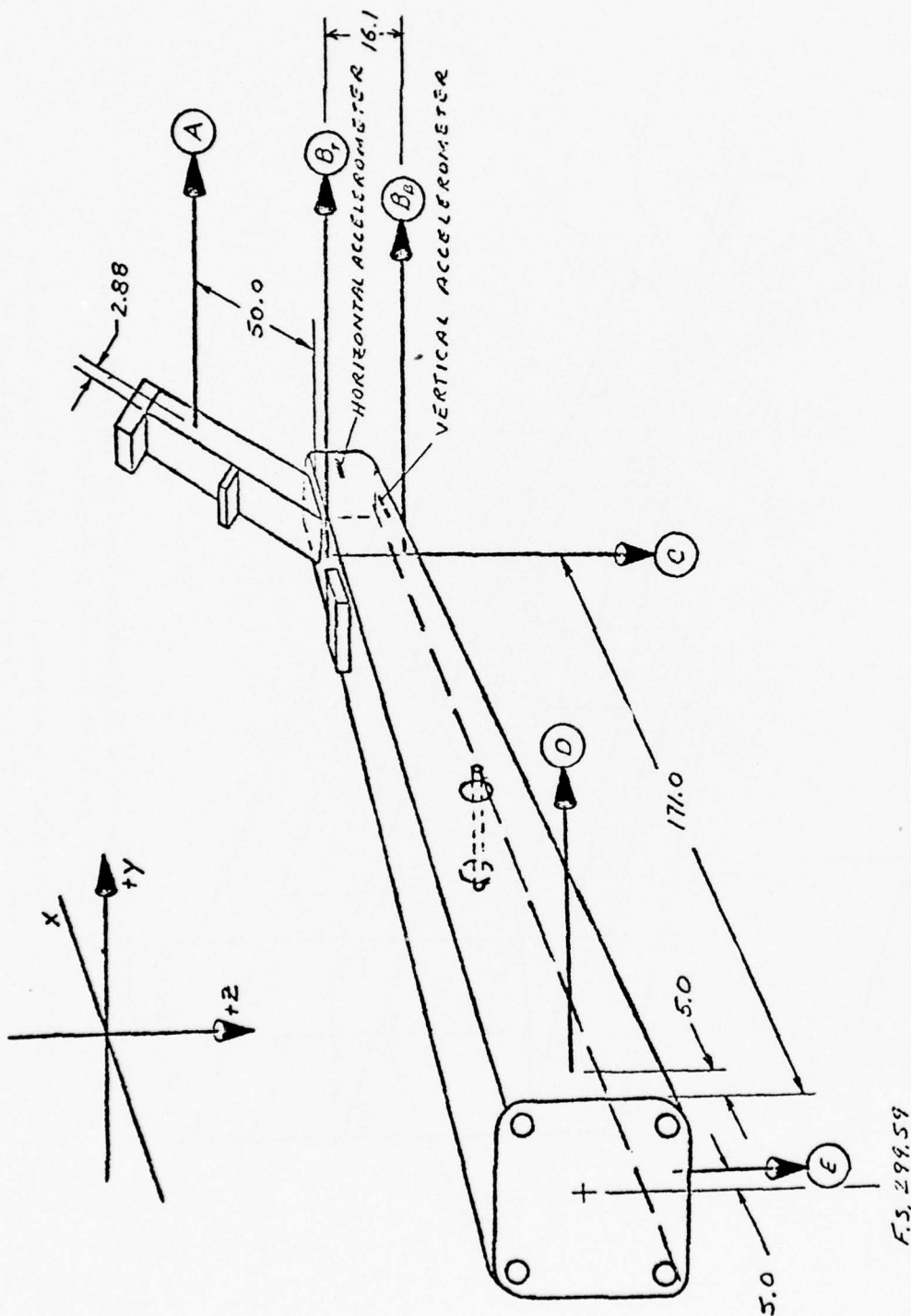
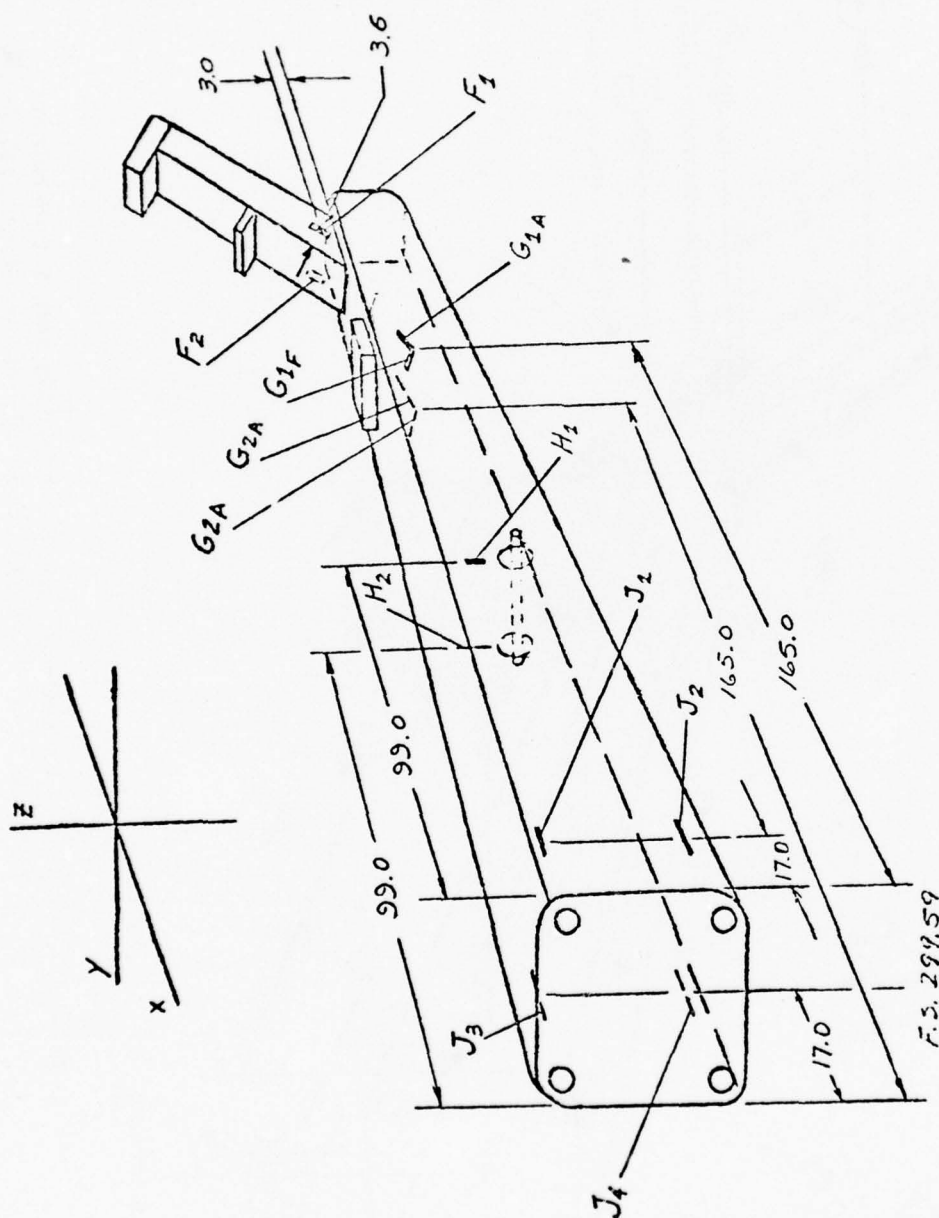
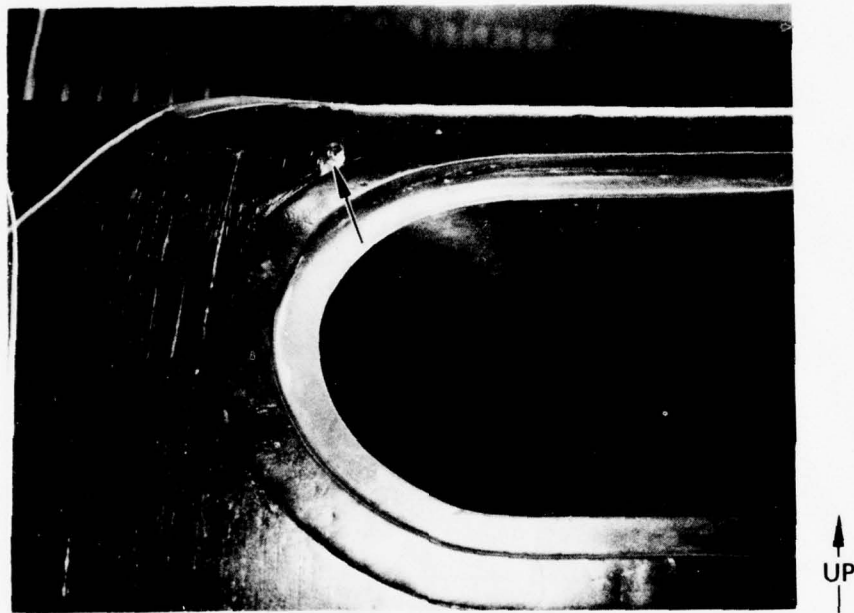


Figure C-4. Schematic Representation of Deflection and Accelerometer Locations for AH-1G Basic Test Tail Boom Structural Tests.



NOTE: F, H, and J gages were used to measure strain, and G gages were used to measure shear.

Figure C-5. Schematic Representation of Strain Gage Locations for the AH-1G Basic Test Tail Boom Structural Tests.



(ARROW) DRILLED IN SIDE OF TAIL BOOM
FOR BULLET HOLE DAMAGE STATIC TEST

Figure C-6. View of Both 0.50-Inch Diameter Holes.

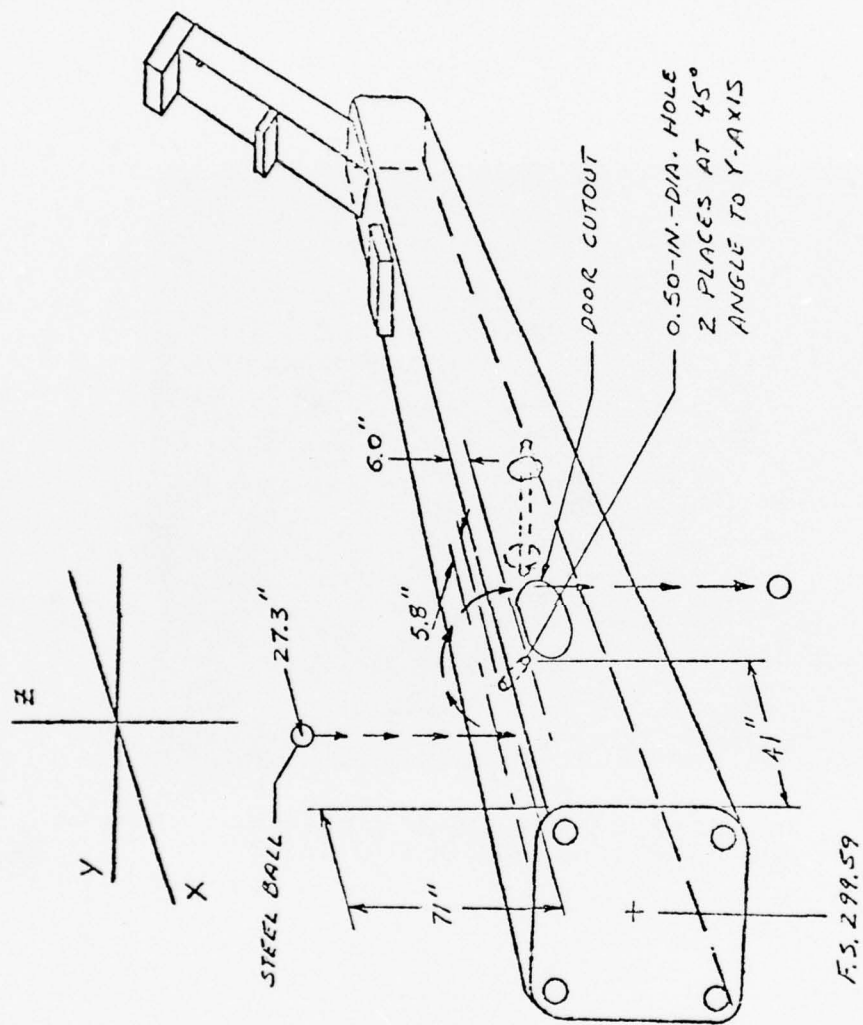


Figure C-7. Schematic Representation of the Location of the 0.50-Inch-Diameter Holes and the Path that the Steel Ball Traveled.

APPENDIX D

AH-1G COBRA TAIL BOOM

STRUCTURAL EVALUATION TEST

OBJECTIVES

The objectives of this test program are:

- To assist in the establishment of the structural integrity of the flight tail boom.
- To calibrate the strain gages for known applied loads and moments.

INTRODUCTION

As per Contract No. DAAJ02-73-C-0079 and in accordance with Engineering Test Request No. AH-BT-02, one 465P-050 basic tail boom test specimen was subjected to a series of static and dynamic natural frequency tests. These tests were conducted at the Hughes Helicopters Structures Test Laboratory, Culver City, California, during the period 8 July through 28 July 1975.

SUMMARY

One basic composite tail boom test specimen was subjected to a series of design limit load static tests and dynamic natural frequency ("bang") tests.

No apparent damage was noted while conducting the tests.

DISCUSSION

TEST SPECIMEN

The test specimen, Part No. 465P-050, consists of the basic fuselage tail boom and vertical tail fin assembly — less doors, portions of the drive shaft, horizontal stabilizer and stabilizer controls, portions of the tail rotor controls, fairings and cover installations, angle gearbox, tail rotor, and tail rotor gearbox. The tail boom section is constructed of a double shell, filament-wound composite fiber sandwich-type monocoque structure composed of Thornel 300 graphite fiber in an epoxy material and a Nomex honeycomb core. The vertical tail fin spar is also a sandwich construction consisting of graphite/epoxy skins and Nomex honeycomb core with longitudinal graphite fibers on the four corners of the spar. The fuselage section and vertical tail fin assembly are permanently attached.

A 2.37-inch-diameter steel pipe was inserted in the horizontal stabilizer attach fittings to apply the stabilizer loads. Fittings were attached to the angle gearbox/fuselage interface and the tail rotor gearbox/vertical fin interface to apply the other test loads.

A schematic of the test specimen, with the location of these fittings and load points, is presented in Figure D-3.

TEST SETUP

1. General. The tail boom test specimen was mounted to a load reaction fixture by means of four NAS 628-88 Attachment Bolts. Each bolt was installed through the reaction fixture and into a barrel nut attachment in the test specimen. Each bolt was torqued to 1100-1300 inch-pounds. Attach bolts were located in the fixture and in the specimen with the aid of a tooling fixture.

Loads were applied to the specimen by means of four load trains that contained a hydraulic actuator and a load cell in each train. The stabilizer loads (P_{Z1} and P_{Z2}) were applied by one load train, then a whiffle tree was attached to each end of the stabilizer support tube. The vertical and horizontal aft inertia loads (P_{Z3} and P_{Y2} , respectively) were applied by two load trains installed at the angle gearbox/fuselage interface. The tail rotor thrust loads (P_{Y1}) were applied by a load train installed on the tail rotor/vertical fin interface. The location of these four load trains is schematically shown in Figure D-3.

2. Static Tests. For the design limit load static tests, the actuators were hydraulically activated by means of an Edison Load Maintainer.

The load cells, read out by a strain indicator, were used to monitor the test loads. Deflection wires were attached to the test specimen and routed over a pulley system and across a sheet of graph paper mounted to a wooden frame. A weight was fastened to the end of each wire to eliminate sag. Tabs were placed on the wires for use as pointers. During testing, pointer travel, which indicated specimen movement, was marked on the graph paper at each increment of load. The deflection locations are schematically shown in Figure D-4.

Axial strain gages (BLH DLB-A35-6A-S6; 350 ohm; 2.04 gage factor) were bonded to the test specimen in the locations shown schematically in Figure D-5. The output of these strain gages was recorded by means of a Baldwin SR-4 Strain Indicator, during the design limit load static tests.

TEST PROCEDURE AND RESULTS

1. Dynamic Natural Frequency Tests. After completion of the static proof tests, dynamic natural frequency tests were conducted in the lateral and vertical directions. An accelerometer was mounted to the aft end of the specimen, and a sharp blow ("banging") was applied in the proper direction. The output of the accelerometer was simultaneously recorded on a Gould Brush Strip Chart Recorder.

Before these tests were conducted, the four load trains were detached from the specimen. The horizontal drive shaft and the angle gearbox were installed. The canted drive shaft and upper gearbox were not available. All other equipment — couplings, control system, etc — were the same as installed during the static tests.

The location of the accelerometer used during these dynamic tests is schematically shown in Figure D-4.

2. Design Limit Load Static Tests. The +15-degree yaw condition (Condition "A") of the design limit load static test was applied to the test specimen in 20-percent incremental load steps to 80 percent, then in 10-percent incremental load steps to 100 percent. Deflection, load, and strain gage readings were recorded at each incremental step. The tail down landing condition (Condition "C") and the -15-degree yaw condition (Condition "B") were then applied, respectively, in the same manner as Condition "A". Again, deflection, load, and strain gage readings were recorded at each incremental load step. After completion of each load condition, a visual inspection of the test specimen was conducted.

Each load condition was completed successfully and no damage was noted during the subsequent inspections. The maximum applied loads are given in Table D-1 together with the resulting deflections and strains.

TEST WITNESSES

These tests were witnessed all or in part by the following personnel:

T. Mazza	Aerospace Engineer-Eustis Directorate
H. T. Lund	Manager-Light Helicopter Division
J. M. McDermott	Chief-Stress Analysis
R. E. Moore	Division Manager-Military Helicopter
J. F. Needham	Design Specialist
G. A. D'Agostino	Senior Research Engineer-Structures Test
G. D. Deveaux	Chief-Structures Test

TABLE D-1. MAXIMUM APPLIED LOADS,
DEFLECTIONS AND STRAINS

Condition	A +15° Yaw, Rec.	B -15° Yaw, Rec.	C Tail Down Land.
Loads, lb ^①			
P _{Y1}	-1592	1325	0
P _{Y2}	-1510	816	0
P _{Z1}	433	462	0
P _{Z2}	433	462	0
P _{Z3}	415	387	-1357
Deflection - inches ^②			
A	-5.08	3.72	-
B (Deg., Min.)	56'	41'	-
B	-2.62	1.88	-
C	0.53	0.48	1.35
D	-0.02	0.02	0
E	-0.12	0.05	0.10
F	-0.06	0.06	0.04
Strain μ - in./in. ^③			
1	-1490	1240	55
2	1775	-1380	40
3	1315	-670	-510
4	1265	-1395	555
5	-1945	815	520
6	-1035	1160	-580

NOTES:

① See Figure D-3 for location and direction of loads.

② See Figure D-4 for location and direction of deflections.

③ See Figure D-5 for location of strain gages - positive indicates tensile strain.



Figure D-1. View of Test Setup of AH-1G Flight Test Tail Boom Static Proof Test.

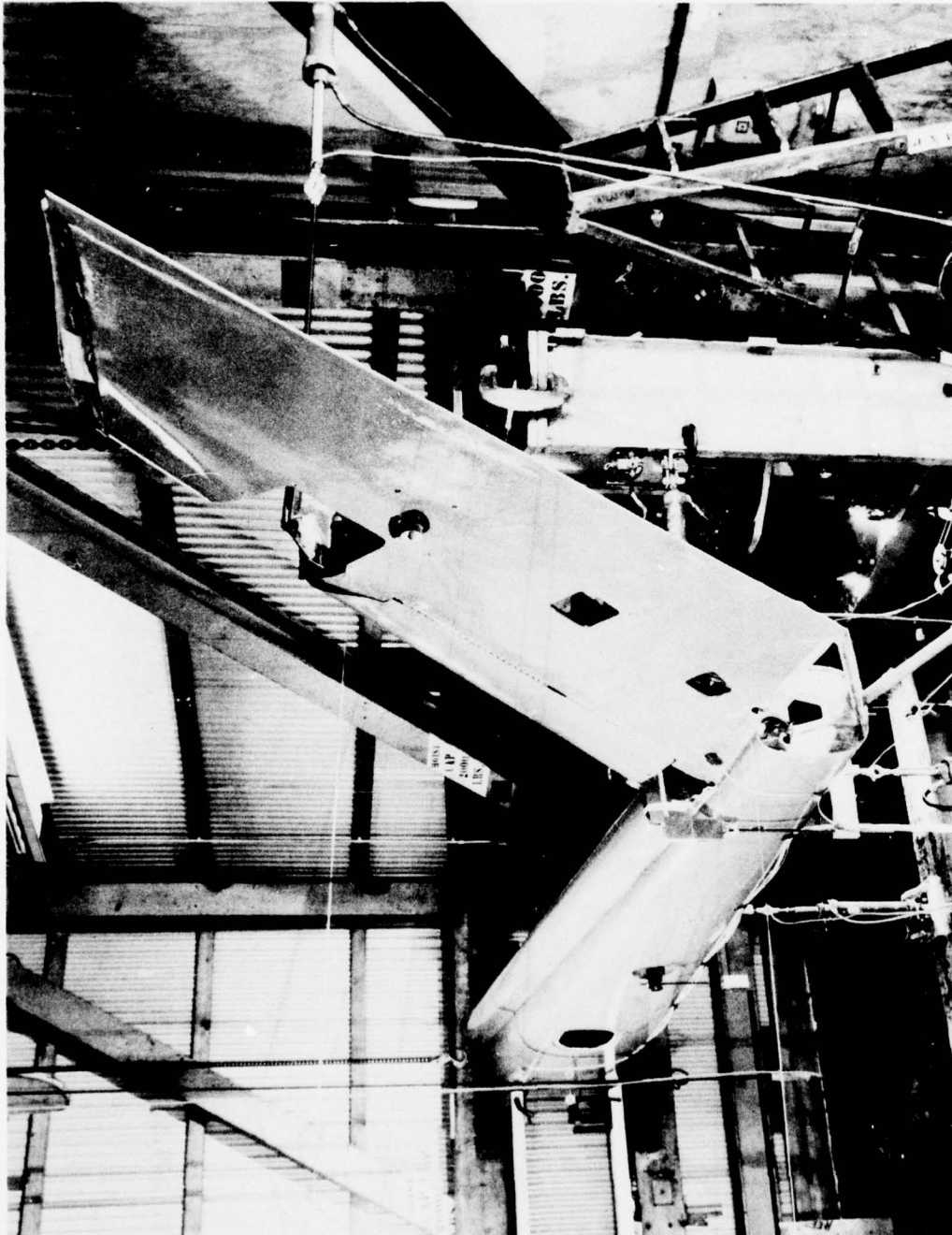


Figure D-2. View of Test Setup of AH-1G Flight Test Tail Boom Static Proof Test.

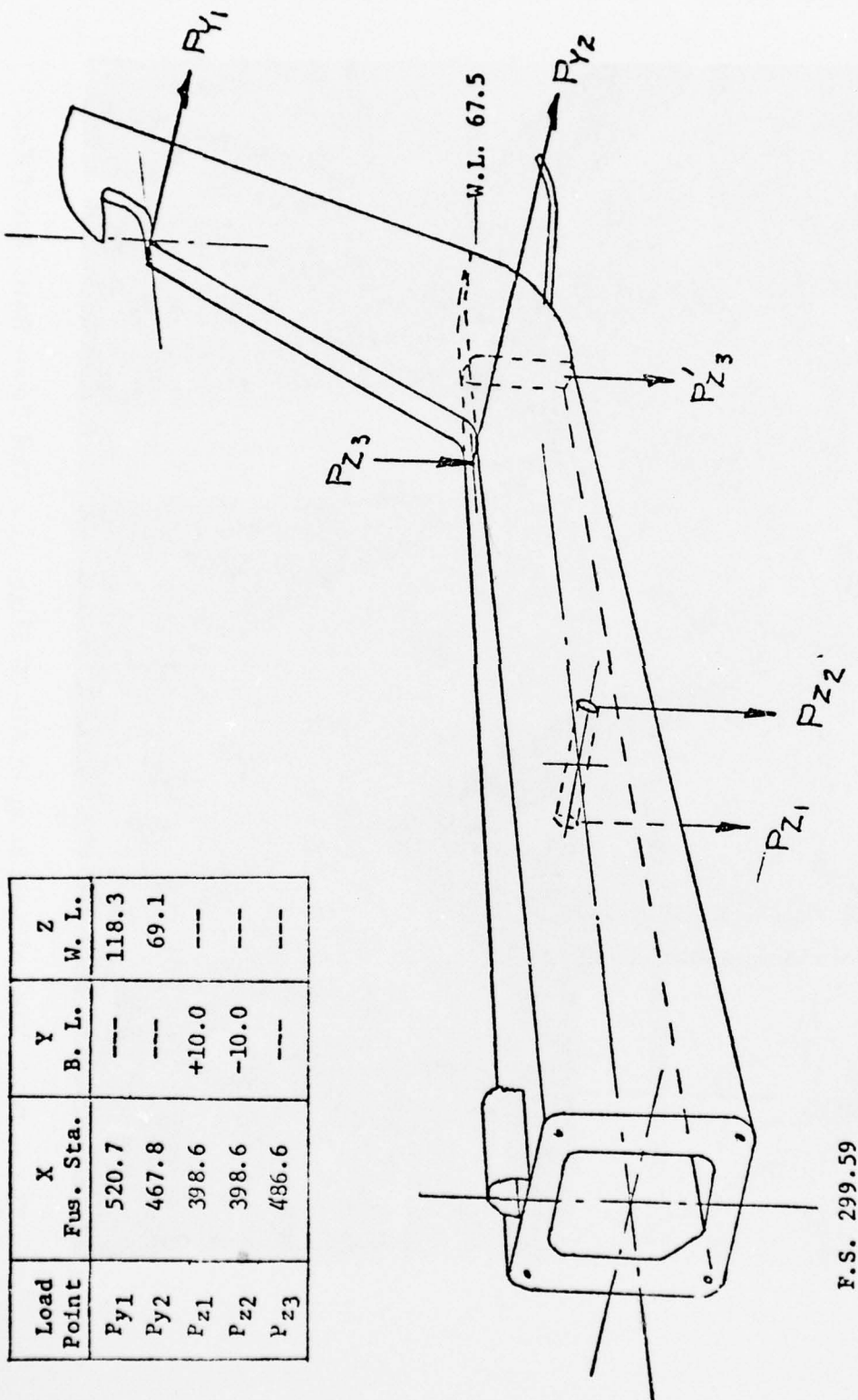


Figure D-3. Schematic Representation of Load Point Locations and Load Direction for the AH-1G Flight Test Tail Boom Structural Test.

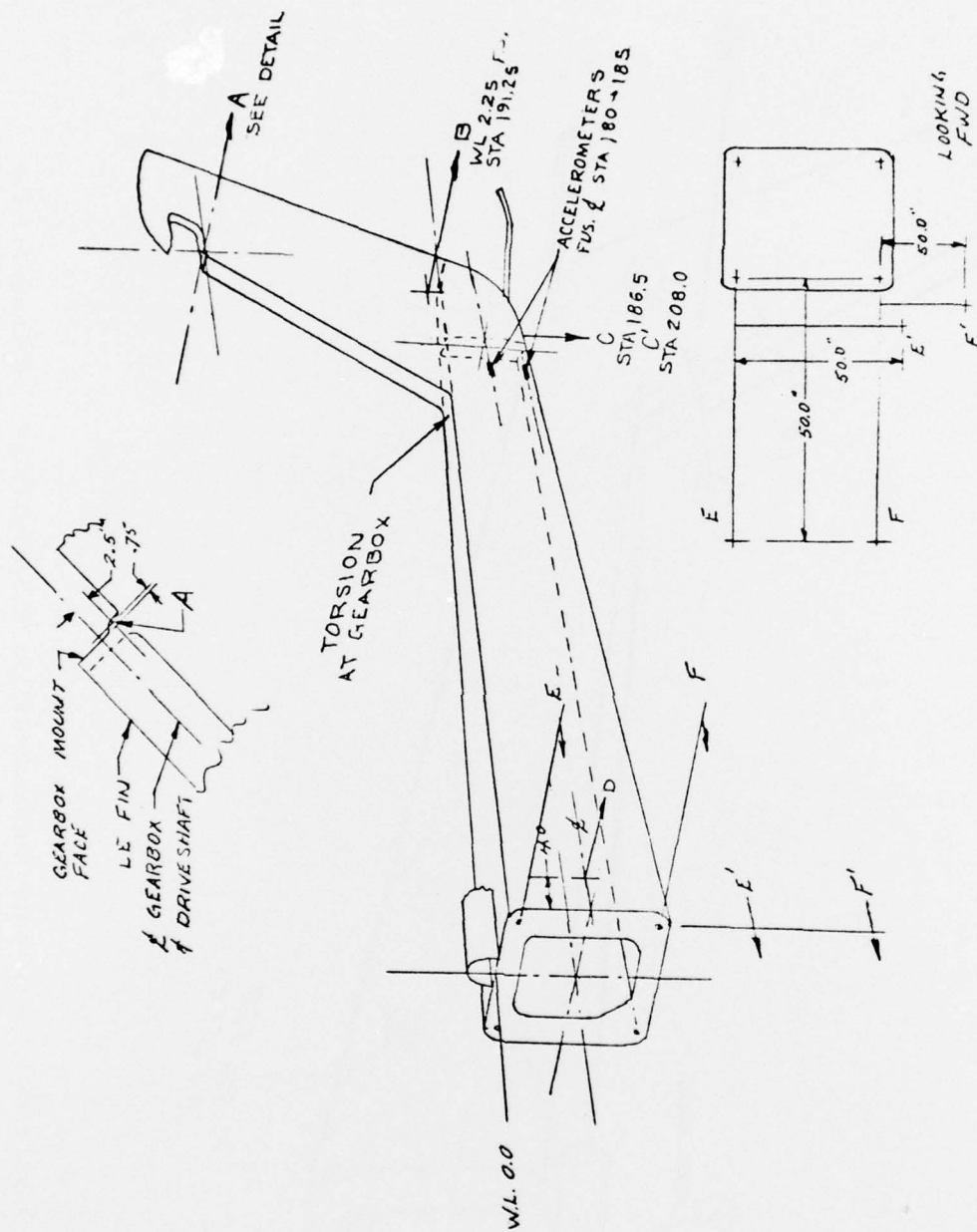


Figure D-4. Schematic Representation of Deflection and Accelerometer Locations for the AH-1G Flight Test Tail Boom Structural Test.

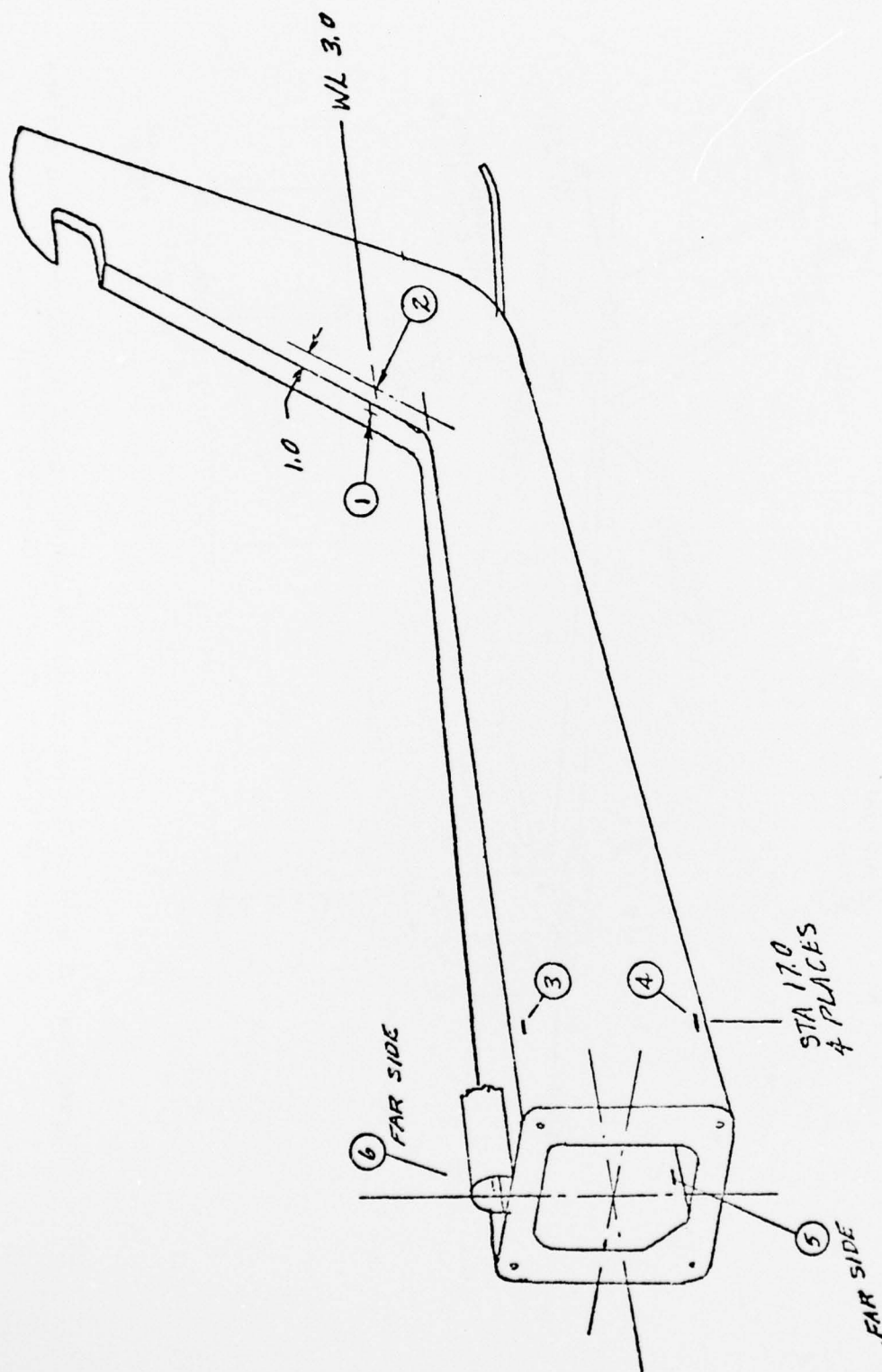


Figure D-5. Schematic Representation of Strain Gage Locations for the AH-1G Flight Test Tail Boom Structural Test.

SYMBOLS

a	Dimension (in.)
A	Cross-sectional area (in. ²)
AI	Cross-sectional area of the fuselage shells inside face (in. ²)
AIC	Enclosed area of the fuselage shells inside face (in. ²)
AO	Cross-sectional area of the fuselage shells outside face (in. ²)
AOC	Enclosed area of the fuselage shells outside face (in. ²)
b	Dimension (in.)
BS	Boom station
BL	Butt line
c	Dimension (in.)
cg	Center of gravity
C _h	Chord length (in.)
e	Elongation (in./in.)
E	Modulus of elasticity (psi)
E'	$\sqrt{E_a E_b}$
EA	Axial stiffness (lb)
EI	Modulus of fuselage shell inside face (psi)
EIY	Flexural stiffness about 'y' axis (lb-in. ²)
EIYI	Flexural stiffness of fuselage shell's inside facing about 'y' axis (lb-in. ²)
EIYO	Flexural stiffness of fuselage shell's outside facing about 'y' axis (lb-in. ²)
EIZ	Flexural stiffness about 'z' axis (lb-in. ²)
EIZI	Flexural stiffness of fuselage shell's inside facing about 'z' axis (lb-in. ²)
EIZO	Flexural stiffness of fuselage shell's outside facing about 'z' axis (lb-in. ²)
EO	Modulus of fuselage shell outside face (psi)
f	Stress (psi)
F	Strength (psi)
FS	Fin Station
g	Load Factor, acceleration
GI	Shear modulus of fuselage shell inside facing (psi)
GK	Shear stiffness (lb-in. ²)
GKI	Shear stiffness of fuselage shell inside facing (lb-in. ²)
GKO	Shear stiffness of fuselage shell outside facing (lb-in. ²)
GO	Shear modulus of fuselage shell outside facing (psi)
h	Dimension (in.)
H	Load (lb.)
HDT	Heat distortion temperature (°F)
I	Moment of inertia (in. ⁴)
IGE	In Ground Effect
K	Torsional constant (in. ⁴), constant

K_m	Buckling coefficient
L	Length (in.)
L/H	Left Hand
LI	Mid-wall length around cross section of fuselage inside skin (in.)
LL	Lower Left
LO	Mid-wall length around cross section of fuselage outside skin (in.)
LR	Lower Right
M	Moment (in.-lb)
MS	Margin of safety
N	Number
P	Load or force (lb)
PSI	Angle (deg)
R	Radius (in.), ratio of actual stress/allowable stress
R/H	Right Hand
R_e	Radius to mid-point of band where winding angle is 90° (in.)
S	Load (lb)
t	Thickness (in.)
T	Torque (in.-lb)
TC	Thickness of sandwich wall core material (in.)
TI	Thickness of sandwich wall inside face (in.)
TO	Thickness of sandwich wall outside face (in.)
U	Transverse shear stiffness (lb-in. ²)
UL	Upper Left
UR	Upper Right
V	Shear load (lb), velocity (kn)
VF	Fiber volume ratio
W	Weight (lb or lb/in.)
WL	Water line
x	Dimension (in.)
Y	} Dimensions, See Figure 10 (in.)
YBI	
YBO	
YI	
YII	
YO	
Z	
ZBI	
ZBO	
ZI	
ZII	
ZO	
α	Winding angle (deg), coefficient of thermal expansion (in./in./°F)
μ	Poisson's ratio - Strain (in./in.)
ρ	Density (lb/in. ³ or lb/ft ³)

SUBSCRIPTS

b	Bending
c	Composite, coil or compression
cu	Compression ultimate
i	Inside
L	Left side
o	Outside, 0° orientation relative to axial axis or initial angle
R	Right side or rear
r	Resultant
s	Shear or skin
su	Shear - ultimate
tu	Tension - ultimate
x	Refer to coordinate axis
y	
z	